ABSTRACT

MESSENGER, ZACHARY J. Deletion of C/EBPβ in Oncogenic Ras-Driven Skin Tumors is a Synthetic Lethal Event Promoting p53-Dependent Apoptosis, a Type I Interferon Response, and Tumor Regression. (Under the direction of Dr. Robert C. Smart).

During tumorigenesis, the developing tumor must overcome a variety of stress phenotypes such as inflammation, genomic instability, and DNA damage all while sustaining a proliferative environment and avoiding growth suppression and death. Therapeutic targeting of specific genetic changes directly or indirectly in cancer has proven to be an effective therapeutic strategy and the concept of synthetic lethality has emerged. Based on previous findings that C/EBPβ$^{-/-}$ mice are refractory to skin tumor development involving oncogenic Ras, we hypothesized that the transcription factor C/EBPβ is required for survival of oncogenic Ras skin tumors and that deletion of C/EBPβ in a pre-existing tumor would promote tumor regression. To test this hypothesis, we developed a mouse model where C/EBPβ could be conditionally deleted in pre-existing oncogenic Ha-Ras skin tumors. Deletion of C/EBPβ in oncogenic Ras tumors resulted in rapid tumor regression. By 10 weeks after C/EBPβ deletion, tumor volume decreased by 98% and 80% of the tumors completely regressed. Regressing tumors displayed elevated levels of apoptosis and the p53 protein while adjacent C/EBPβ depleted skin did not, suggesting C/EBPβ is essential in oncogenic Ras skin tumor cells but not in skin keratinocytes with wild type Ras. In accord, the induced expression of transgenic oncogenic Ras in C/EBPβ$^{-/-}$ epidermis did not alter keratinocyte survival or p53 levels, suggesting that oncogenic Ras tumors have acquired a dependence on C/EBPβ. To determine whether p53 is required for observed increased apoptosis and regression of oncogenic Ras tumors depleted of C/EBPβ, we co-deleted C/EBPβ and p53 in oncogenic Ras tumors and observed that p53 is required for both tumor

regression and elevated levels of apoptosis. RNAseq data analysis of regressing tumors depleted of C/EBPβ showed significant up-regulation of proapoptotic signaling networks including significant activation of death receptor signaling networks involving a type I interferon response and p53. In summary, oncogenic Ras skin tumors are dependent on C/EBPβ for survival, and deletion of C/EBPβ in these tumors is a synthetic lethal event dependent upon p53.

© Copyright 2018 Zachary J Messenger

All Rights Reserved

Deletion of C/EBPβ in Oncogenic Ras-Driven Skin Tumors is a Synthetic Lethal Event Promoting p53-Dependent Apoptosis, a Type I Interferon Response, and Tumor Regression.

by
Zachary J Messenger

A dissertation submitted to the Graduate Faculty of
North Carolina State University
in partial fulfillment of the
requirements for the degree of
Doctor of Philosophy

Toxicology

Raleigh, North Carolina

2018

APPROVED BY:

_____	_____
Dr. Robert Smart Committee Chair	Dr. Jun Ninomiya-Tsuji
_____	_____
Dr. James Bonner	Dr. Jon Horowitz

DEDICATION

For Izzy, Logan, & Sadie

BIOGRAPHY

Zachary J. Messenger was born in York, Pennsylvania to John and April Messenger and raised just outside of Newville, Pennsylvania with his younger brother Ethan. Zach graduated from Big Spring High School before attending The Pennsylvania State University where he earned his Bachelor of Science degree from the Eberly College of Science in Forensic Science. Upon completion in 2008 he married his first wife Elizabeth "Izzy" Royse and the two set off to the big city. Living just north of the Philadelphia line in the small community of Abington, Zach worked toward his Master of Science in Forensic Science which he earned in 2010 at Arcadia University in conjunction with The Center for Forensic Science Research & Education at the Fredric Rieders Family Foundation. During his Masters work Zach was attracted to the field of Toxicology and to the idea of working towards a doctoral degree. His wife Izzy was in full support so long as the considered institutions were located in points south, which in turn led them to North Carolina State University. Two years into the Toxicology doctoral program Zach and Izzy welcomed their son Logan into the family followed 18 months later by their daughter Sadie. Having watched Logan graduate (pre-school), Zach figured he better finish up before he finished high school.

ACKNOWLEDGMENTS

I would like first and foremost to thank my advisor and friend Dr. Robert C. Smart for training and mentoring me. During my time at NC State Rob has patiently and compassionately provided me with guidance, and motivation to improve as a scientist. I would also like to thank Dr. Jonathan Hall for his friendship, help and comradery in the laboratory as well as Dr. Hann Tam, Dr. Songyun Zhu, Dr. John House and Jeanne Burr for their help and support along this journey, Nicholas Clark and Zoe Lindsey-Mills for their assistance, and to Dr. Alexander Bogdan for his help in putting this dissertation together. I would also like to thank my parents, brother, family, friends and the Meadow Run Science Association for their support and encouragement. Finally, to my wife Izzy who has kept this operation in the black for the past 10 years, thank you for your encouragement and confidence when things got tough. I love you.

TABLE OF CONTENTS

LIST OF TABLES

LIST OF FIGURES

Introduction

Chapter 1

Appendix

GENERAL INTRODUCTION

Cancer is not a singular malady but rather a group of diseases characterized by cells which are able to continuously proliferate while evading forces opposing their growth and progression. Cancer is the second leading cause of mortality in the United States [1], with over half a million people dying in 2016 alone [2]. The National Cancer Institute (NCI) estimates that over a third of people in the United States will be diagnosed with a form of cancer during their lifetime. In 2010, Americans spent around $125 billion on cancer treatment and care, and the NCI estimates this annual cost could top $150 billion by 2020 [3]. The human and economic costs incurred by cancer have rightly put an emphasis on research related to its prevention, treatment and understanding.

Cancer

Cancer arises through a process called carcinogenesis, where a single cell acquires genetic alterations (mutations) which allow for clonal expansion into a population of cells that share certain characteristics. These “Hallmarks of Cancer” as described by Hanahan and Weinberg [4] include six established hallmarks and four additional emerging hallmarks: 1.) sustaining proliferative signaling, 2.) evading growth suppressors, 3.) resisting cell death, 4.) inducing angiogenesis, 5.) enabling replicative immortality, 6.) activating invasion and metastasis, 7.) deregulating cellular energetics (metabolism), 8.) avoiding immune destruction, 9.) tumor-promoting inflammation, and 10.) genome instability and mutation (Figure I1). The initial cell the cancer originates from does not exhibit all ten of these characteristics at once, but rather accumulates them over time through a multi-stage process.

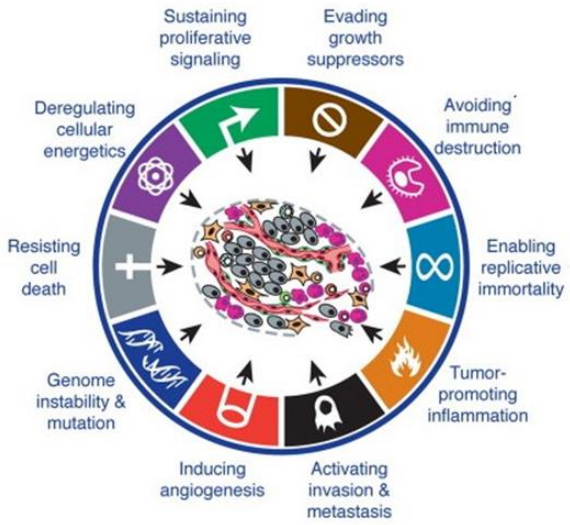

Figure I1: The Hallmarks of Cancer. Adapted from: Hanahan, D. and Weinberg, R.A., Hallmarks of cancer: the next generation. Cell, 2011. 144(5): p. 646-74

The initial step in this process, tumor initiation, is an early genetic change (mutation) which provides a selective advantage and primes the cell for future genetic and epigenetic changes that could arise if the initiated cell is promoted. Tumor promoters are not carcinogenic in themselves but act instead to promote a proliferative environment for the initiated cell. One of the earliest descriptions of the initiation/promotion model was made by Sir Percival Pott in 1775 who found a link between exposure to soot and scrotum cancer in chimney sweeps [5, 6]. Cells can acquire mutations and become initiated through inheritance of genetic abnormalities, exposure to chemicals or environmental factors, or cells can develop initiating mutations spontaneously over time [7]. The greatest risk factor for developing cancer is age [7]. Once initiated the cell needs to be promoted in order to progress to cancer. Promotors can sometimes act as initiators if exposure continues as in UVB induced skin cancer or, the initiator and promotor can be two different factors as in the DMBA/TPA

chemical carcinogenesis protocol explained below. Regardless of source, the initiated cell requires regular promotion to facilitate a proliferative state, while avoiding growth suppression and death. If shielded from arrest/death/differentiation, a hyperplastic population of cells will form and lead to subpopulations gaining additional mutations. Natural selection may impart additional advantages (i.e., acquiring additional hallmarks of cancer). The clonal expansion will then progress *in situ* (i.e., remaining in the original location), eventually forming a tumor. With continued clonal expansion and additional advantageous mutations, the population of cells arising from the original initiated cell may break through the basement membrane of the tissue and metastasize to different regions of the organism. As stated previously cancer is not a single disease, and different forms will develop and manifest differently. For example, the development of a blood cancer such as leukemia would lack the classic "lump" of a solid tumor in breast cancer; however, the monoclonal origin and accumulation of the hallmarks of cancer would remain the same.

Ras

The first and arguably most fundamental, hallmark of cancer is "sustaining proliferative signaling". In normal cells, the act of proliferation is a carefully orchestrated process in which pro-proliferative signals "push" a cell through the cell cycle. A key feature of homeostasis in normal cells is that proliferative signaling is tightly regulated and can be turned off. One important family of proteins involved in the regulation of pro-proliferative signaling is the Ras family. Ras was initially discovered in the 1960's as viral genes able to induce sarcomas *in vivo* or transform cells in culture[8, 9]. Originally known as p21 based on

its 21kDa size [10], the ability of the gene to induce rat sarcoma became the basis for the current nomenclature, Ras. The Ras family of proteins is made up of small, membrane-bound, GTPases that act as signal transducers, relaying extracellular signals through the cell membrane. The three family members are Ha-Ras, Ki-Ras, (named after Harvey [8] and Kirsten [9]) and N-Ras (first identified in a neuroblastoma cell line [11]). Humans have two forms of Ki-Ras stemming from alternative splice variants, KRAS4A and KRAS4B. Ras signaling can occur downstream of receptor tyrosine kinases (RTKs). When, an RTK binds its ligand, the RTK autophosphorylates on tyrosine residues located in the intracellular C-terminal domain. This phosphorylation causes adapter proteins (e.g., Grb2) to bind and recruit guanine exchange factors such as SOS (Son of Sevenless). Ras proteins act as molecular switches; their activity is determined by guanosine diphosphate (GDP) and guanosine triphosphate (GTP) binding. Ras bound to GDP is "switched off", i.e., inactive. The guanine exchange factor causes GTP to replace GDP, leading to the "switching on" of Ras. Once activated, Ras induces the phosphorylation and activation of a variety of downstream pathways including the mitogen-activated protein kinase (MAPK) pathway, phosphoinositide 3-kinase/protein kinase B (PI3K/Akt) pathway, Ral guanine dissociation stimulator (RALGDS) pathway, and phospholipase C (PLC) pathway; these pathways are involved in a variety of biological endpoints including proliferation, survival, transcription, vesicle transport, and calcium signaling. Ras has a very weak intrinsic GTPase activity that can be stimulated through binding of a GTPase activating protein (GAP) such as p120 [12]. Stimulation of this GTPase activity causes the hydrolysis of GTP to GDP, returning Ras to an inactive state and effectively "turning off" Ras signaling.

Oncogenic Ras

Ras is mutated in 20-30% of all human cancer. Some cancers exhibit characteristically high percentages of Ras mutations, such as mutated Ki-Ras in ~90-95% of pancreatic cancers. Ras genes are the most frequently mutated dominant oncogenic drivers in human cancer [13, 14]. Most mutations of Ras occur in the 12^{th}, 13^{th}, or 61^{st} codons, which decrease the already low intrinsic GTPase activity and prevent Ras interaction with GAP effectively leaving Ras in the "on" state [15].

Aside from Ras itself being mutated to the permanently "on" state, there are several other genetic changes in the Ras signaling pathway that can lead to aberrant Ras signaling. Greater than 50% of carcinomas display an overexpression of EGFR (an RTK upstream of Ras) [16], nearly 30% of breast cancer patients exhibit overexpression of HER-2/neu (human epidermal growth factor receptor 2) [17], and 12% and 40% of ovarian cancers have amplifications in AKT2 and PI3K (downstream targets of Ras signaling) respectfully [18]. The tumor suppressor PTEN (phosphatase and tensin homolog), an inhibitor of the PI3K pathway is altered at significant levels in a wide range of cancers [19]. The Ras pathway and its effectors play major roles in a variety of cancers and the ability to target Ras or the various Ras pathways could prove beneficial in anti-cancer therapies.

Unfortunately, Ras itself has proven extremely difficult to target pharmacologically. There are three requirements for Ras signaling: GTP binding, membrane localization, and effective signaling of downstream pathways. These requirements have been investigated as potential blockers of Ras signaling. Prevention of GTP interaction would essentially silence Ras signaling by preventing transduction of the signal to downstream pathways [20].

Antibodies that targeted the twelfth amino acid in oncogenic Ki-Ras prevented the binding of GTP [21]. This important finding confirmed the location of nucleotide binding but also suggested that competitive inhibitors could be a viable therapy option. Another method would be to enhance the intrinsic GTPase activity of Ras. Though the GTPase activity is decreased, oncogenic Ras does not completely lose the ability to hydrolyze a triphosphate as shown by the Scheffzek group [22]. They incubated the GTP analog DABP-GTP (3,4-diaminobenzophenone-phosphonoamidate of GTP) with various forms of mutant Ras and found a high rate of hydrolysis of DABP-GTP to GDP. This suggested that it should be possible to design or screen small molecules that can bind to the active site of oncogenic Ras as a part of future potential therapies. The Gray group was able to synthesize a GDP analogue that did just that [23]. The molecule SML-8-73-1 is a normal GDP with a linker and electrophile. The electrophile in this case was a chloroacetamide which could covalently bind to cysteine 12 of Ki-Ras^{G12C} and inhibit the recruitment of GTP. The downside being the double negative charge of the electrophile prevents passage through the cell membrane. Several other compounds were synthesized and tested with mixed results. All had to be present at high concentrations to compete with endogenous GTP for the binding site (if they could even enter the cell) and were specific to individual mutations. Ras has picomolar affinities for GTP, making competitive inhibition a difficult prospect [24, 25].

The second requirement of Ras activation is the physical location of Ras on the cell membrane [26]. Without membrane association, Ras is unable to signal or induce transformation [27, 28]. Each of the four Ras isoforms have a highly conserved G-domain followed by a hypervariable region on the C-terminus known as a CAAX motif where C:

cysteine; A: aliphatic amino acid; X: any amino acid. Post-translational modification by farnesyltransferase (FTase) adds a farnesyl group to the C-terminal cysteine [29, 30]. Following farnesylation, Ras-converting enzyme 1 cleaves the amino acids adjacent to the farnesyl group and isoprenylcysteine carboxylmethyltransferase-1 methylates the new C-terminal end. At this point only Ki-Ras4B is able to associate with the plasma membrane, the other three isoforms (Ha-Ras, N-Ras, and Ki-Ras4A) require palmitoylation and then vesicular transport to the plasma membrane [26]. FTase inhibitors were early candidates for anti-oncogenic Ras therapy [31-34], however they failed in clinical trials for various reasons [35], such as geranylgeranylation being able to overcome the missing farnesylation in N and Ki-Ras isoforms [36]. Blocking geranylgeranylation and farnesylation simultaneously was found to induce general toxicity which deceased the feasibility of a potential dual therapy [37, 38].

The third requirement of Ras signaling are the downstream signaling pathways themselves. As a membrane bound signal transducer, Ras requires downstream effectors to propagate the signal. Conveniently, many of these downstream effectors are kinases for which small-molecule inhibitors are readily available [39-41]. The Ras-Raf-MEK-ERK signaling cascade has been effectively targeted with drugs currently on the market like Nexavar®/Sorafenib (Raf inhibitor)[42] and Selumetinib (MEK inhibitor) [43]. Unfortunately, targeting this cascade has proven ineffective due to the development of drug resistance and reactivation of ERK [44-46]. Therefore, dual inhibition (i.e., ERK inhibition in conjunction with Raf or MEK inhibition) is an enticing prospect, with compounds like BVD-523 (Ulixertinib, a reversible ERK inhibitor) recently completing a phase 1/2 study

(ClinicalTrials.gov Identifier: NCT02296242) [47]. In addition to the Ras-Raf-MEK-ERK pathway, the Ras-PI3K-AKT-mTOR pathway is another major cascade of Ras effectors. The Downward group has shown that interaction of PI3K with Ras is required for oncogenic Ras induced tumorigenesis [48] and maintenance [49]. The drug Buparlisib is an inhibitor of PI3K that was recently found to be too toxic for effective use [50], but the drug Copanlisib [51] is approved by the FDA as a selective inhibitor of PI3K. The AKT inhibitor Afuresertib [52], and the mTOR inhibitor Everolimus [53] are examples of FDA approved drugs targeting the PI3K-AKT-mTOR pathway. The downside is that there has been little success treating oncogenic Ras tumors with PI3K, AKT, or mTOR inhibitors alone; however combination therapies may prove beneficial going forward, as described by Cantley and Wong [39]. Their study found that a PI3K inhibitor and a MEK inhibitor showed promise when treating murine lung cancers containing a mutated Ki-Ras.

The ”Undruggable” Nature of Ras

Even with all the attention given to oncogenic Ras, the shape/structure, translocation, and downstream effectors of Ras remain difficult targets for inhibiting oncogenic Ras signaling. Ras is a very “smooth” protein in that it lacks deep pockets for compounds to bind and disrupt signaling. Without specific inhibitors for post-translational modifications of Ras, general inhibition of farnesylation, geranylgeranylation, or palmitoylation will have toxic side effects in patients as many other important membrane-localized proteins would be disrupted.

Additionally, Ras signaling is extremely complex. Describing Ras signaling as a web as opposed to a pathway would be a more accurate descriptor as both positive and negative feedback loops exist [54, 55]. These difficulties in targeting Ras have earned it the moniker "undruggable" [56, 57] as nearly four decades of work into anti-Ras therapy have proven largely unsuccessful. Identification of factors that are essential to survival of oncogenic Ras tumors could prove to be valuable in the development of future anti-cancer therapies with targets more responsive to treatment than Ras.

Synthetic Lethality

The hunt for these alternative essential factors has already commenced [58-60]. Synthetic lethality is a phenomenon where deletion/mutation in either one of two genes is compatible with survival, however deletion/mutation of both genes results in death. The related concepts of oncogene addiction and induced essentiality are additional descriptors of this concept where in the presence of oncogenic signaling and/or a tumor microenvironment, expression of certain genes may now be essential to viability, i.e., the tumor is addicted to expression [61, 62]. In the case of oncogenic Ras associated cancers, the search is on for protein targets that when targeted in the presence of oncogenic Ras result in synthetic lethality [60]. The tumor-specific nature of synthetic lethality would theoretically result in decreased side effects as depletion of a target gene in non-cancerous wildtype cells would not affect viability. Many of these searches for oncogenic Ras synthetic lethal targets begin with large scale *in vitro* RNAi screens where several tumor and control cell lines are transfected with thousands of interfering RNAs [63, 64]. These approaches and others have only

exhibited moderate success as many of these synthetic lethal interactions are cell type specific or do not translate to *in vivo* model systems. Recently, we uncovered a synthetic lethal interaction between oncogenic Ha-Ras and the transcription factor C/EBPβ in the dorsal skin of mice using one of the most well studied and defined models of studying oncogenic Ras-driven tumorigenesis: the *in vivo* model of chemical carcinogenesis through dosing with the carcinogen 7,12-dimethylbenz[*a*]anthracene (DMBA) followed by tumor promotion with 12-*O*-Tetradecanoylphorbol-13-acetate (TPA) [65]. DMBA is a pro-carcinogen which is metabolized to a bay-region diol epoxide and forms bulky DNA adducts within the Ha-Ras gene, leading to mutation following replication of the region [66-68].

Skin

The largest organ in the human body is the outer covering; the skin. In addition to protecting the muscular, skeletal, and internal organ systems, skin acts as the front-line defense against exogenous damaging agents [69]. Skin is an extremely dynamic heterogeneous tissue which plays key roles in insulation/temperature regulation, vitamin D synthesis, sensation, and defense against infecting pathogens, as well as acting as a moisture/vapor barrier protecting the body from water loss. Skin can also heal itself through reepithelization wherein keratinocytes, fibroblasts, endothelial cells, and inflammatory cells interact in a complex network stimulating migration to the site of injury and proliferation to replace lost/damaged tissue [70, 71].

Skin is a stratified tissue and can be classified by its layers (Figure I2). The subcutis or hypodermis, predominantly made up of adipocytes and fibroblasts, is the deepest layer and

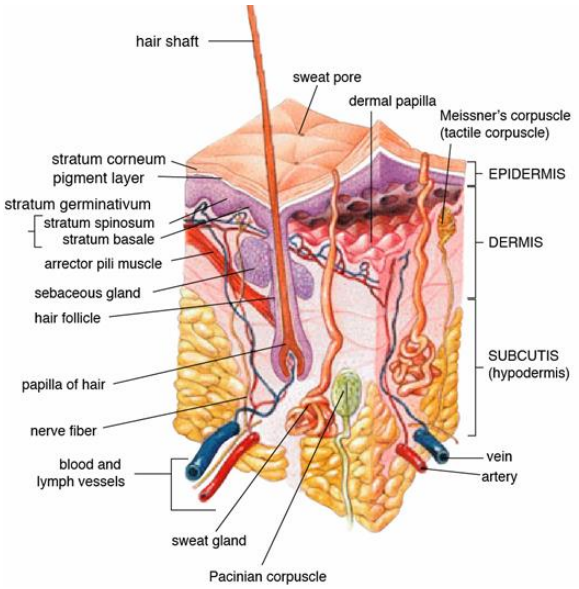

Figure I2: Model of Human Skin. Open source image from https: //seer.cancer.gov/

is important for attachment of the skin to the underlying tissues (bone/muscle) [69]. The dermis, the largest constituent of skin, sits above the hypodermis provides strength, elasticity, and structure to the skin. The dermis is predominantly made up of the extracellular matrix proteins such as collagen, which makes up 70% of the skin's dry weight [72]. Fibroblasts are the predominant cell type and produce the collagen which is constantly being turned over. The fibroblast/collagen network supports the nervous/sensory network, vasculature, hair follicles, and glands, such as the sebaceous gland [72]. The top layer is a squamous epithelium called the epidermis which is made up predominantly of keratinocytes divided into several stratified layers. The basal layer (stratum basale) contacts, and interacts with the fibroblasts of the dermis. Above the basal layer are the stratum spinosum, stratum granulosum and stratum corneum. The multiple layers of the epidermis form tight junctions which are lubricated by lipids excreted by sebaceous glands to form the water-tight barrier of

the skin. The keratinocytes of the epidermis are constantly being turned over through a highly organized system of differentiation associated with the expression of various keratins. Stem cells of the bulge (within hair follicle) will proliferate in response to wound healing and stem cells in the interfollicular regions (between hair follicles in basal layer) will infrequently proliferate to maintain homeostasis and form pockets of transiently amplifying cells in the basal layer which further proliferate to populate the basal layer [73, 74]. These newly created cells will become post-mitotic through differentiation and migrate up through the strata spinosum, granulosum, and corneum. In this way, the stem cell population is "protected" from mutation by infrequent mitosis and by post-mitotic keratinocytes that are free to be exposed to exogenous damaging agents including ultraviolet radiation, chemical exposures, mechanical wounding, or pathogens. The cells of the basal layer are attached to the basement membrane though integrin expression and retain their ability to proliferate through expression of the epidermal growth factor receptor (EGFR) which, as discussed above signals through the Ras-MAPK pathway [75-77]. Upon keratinocyte detachment from the basement membrane of the basal layer, a complex series of events drive the cell forward through the process of differentiation and upward through the layers of the epidermis.

Epidermal Differentiation

The stratified layers of the epidermis are characterized by a calcium gradient which increases as cells move up through the increasingly differentiated layers [78]. The layers of the epidermis express different keratins. The basal layer of the epidermis expresses Keratins 5 (K5) and 14 (K14) and express integrins and interact with fibronectin, laminin and type IV

collagen [79, 80]. As cells become post-mitotic through loss of integrins and EGFR, they increase in calcium concentration and express keratin 1 and 10 in the stratum spinosum. Although post-mitotic, the cells are still transcriptionally active and express the C/EBP transcription factor C/EBPβ (described in detail below) which plays a role in keratin 1 and 10 expression [81]. As the keratinocytes migrate into the stratum granulosum they increase in calcium concentration, accumulate keratohyalin granules, and produce transglutaminases. The transition to the stratum corneum is not a simple accumulation of "dead" skin cells, a common misconception, but rather an organized series of processes which includes the breaking down of organelles, de-nucleation, and cornification (or keratinization). The transglutaminases produced when the keratinocyte resided in the stratum granulosum are Ca^{2+} dependent enzymes which act to crosslink proteins during the transition to the stratum corneum and form the cornified envelope [82]. The cornified envelope is a covalently cross-linked structure that is made up of keratin bundles surrounded by crosslinked proteins and covalently linked lipids. Loricrin, involucrin, and other small proline-rich proteins (SPRs) make up the majority of the cross linked cornified envelope which acts as the initial protective and hydrophobic barrier, protecting the rest of the epidermis, skin, and ultimately the organism [83].

Epidermis and the Immune System

In addition to being a physical barrier between environmental factors and pathogens, the epidermis plays an active role in immunity and pathogen resistance. For example, keratinocytes [84] as well as sebocytes [85] can produce anti-microbial peptides that are

found in the stratum corneum. The keratinocytes of strata granulosum, spinosum, and basale also express pattern recognition receptors (PRRs) which recognize pathogen-associated molecular patterns and can initiate an immune response [86]. Also located amongst the keratinocytes of the epidermis are dendritic cells called Langerhans' cells which play a role in immune response [87] as well as resident $CD8^+$ T cells [88]. As part of their immune response keratinocytes produce a wide range of cytokines and chemokines [89] and can activate a type 1 interferon response [90].

CCAAT/Enhancer-Binding Proteins

CCAAT/Enhancer-Binding Proteins (C/EBP) are a conserved family of basic leucine zipper (b-zip) transcription factors along with Jun/Fos, CREB/ATF, PAR-domain proteins, and CHOP [91, 92]. First isolated by the McKnight group [93] the C/EBP family now comprises six members identified by Greek letters in the order of their discovery: **C/EBPα** (initially described by the McKnight group as RcC/EBP1), **C/EBPβ** (NF-IL6, IL-6DBP, LAP, CRP2, NF-M, AGP/EBP, ApC/EBP), **C/EBPγ** (Ig/EBP-1), **C/EBPδ** (NF-IL6b, CRP3, CELF, RcC/EBP2), **C/EBPε** (CRP-1) and **C/EBPζ** (CHOP-10, GADD153) [92, 94-100]. Each member contains a C-terminal bZIP domain which shares greater than 90% homology between isoforms. The conserved region allows for dimerization through the "leucine zipper" domain as well as binding to DNA consensus sequences (Figure I3). C/EBPs bind to a dyad consensus sequence of RTTGCGYAAY where R is a purine and Y is a pyrimidine; however, many exceptions to this consensus exist [101, 102]. Each isoform is intronless except for C/EBPε which has one intron [103] and C/EBPζ which has three [104]. The N terminus is

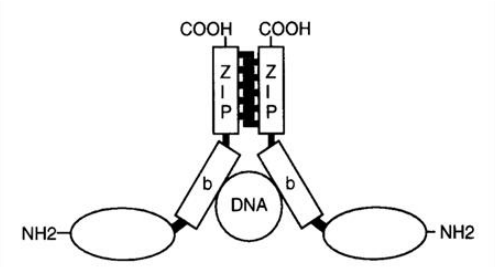

Figure I3: Model of C/EBP Dimerization. Taken from : Wedel, A. and Ziegler-Heitbrock, H.W., The C/EBP family of transcription factors. Immunobiology, 1995. **193**(2-4): p. 171-85

less conserved exhibiting > 20% homology of amino acid sequence between isoforms, allowing for a diverse range of activating signals and transcriptional activity. Adding to the diversity of the six family members, different translational start sites can lead to isoforms of varying lengths within a single-family member [105-107]. Additionally, C/EBPε has also been shown to undergo alternative splicing [108].

Transcriptional activity is stimulated through phosphorylation at various points in the un-conserved N-terminal region's transactivation domain which causes C/EBP isoforms to homo or hetero-dimerize, bind a consensus sequence, and aid in the induction of gene transcription. Interestingly, the isoform C/EBPγ can heterodimerize as it has the conserved C-terminal b-zip region however it has a severely truncated N-terminus which lacks any transactivation domain causing it to inhibit transcriptional activity when it dimerizes with other family members [109]. Three isoforms of C/EBPβ exist, and like C/EBPγ, one of them is truncated and acts as an inhibitor. LAP* (38kDa), LAP (35kDa), and LIP (20kDa) arise from three separate translational start codons in the C/EBPβ mRNA [106]. The shortest C/EBPβ isoform, LIP, is missing a large portion of the N-terminal domain and is able act as a

dominant negative inhibitor upon dimerization. In addition to homo- and heterodimerization within the C/EBP family, C/EBPs can also form protein-protein interactions with other bZIP and non-bZIP transcription factors which increases the diversity of cellular processes C/EBPs can act upon [110-112].

C/EBPs are expressed in a variety of tissues and are involved in many key cellular processes including differentiation, metabolism, inflammation, and proliferation [113]. For example, C/EBPβ is expressed in adipose tissue [99], liver [94-97], skin [114, 115], stomach [95], lung [96, 97], heart [95, 97], kidney [96, 97], spleen [95, 97], chondrocytes [116] and others. In adipocytes, C/EBPβ and C/EBPδ expression is greatly increased following induction of differentiation which can be sped up if additional C/EBPβ and C/EBPδ are supplemented [117]. Additionally preadipocytes lacking C/EBPβ or C/EBPδ are unable to differentiate [118]. Early C/EBPβ and C/EBPδ expression in the adipocytes is followed by the upregulation of C/EBPα before being downregulated following completion of differentiation [99]. Furthermore, both C/EBPα and C/EBPβ are expressed in the early liver bud of mice which distinguishes these cells from early pancreatic progenitor cells [119]. C/EBPα is especially important for liver function as it regulates several genes involved in gluconeogenesis, and deletion of C/EBPα in mouse liver is lethal [120]. C/EBPα and C/EBPβ are also expressed in the skin of both humans and mice [81, 115, 121, 122]. Expression in the epidermis follows patterns associated with stratified squamous differentiation and both C/EBPα and C/EBPβ are expressed in the sebaceous glands of the dermis [123-125]. In the epidermis, both C/EBPα and C/EBPβ are expressed predominantly in the suprabasal compartment of post-mitotic keratinocytes suggesting roles in keratinocyte differentiation

[115]. C/EBPα and C/EBPβ are co-localized in the epidermis and sebaceous glands and deletion of one or the other does not produce major skin phenotypes; however, simultaneous ablation of both leads to striking morphological defects including hyperplasia, dysplasia, and hyperkeratosis as well as molecular defects in squamous differentiation [81, 125, 126]. This finding suggests a compensatory mechanism may be at work where loss of one can be overcome through potential functional redundancies as supported by a study that found that replacing C/EBPα with C/EBPβ at the C/EBPα locus rescues the mice from the lethal phenotype [127].

C/EBPβ and Oncogenic Ras Driven Skin Tumorigenesis

As previously mentioned C/EBPβ plays important roles in cellular processes such as differentiation, inflammation, survival, and energy metabolism [113, 128, 129]. C/EBPβ is activated by numerous cytokines [130-132], as well as by oncogenic Ras [133, 134], RTKs [135], and Toll-like receptors [136, 137]. In some cell types, C/EBPβ has been implicated in the regulation of acute phase response cytokines including IL-6, IL-8, IL-1β, and TNF [113, 129, 130, 138-140], with several cytokines regulated cooperatively with NFkB [130, 141-143]. C/EBPβ levels are increased in numerous human cancers, and often associated with poor prognoses and invasive growth [144-153]. In numerous cancer cells, C/EBPβ has a pro-survival function as well [134, 150, 154-157]. C/EBPβ is known to be highly expressed in murine liver, lung, and adipose tissue; however, C/EBPβ mRNA level in the epidermis has been shown to have the highest expression levels. C/EBPβ protein is also highly expressed in various murine skin neoplasms, such as epidermal hyperplasia, squamous papilloma, and

squamous cell carcinoma driven by oncogenic Ras [115] which led the Smart group to investigate the role C/EBPβ plays in oncogenic Ras driven skin tumorigenesis. Murine skin tumors initiated with the chemical carcinogen DMBA and promoted with TPA have a reported 95-100% mutation rate in Ha-Ras causing a A to T transversion at the 182nd base, leading to a Q to L substitution at the 61st codon [158, 159]. The chemical carcinogen *N*-methyl-*N*'-nitro-*N*-nitrosoguanidine (MNNG) is a direct-acting carcinogen that induces papillomas with 85-90% contain an oncogenic mutation at the 12th codon of Ha-Ras or Ki-Ras [158, 160]. C/EBPβ nullizygous mice were completely refractory to DMBA and MNNG induced skin tumorigenesis [134]. The Tg.AC mouse model system has an oncogenic Ras transgene (v-Ha-Ras) under the control of a partial ζ-globin promoter which allows for skin tumor development following promotion (e.g., with TPA) without an initial carcinogen exposure [161]. When this mouse was crossed with C/EBPβ$^{-/-}$ mice the number of developed skin tumors was significantly decreased [134]. It was also demonstrated that: i) Ha-Ras can stimulate C/EBPβ transcriptional activity in both immortalized and primary mouse keratinocyte cell lines; ii) C/EBPβ can enhance Ha-Ras induced transformation of NIH-3T3 (mouse embryonic fibroblast) cells, and; iii) that activation of C/EBPβ downstream of Ras occurs through phosphorylation by ERK and cyclin dependent kinases, CDK1 and CDK2 [134, 162]. In addition to expressing high levels of C/EBPβ, mouse epidermis also expresses high levels of C/EBPα and C/EBPδ. DMBA tumorigenesis experiments where C/EBPα or C/EBPδ were conditionally deleted in mouse epidermis gave different phenotypes than the C/EBPβ$^{-/-}$ experiments. Ablation of C/EBPδ in the epidermis had no effect on DMBA/TPA tumor phenotype when compared to controls. C/EBPα deletion in the epidermis of mice had

the opposite effect of C/EBPβ deletion; C/EBPα skin knockout mice developed squamous papillomas sooner and developed more of them over time, suggesting that C/EBPα plays an inhibitory role downstream of oncogenic signaling whereas C/EBPβ plays an activating role in promoting survival and proliferation [126, 163].

These initial experiments were key in demonstrating that: i) C/EBPβ is expressed in the epidermis of mice; ii) C/EBPβ transcriptional activity is induced by oncogenic Ras signaling; and iii) C/EBPβ is required for the development of squamous papillomas driven by oncogenic Ha-Ras. When taken with other findings that C/EBPβ is key for the survival of macrophages transformed with Myc/Ras [157], CCl_4 treated hepatic stellate cells [154], and Wilms tumor cell lines [150], and that C/EBPβ is overexpressed in a variety of human and murine cancers [144-153], we can start to paint the picture that C/EBPβ may play an important role in the survival and progression of a variety of cancer cells. The first hint to the mechanism of this tumor survival is that DMBA-treated systemic and skin conditional C/EBPβ$^{-/-}$ mice displayed elevated levels of apoptosis [134, 163] which was later found to be associated with, and dependent upon, the tumor suppressor p53 [164].

The tumor suppressor p53

Referred to as the "Guardian of the Genome", p53 is the most frequently mutated gene in human cancer and plays its traditional role as a transcription factor but also has non-transcriptional activity [165-167]. Originally p53 was thought to be a tumor promoting oncogene [168]; however, it was not until nearly a decade later when the gene *Trp53* had been thoroughly characterized did the research community realize that this was the mutated

form and that the wildtype protein is in fact a tumor suppressor [169-171]. p53 activation and signaling has been extensively studied for over three decades and a complex network of interactions has been established. In normal cells (including those of the epidermis), p53 acts as a major signaling node in a cell's DNA damage response. p53 can be induced downstream of a variety of stresses including oncogenic signaling, DNA damage, nutrient starvation, viral infection, hypoxia, and changes in pH. The cellular responses to these stressors act to stabilize p53 and allow it to carry out its function. Cells are constantly producing p53 protein and in its unmodified state, p53 undergoes constitutive ubiquitylation by ubiquitin ligases such as Mdm2, and subsequent proteasomal degradation [172, 173]. This tightly regulated balancing act prevents over expression from killing the cell or under expression from putting the cell at risk of carcinogenesis. When the cell is exposed to an extrinsic or intrinsic stressor, p53 is post-translationally modified through phosphorylation, acetylation, methylation, glycosylation, ribosylation, sumoylation, and/or neddylation which prevents interaction with ubiquitin ligases (e.g., Mdm2) and thereby stabilizes p53 [174, 175]. Stabilized p53 tetramerizes and can potentially bind to thousands of promoter elements to directly up- or down-regulate gene transcription [176-178]. Downstream of cellular stressors, p53's diverse web of activators and effectors allow for the induction of cell cycle arrest and DNA repair, senescence, or apoptosis. Oncogenic signaling, including from Ras, can act to stabilize p53 through the upregulation of the tumor suppressor gene *p19Arf* which directly inhibits Mdm2 [179]. Mice lacking C/EBPβ have increased levels of p19Arf protein; however, the resistance to oncogenic Ras driven skin tumorigenesis in C/EBPβ$^{-/-}$ mice was determined to be independent of p19Arf [155]. Following DNA damage from sources including ionizing or

UV radiation, p53 can stimulate transcription of the CDKN1A gene coding for the cyclin dependent kinase inhibitor p21 which in turn activates the G_1/S cell cycle checkpoint leading to cell cycle arrest [180]; alternatively, if the damage occurred after S-phase, p53 could activate GADD45 (growth arrest and DNA damage) which would induce cell-cycle arrest at the G_2/M checkpoint instead [181]. p53's regulation of senescence was first observed after mutant p53 helped stimulate post-mitotic senescent cells to initiate mitosis. Senescence is an event in somatic cells normally initiated by telomere shortening. This replicative (telomere dependent) senescence is dependent on p53 and is believed to protect cells from tumorigenesis by entering a quiescent state before the eventual degradation of telomeres [182]. Cells can also undergo telomere-independent senescence through oncogenic Ras signaling [183], constitutive MAPK signaling [184], or via the E2F1 transcription factor [185]. If the damage to a cell's DNA is too great to repair through cell cycle arrest and/or senescence is not an option, p53 can induce apoptosis.

Apoptosis and p53

Apoptosis is a form of programmed cell death that is required for normal tissue homeostasis. Apoptosis can play a negative role in disease, especially neurodegenerative diseases such as Alzheimer's disease, Parkinson's disease, ALS, and Huntington's disease where increased apoptosis leads to disease phenotypes [186]. In cancer, the opposite is typically the case as progression can only take place if the early neoplasms are able to adapt and avoid apoptotic signaling. Several morphological changes associated with apoptosis can be used to identify an apoptotic cell from a normal living cell or a cell undergoing a necrotic

cell death. Condensation of nucleic acids and shrinking of the cell membrane leads to pyknosis (small dense nuclei), detachment from the surrounding tissue, and a condensed cytoplasm [187]. Hematoxylin and eosin (H&E) staining is a common histological staining procedure that can be used to visualize apoptotic cells in certain tissues. Apoptosis in epidermis is characterized by the presence of small dark pyknotic nuclei, areas of "white space" surrounding the cell indicating detachment from the surrounding tissue, and an eosinophilic (pink) hue of the condensed cytoplasm [134]. Apoptosis is a tightly controlled event which is very "clean" compared to necrosis in that the membrane remains intact which prevents intracellular components from leaking out and causing an inflammatory response. Blebbing of the plasma membrane and karyorrhexis occur next followed by budding of the cell into small apoptotic bodies which are then phagocytosed by macrophages and surrounding cells [188]. As stated previously, p53 is a potent inducer of apoptosis downstream of DNA damage and plays a regulatory role in both the intrinsic and extrinsic apoptotic pathways.

The intrinsic apoptotic pathway can be regulated by p53 downstream of DNA damage, ROS, oncogenic signaling, and stress, and its avoidance is one of the hallmarks of cancer. After stabilization downstream of various stressors, p53 can transcriptionally upregulate pro-apoptotic and downregulate pro-survival genes. For example, Xaf1 [189, 190], Bax [191], Puma [192], Noxa [193], and Bid [194] are examples of pro-apoptotic genes regulated by p53. Once translated, Xaf 1 acts to inhibit x-linked inhibitor of apoptosis (XIAP) as well as feedback to p53 through PTMs, Noxa and Puma act to inhibit the anti-apoptotic factor Bcl-2, and Bax and Bid act to release cytochrome c and other pro-apoptotic

proteins from the mitochondria. Cytochrome c then binds cytosolic Apaf-1 to form the "apoptosome" which acts to cleave caspase-9, ultimately leading to caspase-3 cleavage. The protease activity of the cleaved caspases are the driving forces behind the cell death [195, 196].

Unlike the intrinsic apoptotic pathway that is initiated from internal damage/stress and is mediated through the mitochondria, extrinsic apoptosis is stimulated through transmembrane receptors. Death receptors are part of the tumor necrosis factor receptor (TNFR) superfamily and include a wide variety of related receptors. Locksley et al. [197] compiled a list of receptors and their alternative names. Some examples include the generic TNFR, TNF-related apoptosis-inducing ligand (TRAIL) receptors (also known as death receptors (DR)) [198], and Fas receptors [199]. Generally, once the ligand binds to the extracellular receptor, cytoplasmic adapter proteins such as FADD, TRADD, and RIP are recruited to form the death-inducing signaling complex (DISC), activating caspase-8 cleavage [200]. Regulation of extrinsic apoptosis can occur by inhibiting the DISC/Caspase-8 interaction through C-Flip (C-Flar) [201] or by decreasing the number of cell surface receptors [200]. Like the intrinsic pathway, cleaved caspase 8 then induces cleavage of caspase-3 and like the intrinsic pathway p53 can play a role in the regulation of extrinsic apoptosis through transcriptional regulation of both the Fas receptor [202, 203] and Fas ligand [204] as well death receptor 5 (DR5) [205].

Apoptosis, p53, and Interferon

In addition to the canonical activities of p53 downstream of DNA damage (cell cycle arrest, senescence, and apoptosis), p53 is also active in the innate immune response and the type 1 interferon response through regulation of interferon-stimulated genes (ISGs) such as *Irf9, Stat1, Stat2, Tnf, Tnfsf10, Isg15,* and *Pml* [189, 206-208]. Irf9, Stat1, and Stat2 form the interferon-stimulated gene factor 3 (ISGF3) signaling complex that functions to induce numerous ISGs as well as activate p53 [209]. The "ISGs activating p53 to induce the expression of ISGs" creates a feedforward loop at the intersection of the extrinsic apoptotic and interferon pathways [208]. The type 1 interferon response is traditionally considered to be downstream of pathogenic infection as part of the innate immune system; however, the role of ISGs is continuing to expand and it has been shown that DNA damage including double stranded breaks can induce expression of interferons such as IFNβ [210]. IFNβ is a type 1 interferon which has pro-apoptotic activity [211, 212] and stimulates the induction of ISGF3. Recently our lab has uncovered a synthetic lethal relationship in oncogenic Ha-Ras driven skin tumors following the deletion of the transcription factor C/EBPβ. The synthetic lethality was associated with enrichment of a type I interferon response with many p53 regulated ISGs being upregulated instead of the classical p53 apoptotic mediators.

RESEARCH RATIONALE AND HYPOTHESIS

Around 30% of all human cancer contains an oncogenic Ras mutation which can act as a tumorigenic driving force to push cells through the cell cycle. During tumorigenesis, cells must respond to, and overcome cellular stresses arising from a variety of sources such as DNA damage, oncogenic signaling, and ROS as they engage pro-survival and anti-death signaling pathways. Regulation of key genes and pathways to overcome these oncogenic stressors may be potential sites of therapeutic importance as their disruption in a tumor cell may tip balance from survival to death.

Previous findings in our lab have identified the b-zip transcription factor C/EBPβ as being required for oncogenic Ras driven skin tumorigenesis. Mice lacking C/EBPβ both systemically or conditionally in the epidermis are refractory to tumorigenesis induced by oncogenic Ras activating chemical carcinogens [134, 163]. Our lab has also shown that mice lacking C/EBPβ in the epidermis have an enhanced p53 dependent apoptotic response downstream of DNA damage [155, 164]. Based on these results we hypothesized that C/EBPβ is required for oncogenic Ras skin tumor survival and that deletion of C/EBPβ in a pre-existing tumor would result in tumor regression.

CHAPTER ONE

C/EBPβ Deletion in Oncogenic Ras Skin Tumors Induces Synthetic Lethality via Type-1 Interferon Responses and p53

Zachary J Messenger1, Jonathan R Hall1,2,3, Dereje Jima3,4, John S. House3,4 Debra A Tokarz3,5, Robert C Smart1,2,3

1Toxicology Program, 2Department of Biological Sciences, 3Center of Human Health and the Environment, 4Bioinformatics Research Center, 5Department of Population Health and Pathobiology, North Carolina State University, Raleigh, NC, USA

Funding: NCI Grant# CA046637, NIEHS Grant# ES024471, ES007046, P30ES025128

CORRESPONDING AUTHOR:

Robert C Smart

NCSU Campus Box 7633

Raleigh, NC 27695

rcsmart@ncsu.edu

MANUSCRIPT ABSTRACT

Therapeutic targeting of specific genetic changes in cancer has proven to be an effective therapy. Based on previous findings that C/EBPβ$^{-/-}$ mice are refractory to skin tumor development involving oncogenic H-Ras, we hypothesized C/EBPβ is essential for survival of oncogenic Ras^{Q61L} skin tumors and its deletion would promote tumor regression. C/EBPβ deletion in H-Ras^{Q61L} mouse skin tumors resulted in tumor regression. Regressing tumors exhibiting elevated levels of apoptosis and p53 while adjacent C/EBPβ-depleted skin did not suggesting C/EBPβ is essential for survival of Ras^{Q61L} tumor cells but not normal keratinocytes. Co-deletion of C/EBPβ and p53 in Ras^{Q61L} tumors showed p53 is required for tumor regression and elevated apoptosis. Regressing tumors showed significant activation of death signaling networks involving a type I interferon response and p53. In summary, oncogenic Ras skin tumors are dependent on C/EBPβ for survival, and deletion of C/EBPβ in these tumors is a synthetic lethal event dependent upon p53.

INTRODUCTION

Ras proteins are small GTPase membrane bound signal transducers, and the coding genes are the most frequently mutated dominant oncogenic drivers in human cancer [1-3]. At least one of the three family members (Ha, N or Ki-RAS) is mutated in 20-30% of all human cancers, with some cancers exhibiting high percentages of Ras mutation; for example, >90% of pancreatic cancers contain mutated Ki-RAS [1]. Once mutated, oncogenic Ras signaling promotes proliferation through activation of the RAF-MAPK, PI3K and RAL-GDS pathways [4-9]. These pathways also downregulate pro-apoptotic genes, leading to conditions which favor expansion while evading cell death [10]. Despite this significance of Ras in a variety of cancer types, three decades of work into drug therapy led to suggestions that Ras was "undruggable", although improved structural data has recently provided new approaches [1, 11]. Identification of factors that are essential to survival of oncogenic Ras tumors would be valuable in the development of future anti-cancer therapies with targets more responsive to treatment than Ras[12].

CCAAT/enhancer binding protein-β (C/EBPβ), a basic leucine zipper transcription factor, plays important roles in cellular processes including differentiation, inflammation, survival and energy metabolism [13-15]. C/EBPβ is also known as NF-IL-6 (nuclear factor for IL-6) [13, 16] and is activated by numerous cytokines [16-18], as well as by oncogenic Ras [19, 20], RTKs [21], and Toll-like receptors [22, 23]. In some cell types, C/EBPβ has been implicated in the regulation of acute phase response cytokines including IL-6, IL-8, IL-1β, and TNF [13, 14, 16, 24-26], with several cytokines regulated cooperatively with NFkB [16, 27-29].

C/EBPβ levels are increased in numerous human cancers, and often associated with poor prognoses and invasive growth [30-39]. In numerous cell types C/EBPβ has a pro-survival function [20, 36, 40-43]. In order for tumor cells to acquire the hallmark traits of cancer, tumor cells must respond to and overcome the cellular stresses associated with tumorigenesis. These stresses are often referred to as the stress phenotypes of tumorigenesis/cancer and include DNA damage and DNA replicative stress, mitotic stress, metabolic stress, proteotoxic stress and oxidative stress [44, 45]. Loss of a pathway(s) that confers adaptability to a stress phenotypes of tumorigenesis could result in selective tumor cell killing [45]. These ideas form the conceptual framework of synthetic lethality, where targeting a specific pathway results in death of tumor cells with a specific oncogenic mutation, while normal cells without the oncogenic mutation survive[12, 46-48].

C/EBPβ contributes to cell survival in response to DNA damage [41, 49], toxicants [40] or oncogenic stress [43], and knockdown of C/EBPβ results in cell death in some cancer cell types [36, 42]. Mice lacking C/EBPβ in their epidermis are highly resistant to the development of skin tumors induced by oncogenic Ras, as well as by chemical carcinogens that produce mutations in Ras [20]. While mechanisms responsible for this resistance to skin tumor development are unknown, it may involve increased apoptosis resulting from loss of C/EBPβ [20]. Based on the key finding that C/EBPβ$^{-/-}$mice are refractory to skin tumor development involving oncogenic Ras, we hypothesized C/EBPβ is essential for oncogenic Ras skin tumors and its deletion would promote tumor regression and apoptosis. Our results demonstrate that deletion of C/EBPβ in oncogenic Ras-driven skin tumors is a synthetic lethal event promoting p53-dependent apoptosis and tumor regression. The synthetic lethality

was associated with enrichment of a type I Interferon response with many p53 regulated interferon stimulated genes being upregulated which can in turn upregulate p53 through feedback loops. This coupled with alterations in TNF and death receptor signaling suggest that deletion of C/EBPβ□primes tumor cells for p53 mediated cell death and make the targeting of C/EBPβ an interesting and promising target for future potential anti-cancer therapies.

MATERIALS AND METHODS

Animal care, treatment/doses, tumor measuring

All animal husbandry, care, and experimentation was conducted per NIH guidelines and approved by the NCSU Institutional IACUC committee. K14-CreER^{tam} mice [50] were crossed with *C/ebpβ$^{flox/flox}$* mice [51], and *p53$^{flox/flox}$* mice (from NCI Mouse Repository FVB.129-Trp53^{tm1Brn}(p53$^{flox/flox}$)[52] to obtain the following genotypes which have been maintained on a 50:50 C57BL/6J:SV129 background. *K14-CreER^{tam}* (Cre), *K14-CreER^{tam};C/ebpβ$^{flox/flox}$* (IKOβ), *K14-CreER^{tam};p53$^{flox/flox}$* (IKOp53) and *K14-CreER^{tam};C/ebpβ$^{flox/flox}$;p53$^{flox/flox}$* (DIKO). To induce tumors, mice aged 8-12 weeks were dorsally shaved while in telogen hair growth phase and given a single topical dose of 200nmol 7,12-Dimethylbenz[a]anthracene (DMBA) (Sigma, D3254, St. Louis MO, USA) in acetone followed one week later by thrice weekly dosing of 5nmol 12-O-Tetradecanoylphorbol-13-acetate (TPA) (Cayman Chemical, 10008014, Ann Arbor, MI) in acetone for the entirety of tumor studies. Activation of the K14-CreER^{tam} was accomplished via dosing 2.5mg (6.73μmol) of Tamoxifen (Sigma, T5648, St. Louis MO, USA) dissolved in corn oil with 5% ethanol intraperitoneal (*ip*) injected daily, 5 days/week for two weeks. Tumor numbers were tabulated weekly with tumor volume being calculated by measuring height, width, and length of tumors. *In vivo* 5-Bromo-2'deoxyuridine (BrdU) labeling was carried out as previously described [41] by *ip* injecting BrdU (Sigma, B5002, St. Louis MO, USA) suspended in phosphate buffered saline (PBS, pH 7.4) 1 hour before sacrifice at a dose of 100mg BrdU per kg body mass.

DNA Sequencing

Whole tumor DNA was collected and Sanger sequencing was performed by the North Carolina State University Genomic Sciences Laboratory (Raleigh, NC, USA). The 61st codon of Ha-Ras was amplified using forward primer ACTCCTACCGGAAACAGGT and reverse primer: GAGGACATCCATCAGTACAG and sequenced using the reverse primer. Exons 3-9 of p53 were amplified and sequenced using the following primer sets previously described. [53] Exon 3-4 Fw: CCTGGGATAAGTGAGATTCTGTC, Exon 3-4 Rev: GCACAGTCTACAGGCTGAAGAG Exon 5-6 Fw: CCTTGACACCTGATCGTTACTCG, Exon 5-6 Rev: AGAAAGTCAACATCAGTCTAGGC, Exon 7 Fw: TGTGCCGAACAGGTGGAATATCC, Exon 7 Rev: ACTCGTGGAACAGAAACAGGCAG Exon 8-9 Fw: GGCCTAGTTTACACACAGTCAGG, Exon 8-9 Rev: CACGGCTAGAGATAAAGCCACTG.

Preparation of epidermal lysates for SDS-PAGE

In brief, as previously described in Thompson et al. [54] mice were euthanized by cervical dislocation and shaved dorsal skin was removed and submerged in 60°C dH_2O for 6 s followed by 10 s in ice water. Following the heat shock, the epidermis was scraped off and placed in RIPA buffer (1% NP-40, 0.5% sodium deoxycholate, 0.1% sodium dodecyl sulfate, 1 mM dithiothreitol, 1 mM sodium orthovanadate, 1 mM AEBSF, and 1 x protease inhibitor cocktail (Roche, Indianapolis, IN, USA) in PBS. Collected samples were sonicated on ice and centrifuged at 14000 x g for 10 min. Equal amounts of protein were resolved via SDS-

PAGE transferred to PVDF membrane, and probed using the following antibodies: C/EBPβ (Santa Cruz, sc-150, 1:5000), α-Tubulin (Santa Cruz, sc-8035, 1:8000), p53 (Cell Signaling, 2524, 1:5000)

H&E staining, detection of apoptosis and inflammatory cell infiltration

Shaved mouse dorsal skin was fixed in 10% Neutral Buffered Formalin for 24 h, changed to 70% ethanol and embedded in paraffin, or tissues were fixed in PAXgene tissue fixative (PreAnalytiX, 765312, Hombrechtikon, Switzerland) for 24 h, changed to PAXgene stabilizer (PreAnalytiX, 765512, Hombrechtikon, Switzerland) and hand embedded in paraffin. Tissue sections (5 μM) were stained with hematoxylin and eosin. Apoptotic cells were scored as positive if they met all three criteria: 1. Dark pyknotic nuclei, 2- cytoplasmic eosinophilia, 3- detachment from adjacent cells. [20] Apoptotic positive cells were expressed as positive cells per mm^2 area of parenchyma as measured using ImageJ software. [55] Apoptosis in the normal epidermis adjacent to tumors was scored in the interfollicular epidermis as previously described [20] and expressed as positive cells per cm skin. Inflammation was scored separately for intratumoral and extratumoral skin using a scoring system adapted from a method previously described [56] on a scale of 0-3 where 0: none present, 1: few present, 2: moderate occurrence, 3: abundant occurrence. Intratumoral included the epidermal components of the papillomas with the subjacent dermis and subcutis. All slides were scored by D.Tokarz, who was blinded as to treatment group, with the exception of slides labeled as controls. Slides were scored in a random order.

Immunohistochemical staining

Total RNA was extracted from whole tumors collected from Cre and IKOβ mice following cessation of Tamoxifen treatment as described above (week 21 of TPA) and were Shaved mouse dorsal skin was fixed in 10% Neutral Buffered Formalin for 24 h, changed to 70% ethanol and embedded in paraffin, or tissues were fixed in PAXgene tissue fixative (PreAnalytiX, 765312, Hombrechtikon, Switzerland) for 24 h, changed to PAXgene stabilizer (PreAnalytiX, 765512, Hombrechtikon, Switzerland) and hand embedded in paraffin. Tissue sections (5 μm) were deparaffinized, peroxidases were inactivated with 3% H_2O_2 and subjected to antigen retrieval using a 2100 retriever (Aptum, Southampton, UK) with citrate buffer (pH 6). Next, sections were treated with 3% H_2O_2 once more before being blocked with normal goat serum (or normal horse serum) before incubation overnight at 4°C with the following antibodies: C/EBPβ (Santa Cruz, sc-150, 1:4000), p53 (Cell Signaling, 2524, 1:1000), Keratin 5 (Covance, PRB-160P, 1:2000), Keratin 10 (Covance, PRB159P, 1:2000), Ki67 (Bethyl Labs, IHC-00375, 1:500), γH2AX (Bethyl Labs, A300-081A, 1:2000), or cleaved caspase 8 (Novus Biologicals, 56116, 1:2000). Staining was visualized using species appropriate secondary antibodies from Vectastain Elite ABC kits (Vector Labs, mouse:PK-6102 rabbit:PK-6101, Burlingame CA, USA) and DAB Peroxidase Substrate Kit (Vector Labs, SK-4100, Burlingame CA, USA) Sections were counterstained with hematoxylin and quantitation was calculated as positive cells per mm^2 area of parenchyma as measured using ImageJ software. [55] Positively stained cells in the normal epidermis adjacent to tumors was scored in the interfollicular epidermis and expressed as positive cells per cm skin. Immunohistochemical staining for BrdU was carried out as previously described

[41] by deparaffinizing 5 μm sections and incubating in the following, 2 M HCl for 30 min at 37°C, boric acid-borate buffer for 3 min at room temperature, 0.05M Tris-HCl (pH 7.8 in 0.1% $CaCl_2$) with 0.01% trypsin for 3 min at 37°C, and 3% H_2O_2 for 10 min at room temperature. Sections were blocked in normal horse serum for 30 min and then incubated for 1 hour at room temperature with anti-BrdU IgG primary antibody (BD Biosciences, 69138, 1:100). Staining was visualized and quantified as described above. Immunohistochemical staining for mouse CD4, mouse CD8a and mouse F4/80 was performed by the Animal Histopathology and Lab Medicine Core located at the University of North Carolina School of Medicine (Chapel Hill, NC). Immunohistochemical analysis for Mouse CD4 (14-9766, eBioscience) was performed on paraffin slide specimens. Antigen retrieval was performed using Ventana's CC1 (pH 8.5), for 72 minutes @ 100 degrees Celsius, followed by the primary antibody diluent (1:25) for 4 hours at room temperature using Discovery PSS Diluent, 760-212. The slides were then given a post primary peroxidase incubation for 8 mins, followed by the secondary antibody (Ventana Omap OmniMap anti Rat HRP, 760-4457, Ready to Use) for 32 minutes at room temperature. The slides were then treated with DAB, counterstained with Hematoxylin II for 12 minutes, and then Bluing Reagent for 4 minutes. The slide staining was performed using Ventana's Discovery Ultra Automated IHC staining system. Immunohistochemical analysis for anti-Mouse CD8a (14-0808, eBioscience) was performed on paraffin slide specimens. Antigen retrieval was performed using Ventana's CC1 (pH 8.5), for 64 minutes @ 100 degrees Celsius and given a peroxidase step for 8 minutes, followed by the primary antibody diluent (1:100) for 2 hours at room temperature using Discovery PSS Diluent, 760-212, and then the secondary antibody (Ventana Omap

OmniMap anti Rat HRP, 760-4457, Ready to Use) for 32 minutes at room temperature. The slides were incubated in Discovery Purple, 760-229 for 32 minutes. The slides were then treated with DAB, counterstained with Hematoxylin II for 12 minutes, and then Bluing Reagent for 4 minutes. The slide staining was performed using Ventana's Discovery Ultra Automated IHC staining system. Immunohistochemical analysis for Rat Anti-Mouse F4/80 Antibody: CI:A3-1 (AbD Serotec, Cat # MCA497RT) was performed on paraffin slide specimens. Antigen retrieval was performed with Protease 2 (760-2019) for 12 minutes at 37 degrees Celsius and given a protein block for 1 hour. Next, the slides were incubated in the primary antibody diluent (1:25) for 1 hours at 37 degrees Celsius using AB Discovery Diluent (760-108), followed by the secondary antibody (Ventana Omap OmniMap anti Rat HRP, 760-4457, Ready to Use) for 32 minutes at room temperature, and a post peroxidase step for 12 minutes. The slides were incubated in Discovery Purple, 760-229 for 32 minutes. The slides were then treated with DAB, counterstained with Hematoxylin II for 12 minutes, and then Bluing Reagent for 4 minutes. The slide staining was performed using Ventana's Discovery Ultra Automated IHC staining system.

RNA isolation and next generation sequencing

Total RNA was extracted from whole tumors collected from Cre and IKOβ mice following cessation of Tamoxifen treatment as described above (week 21 of TPA) and were homogenized in Qiazol (Qiagen, 79306, Hilden, Germany). RNA extraction was carried out using the Quick-RNA MiniPrep Kit (Zymo Research, 11-328, Irvine, CA). Total RNA samples were submitted to the North Carolina State University Genomic Sciences Laboratory

(Raleigh, NC, USA) for Illumina RNA library construction and sequencing. Sample integrity and concentration were evaluated using an RNA 6000 Nano Chip on the Agilent Bioanalyzer 2100 (Agilent, CA, USA), Purification of messenger RNA (mRNA) was performed using the oligo-dT beads provided in the NEBNext Poly(A) mRNA Magnetic Isolation Module (New England Biolabs, USA). NEBNext Ultra Directional RNA Library Prep Kit (NEB, MA, USA) and NEBNext Multiplex Oligos for Illumina (NEB, MA, USA) were used to make the cDNA libraries for Illumina sequencing using the manufacturer-specified protocol which involved chemically fragmenting the mRNA and priming it with random oligos for first strand cDNA synthesis. Second strand cDNA synthesis was then carried out with dUTPs to preserve strand orientation information. The cDNA was purified, end repaired, and "a-tailed" for adaptor ligation. Next the samples were selected for a final library size of 400-550 bp using sequential AMPure XP bead isolation (Beckman Coulter, USA). Library enrichment was performed and specific indexes for each sample were added during the protocol-specified PCR amplification. The amplified library fragments were purified and checked for quality and final concentration using an Agilent 2200 Tapestation (Agilent, CA, USA). The final quantified libraries were sequenced using Illumina's NextSeq 500 DNA sequencer, utilizing a 75 bp paired end kit (Illumina, CA, USA) which gave around 200 million reads for the eight samples (4 samples/group) which works out to ~25 million reads/sample. The software package Real Time Analysis (RTA), was used to generate raw bcl, or base call files, which were then de-multiplexed by sample into fastq files for data submission.

RNA-Seq data analysis was conducted in consultation with the Bioinformatics Core of the NCSU Center of Human Health and Environment. The quality of raw sequence data was

assessed using FastQC and the first 12 poor-quality bases were trimmed based on the quality matrix from the FastQC application. The remaining good quality reads were aligned to the mouse reference genome (mm38 version 87) using STAR[57] aligner. For each replicate sample, per-gene counts of uniquely mapped reads were calculated using htseq-count script from the HTSeq python package. The count matrix was imported and normalized for sequence depth and distortion, and dispersion was estimated using DESeq2[58] Bioconductor package in the R statistical computing environment. We fit a leaner model using treatment levels (Cre and IKOβ) and differentially expressed genes were identified after applying multiple testing correction using the Benjamini-Hockeberg procedure [59] (padj<0.05).

Gene Set Enrichment analysis

We used Gene Set Enrichment analysis (GSEA) to understand the biology underlying the differential gene expression profile using GSEA software[60]. Briefly, the genes from differential expression were ranked based *on signed fold change * –log10 p-value.* The rank file contains gens with the strongest up-regulation(top), strongest down-regulation(bottom), and not changing are in the middle. The analysis was preformed using *GseaPreranked* application in the GSEA software suing mouse C2 MSigDB gene set and default settings. Finally, the enriched pathways (padj<0.05) were plotted using Enrichment Map Visualization in the same software package and plotted the bar plot for the top 20 enriched pathways.

For visualization of specific pathways, normalized counts from DESeq2 [58] were row scaled (by gene), grouped by average linkage, and heatmaps generated. Data for each ontology along with adjusted p-values are provided in Supplemental Tables 2-5. Ontologies

were retrieved and combined in the following fashion from the curated C2.GSEA MSigDB database: Interferon – ("INTERFERON-GAMMA SIGNALING PATHWAY%PANTHER PATHWAY%P00035" plus "INTERFERON GAMMA SIGNALING%REACTOME%R-HSA-877300.1" plus "INTERFERON SIGNALING%REACTOME%R-HSA-913531.1" plus "INTERFERON ALPHA BETA SIGNALING%REACTOME%R-HSA-909733.1" plus 10 additional OAS genes), p53 – (“HALLMARK_P53_PATHWAY%MSIGDB_C2%HALLMARK_P53_PATHWAY“), TNF – (“HALLMARK_TNFA_SIGNALING_VIA_NFKB%MSIGDB_C2%HALLMARK_TNFA_SIGNALING_VIA_NFKB“), and Death Receptor – ("BIOCARTA_DEATH_PATHWAY%MSIGDB_C2%BIOCARTA_DEATH_PATHWAY" plus "DEATH RECEPTOR SIGNALLING%REACTOME DATABASE ID RELEASE 59%73887").

RESULTS

Spatial and temporal regulation of C/EBPβ in epidermis and in pre-existing oncogenic Ras skin tumors

As shown in Figure 1A, C/EBPβ is abundantly expressed throughout the epithelial portion (parenchyma) of oncogenic Ras containing mouse skin tumors arising from the DMBA/TPA protocol. Based on the robust C/EBPβ levels in skin tumors, along with previous findings that mice lacking C/EBPβ in their epidermis are highly resistant to development of skin tumors induced by chemical carcinogens (DMBA) that produce mutations in Ha-Ras^{Q61L} [20], we hypothesized C/EBPβ is essential for the survival of oncogenic Ha-Ras skin tumors and its deletion would promote tumor regression.

To test this hypothesis, we developed a mouse model, *K14CreER^{tam};C/ebpβ$^{flox/flox}$* (IKOβ), in which C/EBPβ could be conditionally deleted in epidermis, and presumably also in pre-existing oncogenic Ha-Ras skin tumors. In this model, the keratin 14 (K14) promoter directs expression of a CreER^{tam} recombinase fusion protein to the basal keratinocytes of the epidermis/tumor. Tamoxifen treatment activates Cre recombinase which then removes the floxed *C/ebpβ* alleles [15, 50] (Fig 1B). As shown in Figure 1C/D, dosing IKOβ mice with tamoxifen *ip* (1x/day for 5 days/week for 2 weeks) resulted in loss of C/EBPβ protein in the epidermis while dermal C/EBPβ protein levels were unaffected.

To test whether C/EBPβ could be deleted in pre-existing skin tumors in this mouse IKOβ model, we generated skin tumors in IKOβ mice using a DMBA/TPA tumorigenesis treatment protocol. Tumor bearing mice were then treated with tamoxifen *ip* or vehicle *ip* (1x/d for 5 days/week for 2 weeks) and tumors were harvested 2 weeks after the start of

tamoxifen treatment. As shown in Figure 1E, tamoxifen treatment resulted in the loss of C/EBPβ protein in the parenchyma portion of the tumor, but not in the stroma. We conducted DNA sequencing of DMBA/TPA tumors from *K14CreER^{tam}* (Cre) to verify mutations in Ha-Ras and found that 26/26 tumors contained the expected A->T mutation in the 61st codon of Ha-Ras (Q61L) (Fig 1F) [61]. These results demonstrate that the DMBA/TPA treated IKOβ mouse is a tractable model to test the hypothesis that deletion of C/EBPβ in oncogenic Ras skin tumors will result in tumor regression.

Oncogenic Ras skin tumors depend on C/EBPβ for survival

Cre and IKOβ mice were initiated with a single topical application of DMBA and promoted thrice weekly with topical treatments of TPA for the duration of the tumor experiment (30 weeks). By week 19 of TPA treatment 100% of mice from both genotypes had tumors with an average of ~5 tumors/mouse. Starting at week 19, mice were treated with tamoxifen *ip* (1x/day for 5days/week for 2 weeks) while continuing thrice/weekly TPA promotion. As shown in Figure 2A, tamoxifen-treated Cre mice continued to develop additional tumors while skin tumors of tamoxifen-treated IKOβ mice began to rapidly regress. Approximately 50% of tumors completely regressed by two weeks after the start of tamoxifen treatment. At 10 weeks after the start of tamoxifen treatment, ~80% of the IKOβ tumors had completely regressed (Fig 2A) and the percentage of mice with tumors decreased from 100% to ~25% (Fig 2B). Tumor volume was also monitored following tamoxifen treatment (Fig 2C). Using tumor volume at 19 weeks as a standard, after 10 weeks of

tamoxifen treatment, tumor volume in Cre mice tripled, and decreased by 98% in IKOβ mice. A representative IKOβ mouse before and after tamoxifen treatment is shown in Figure 2D.

To determine if more progressed skin tumors also regress upon the C/EBPβ deletion, we conducted another tumor study using mice initiated with DMBA and then promoted with TPA for 40 weeks. At 34 weeks of TPA treatment (compared to 19 weeks in the previous tumor experiment) mice were treated with tamoxifen *ip* (1x/day for 5 days/week for 2 weeks). Similar to the previous tumor experiment, Cre mice continued to develop additional tumors, while skin tumors of tamoxifen-treated IKOβ mice regressed rapidly. Six weeks after initiation of tamoxifen treatment, ~80% of IKOβ mouse tumors completely regressed (Fig 2E), and the percentage of mice with tumors decreased to 50% (Fig 2F). This tumor experiment was terminated at 40 weeks, as some tumor bearing mice developed a cachexia-like phenotype. In summary, these results demonstrate that deletion of C/EBPβ in oncogenic Ras tumors results in rapid tumor regression indicating that C/EBPβ is required for the survival of Ras skin tumors.

Regressing tumors display elevated levels of apoptosis and p53 protein while adjacent C/EBPβ-depleted skin does not

To gain insight into the mechanism of tumor regression, we analyzed for a variety of endpoints including apoptosis, p53 protein levels, DNA damage, proliferation, senescence, inflammation, and differentiation in PAX gene-fixed paraffin-embedded (PFPE) sections from regressing (tamoxifen dosed, C/EBPβ deleted) and non-regressing (vehicle dosed) tumors. IKOβ mice were initiated with DMBA, promoted with TPA, and at 19 weeks of TPA

treatment, mice were dosed with either tamoxifen or a vehicle control (corn oil) *ip* (1x/day for 5 days/week for 2 weeks). Tumors, along with adjacent skin, were collected 2 weeks after the first treatment with tamoxifen or vehicle, and PFPE sections were prepared. The deletion of C/EBPβ in regressing tumors and adjacent skin was confirmed by lack of IHC staining for C/EBPβ protein Fig 3A. Based on the characteristic morphology of apoptotic cells in H&E stained sections, we observed a ~7-fold increase in apoptotic cells in in the parenchyma of regressing tumors (C/EBPβ deleted) compared to the parenchyma of non-regressing tumors (C/EBPβ$^{+/+}$) (Fig 3B). Both TUNEL staining and cleaved caspase-3 staining produced similar numbers of apoptotic cells as observed in the H&E sections (data not shown). The increase in apoptosis in the regressing tumors was accompanied by a ~9-fold increase in p53 positive tumor cells compared to tumor cells of the non-regressing tumors (Fig 3C, D). In stark contrast to the tumor results, there were no significant differences in apoptosis or p53 levels between C/EBPβ depleted epidermis adjacent to the tumor and C/EBPβ$^{+/+}$ epidermis adjacent to the tumor (Fig 3E-F). Moreover, the levels of apoptosis and p53 were low in the adjacent normal epidermis, regardless of C/EBPβ status (Fig 3E-F). These results indicate that; i) the loss of C/EBPβ leads to increased levels of p53 and apoptotic cell death in oncogenic Ras skin tumor cells but not in adjacent epidermal keratinocytes with wild type Ras, ii) the loss of C/EBPβ is a synthetic lethal event in oncogenic Ras skin tumor cells.

Skin tumors exhibit increased levels of DNA damage, a stress phenotype of tumorigenesis

Prior work in our lab has demonstrated that C/EBPβ knockout mice treated with DNA damaging agents display increased levels of p53 and apoptosis in their epidermis compared to similarly treated wild type mice [41]. In the current study, the presence of DNA damage and subsequent stress phenotypes in oncogenic Ras skin tumors could provide a mechanism through which loss of C/EBPβ results in increased sensitivity to DNA damage, leading to increased p53 levels and apoptosis. To test for such DNA damage, we measured γH2AX, a marker of double strand breaks [62] in both tumors and adjacent epidermis. We observed very low numbers of γH2AX positive cells in the adjacent epidermis of regressing and non-regressing tumors (Fig 4A), however γH2AX IHC positive cells were significantly and similarly increased in both regressing and non-regressing tumors (Fig 4B). These results indicate that regressing and non-regressing skin tumors display a hallmark tumor stress phenotype [62] involving replicative/mitotic/DNA damage stress.

Regressing C/EBPβ-deficient tumors do not display differences in, proliferation, senescence, differentiation or inflammation

Next, we examined regressing and non-regressing tumors for differences in; i) cell proliferation (Fig 4C), ii) Ki67 staining as an indicator of senescence as decreased Ki67 staining would indicate cells have exited from the cell cycle, i.e. increased numbers of G_0 cells (Fig 4D), iii) differentiation with respect to the pattern of the keratin 5 (K5) and keratin 10 (K10) compartment (Fig 4E), and iv) tumor inflammation (Fig 4F-K). As shown in

Figures 4F-K, there were no differences in infiltration by neutrophils, mononuclear leukocytes, CD4+ T cells, CD8+ T cells, or F4/80 expressing macrophages in regressing versus non-regressing tumors. In summary, of the cellular processes evaluated, only increased apoptosis and increased p53 levels are associated with the regressing tumor phenotype suggesting increased p53-mediated apoptosis is a key event in tumor regression following the deletion of C/EBPβ.

Development of a mouse model for the inducible conditional co-deletion of C/EBPβ and p53 in epidermis and in pre-existing oncogenic Ras skin tumors

To determine if tumor regression and the associated increase in apoptosis following deletion of C/EBPβ requires p53, we developed an inducible conditional C/EBPβ-p53 double knockout mouse *K14CreER^{tam};C/ebpβ$^{flox/flox}$;p53$^{flox/flox}$* (DIKO) (Fig 5A) in which C/EBPβ and p53 could be conditionally co-deleted in epidermis, and presumably in pre-existing oncogenic Ha-Ras skin tumors. As shown in Figures 5B-C, dosing DIKO mice with tamoxifen *ip* (1x/day for 5 days/week for 2 weeks) resulted in the loss of both C/EBPβ and p53 protein in the epidermis. To test whether C/EBPβ and p53 could be co-deleted in pre-existing skin tumors, we generated skin tumors in DIKO mice using a DMBA/TPA tumorigenesis treatment protocol. DIKO tumor bearing mice were treated with tamoxifen *ip* (1x/d for 5 days/week for 2 weeks) or vehicle and tumors were harvested following cessation of treatment. As shown in Figure 5D, C/EBPβ and p53 are expressed in skin tumors, and tamoxifen treatment resulted in loss of C/EBPβ and p53 expression in the epithelial (parenchyma) portion of the tumor. These results show the DIKO mouse is a suitable model

to test whether the regression oncogenic Ras tumors resulting from the deletion of C/EBPβ is p53-dependent.

Oncogenic Ras skin tumors are dependent on C/EBPβ for survival and deletion of C/EBPβ in these tumors is a synthetic lethal event dependent upon p53

Skin tumors were generated in Cre and DIKO mice using the same DMBA/TPA tumorigenesis treatment protocol as before for the duration of the tumor experiment (30 weeks). As in previous experiments mice were treated with tamoxifen *ip* (1x/day for 5 days/week for 2 weeks) beginning at week 19 of TPA treatment. Tamoxifen-treated Cre mice continued to develop additional tumors (Fig 5E). No tumor regression was observed in the tamoxifen-treated DIKO and these mice, like the Cre mice, continued to develop additional tumors (Fig 5E/F). Both Cre and DIKO mice displayed an increase in tumor volume after tamoxifen treatment (Fig 5G) and no decrease in the percent mice with tumors was observed in either group (Fig 5F). DNA sequence analysis of p53 exons 3-9 in Cre tumors demonstrated that p53 was wild-type in 26/26 skin tumors and therefore lack of tumor regression was not due to the presence of mutant p53 (data not shown).

As part of the experiment described above, a small group of IKOβ and IKOp53 mice were also initiated, promoted and treated with tamoxifen. IKOβ mice displayed tumor regression, IKOp53 mice showed no regression, and tumors from these mice, along with tumors from DIKO and Cre mice were collected 2 weeks after the start of tamoxifen treatment (data not shown). PFPE sections were analyzed for apoptosis and γH2AX levels. As shown in Figure 5H, the majority of apoptosis observed in the IKOβ mouse tumors was

p53 dependent. All tumors displayed the significant and similar numbers of γH2AX positive cells (Fig 5I). Collectively these results demonstrate oncogenic Ras skin tumors are dependent on C/EBPβ for survival and deletion of C/EBPβ in these tumors is a synthetic lethal event dependent upon p53.

Regressing tumors display enrichment of a type I interferon response, p53 and TNF/death receptor signaling networks.

RNAseq analysis was conducted on RNA isolated from 3 non-regressing tumors (Cre mice) and 3 regressing tumors (IKOβ mice) at 2 weeks after the start of tamoxifen treatment. Deletion of C/EBPβ in the tumors had a profound effect on transcriptional responses. We identified a total of 2,287 genes (880 up-regulated and 1,407 down-regulated out of a data set of 17,431 genes) that were altered in the regressing tumors compared to the non-regressing tumors (FDR $p \leq 0.1$) (Figure 6A and Table S1). Gene set enrichment analysis (GSEA) was performed using gene sets from within the Molecular Signature Database (MSigDB). Unexpectedly, GSEA revealed that interferon pathways were the most highly enriched pathways in the regressing tumors (Fig 6B, Fig S1). While pathway analysis indicated activation of a type 1 interferon response, interferon-β (Ifnβ1) was not present in our RNAseq data set. Ifnβ1 is a potent cytokine and often expressed at very low levels that may not be detected in an RNAseq experiment. Therefore, we conducted TaqMAN qRT-PCR analysis for Ifnβ1 using RNA isolated from regressing and non-regressing tumors. This analysis revealed that Ifnβ1 transcripts were not detectable in non-regressing tumors (40 cycles); however, Ifnβ1 transcripts were increased ~115–fold (average Ct 33) in the

regressing tumors (Fig 6C). Further analysis of the MSigDB combined interferon gene showed that 49/161 genes were significantly altered in the regressing tumor (FDR $\leq$ 0.1) (Fig 6D and Table S2). Several of the up-regulated interferon stimulated genes (ISG) included genes known to be regulated by p53 such as *Irf9*, *Stat1*, *Stat2*, *Tnf*, *Tnfsf10*, *Isg15* and *Pml* (Tables S2, S4) [63-65]. Importantly IRF9, STAT1, and STAT2 come together to form the ISGF3 (Interferon-stimulated gene factor 3) signaling complex that functions to activate the transcription of numerous ISGs as well as to activate p53. This combination of ISGs that activate p53 and ISGs that are regulated by p53 result in a p53 feed forward loop in the interferon pathway. Furthermore, genes that increase p53 stability/function such as Xaf1 and Mdm2 were also significantly altered in the regressing tumors. The p53 pathway (53/191 genes) was also highly enriched in the regressing tumor as genes including *Cdkn1a*, *Mdm2*, *Pcna*, *Fox03*, and *Apaf1* were significantly upregulated (FDR $\leq$ 0.1) (Fig 6E and Table S3). Surprisingly, we did not observe upregulation of classic p53 regulated genes involved in the intrinsic apoptosis pathway (for example *Bax*, *Puma*, and *Noxa*).

TNF receptor pathway (FDR $\leq$ 0.1) and death receptor pathway (FDR $\leq$ 0.1) were highly enriched in the regressing tumors. Analysis of the genes in TNF receptor and death receptor pathways revealed that 53/195 genes (Fig 6F and Table S4) and 12/58 genes (Fig 6G and Table S5) respectively were significantly altered in the regressing tumors (FDR p$\leq$0.1). These genes include *Tnf*, *Tnfsf10*, *Cflar*, *Traf2*, *Tnfrsf9* and *Tnfrs19*. *Xaf1* and *Tnfsf10* (TRAIL), ISGs upregulated in the regressing tumor, are major mediators of the extrinsic cell death pathway where XAF1 significantly increases the cellular sensitivity to the pro-apoptotic actions of TRAIL [66]. Activation of caspase-8 is essential to the activation of the

extrinsic TNF/death receptor pathway, and IHC analysis indicated regressing tumors display ~14-fold increase in cleaved caspase-8 [67] (Fig 6H). Based on the results in this manuscript and previous findings, we propose the model that C/EBPβ is required for tumor cell survival through repression of the DNA damage and p53 activated innate immune response following oncogenic Ras induced DNA damage (Fig 6I). The deletion of C/EBPβ in pre-existing oncogenic Ras skin tumors is synthetically lethal and results in the robust activation of p53, innate immune interferon response, and extrinsic cell death TNF and death receptor pathways resulting in dramatic skin tumor regression.

DISCUSSION

In this study, the development of a mouse model where C/EBPβ could be deleted in pre-existing oncogenic Ras skin tumors revealed that C/EBPβ is essential for the survival of these tumors. Deletion of C/EBPβ in Ras tumors resulted in rapid tumor regression that was accompanied by elevated levels of apoptosis and p53. This increase in apoptosis and p53 was tumor specific as neither was increased in C/EBPβ-depleted epidermis adjacent to the tumor. Thus, while the deletion of C/EBPβ in keratinocytes of the epidermis had no effect on apoptosis and p53, the deletion of C/EBPβ in oncogenic Ras containing skin tumors cells, which are derived from the keratinocytes of the epidermis, resulted in elevated levels of apoptosis and p53. Using a mouse model where both C/EBPβ and p53 could be co-deleted in pre-existing oncogenic Ras tumors, we demonstrated that tumor regression and the increased levels of apoptosis in C/EBPβ depleted tumors are dependent on p53. Collectively, these results indicate the deletion of C/EBPβ in oncogenic Ras skin tumors is a synthetic lethal event dependent upon p53. Large scale synthetic lethal screens using cultured cells and RNA interference have been carried out to identify genes that are required for survival of oncogenic Ras containing cells [46]. In general, these screens have not yielded the positive results initially anticipated and it has been suggested that this is, in part, due to the *in vitro* screening methods utilized which do not replicate the selective pressures experienced by tumor cells *in vivo* [46]. While our *in vivo* studies have overcome this *in vitro* issue, most human tumors with a mutant Ras display Ki-Ras [1] mutations and our *in vivo* mouse skin model exclusively involves Ha-Ras^{Q61L} mutations. Future studies will be required to determine if the synthetic lethal effect of C/EBPβ deletion *in vivo* is unique to oncogenic Ha-

Ras^{Q61L} skin tumors or if other oncogenic Ras (Ha, Ki, N) containing p53 proficient tumor types would commit to apoptosis upon deletion/inhibition of C/EBPβ. Based on our results these future studies would be best conducted on oncogenic Ras tumors known to express high levels of the C/EBPβ and wild type p53.

C/EBPβ can be activated by Ha-Ras [19] and this may contribute to tumor cell survival in our model. In addition, previous studies showed C/EBPβ knockout mice treated with DNA damaging agents including chemical carcinogens, UVB radiation and alkylating chemotherapeutic agents display elevated levels of p53 and p53-mediated apoptosis compared to similarly treated wild type mice [41, 49]. These findings indicate that C/EBPβ functions to suppress p53 levels/activity and increase cell survival in response to exogenously induced DNA damage, consequently, the deletion of C/EBPβ influences cell fate death decisions in favor of cell death and sensitizes keratinocytes to DNA damage and p53-mediated apoptosis. In the current study, we observed that oncogenic Ras skin tumors display elevated levels of DNA damage based on increased levels of γH2AX [62]. DNA damage in tumors occurs through stalled replication forks (double strand breaks) and reactive oxygen species [45, 68]. The deletion of C/EBPβ in these tumors resulted in elevated levels of apoptosis and p53, suggesting that endogenous DNA damage stress present in the tumors may be the trigger of apoptosis and tumor regression. Increased endogenous DNA damage stress is a tumorigenic stress phenotype that tumors are forced to contend with in order to survive [45, 68] and in doing so we propose the tumor may become over reliant on genes like C/EBPβ to suppress apoptosis downstream of DNA damage. Luo et al. [45] suggested selective tumor cell killing could be accomplished by stress sensitization or stress overload.

Stress sensitization involves blocking a pathway(s) the tumor has evolved to depend on to handle the increased tumorigenic stress, while stress overload involves causing additional stress to the tumor to overload the already stretched capacity of the tumor. Our results are consistent with the notion that the deletion of C/EBPβ removes a critical stress survival pathway in the tumor. Deletion of C/EBPβ sensitizes tumor cells to oncogenic stress and tumorigenic stress-induced endogenous DNA damage to stimulate apoptotic cell death and tumor regression through p53 and type 1 interferon responses.

Gene set enrichment analysis (GSEA) of RNAseq data from regressing tumors deleted of C/EBPβ showed significant up-regulation of proapoptotic signaling networks involving type I interferon response, TNF, death receptors and p53. The enrichment of interferon, TNF and death receptor gene sets was unexpected as was the observation that canonical p53 target genes involved in the intrinsic apoptotic pathway such as Puma, Bax and Noxa were not upregulated in the regressing tumors. Initially, these results appeared incongruent with the p53-dependent nature of apoptosis and tumor regression observed in the C/EBPβ depleted tumors. However, further analysis revealed that expression of several key ISGs are regulated by p53 and several ISGs, in turn positively regulate p53 [69]. Emerging evidence suggests that p53 has an important role as a guardian of the innate immune response [63-65]. Thus, it appears that the depletion of C/EBPβ removes a mechanism to inhibit p53 mediated cell death in response to DNA damage and cellular stress.

Based on the GSEA results and some of the key genes significantly altered in these data sets we have developed a feed forward working model (Fig 7) whereby we link our results involving oncogenic Ras, DNA damage, type I interferon response, TNF, death

receptors and p53 pathway to the profound apoptotic response observed in C/EBPβ depleted regressing tumors. In this model, the upregulation/activation of p53 uniquely results in the feed forward upregulation of the type I interferon innate immune response as well as direct upregulation of p53 genes including *Tnf and Tnfsf10* (TRAIL) which can initiate apoptosis through the TNFR/death receptor/caspase 9 pathways. Additionally, the upregulation Xaf1 can inhibit IAP [70] function, contributing to the caspase-dependent cleavage of substrates, apoptotic cell death and tumor regression. The model is consistent with our results which indicated both the extrinsic and intrinsic pathways of apoptosis are activated. In summary, oncogenic Ras skin tumors are dependent on C/EBPβ for survival and deletion of C/EBPβ in these tumors is a synthetic lethal event dependent upon p53 and interferon type 1 responses. While additional studies are required, these results highlight that the targeting of C/EBPβ could hold promise as future potential anti-cancer therapy.

REFERENCES

1. Stephen, A.G., et al., *Dragging ras back in the ring.* Cancer Cell, 2014. **25**(3): p. 272-81.
2. Pylayeva-Gupta, Y., E. Grabocka, and D. Bar-Sagi, *RAS oncogenes: weaving a tumorigenic web.* Nat Rev Cancer, 2011. **11**(11): p. 761-74.
3. Malumbres, M. and M. Barbacid, *RAS oncogenes: the first 30 years.* Nat Rev Cancer, 2003. **3**(6): p. 459-65.
4. Sun, H., N.K. Tonks, and D. Bar-Sagi, *Inhibition of Ras-induced DNA synthesis by expression of the phosphatase MKP-1.* Science, 1994. **266**(5183): p. 285-8.
5. Jimenez, C., et al., *Identification and characterization of a new oncogene derived from the regulatory subunit of phosphoinositide 3-kinase.* EMBO J, 1998. **17**(3): p. 743-53.
6. Khosravi-Far, R., et al., *Oncogenic Ras activation of Raf/mitogen-activated protein kinase-independent pathways is sufficient to cause tumorigenic transformation.* Mol Cell Biol, 1996. **16**(7): p. 3923-33.
7. Urano, T., R. Emkey, and L.A. Feig, *Ral-GTPases mediate a distinct downstream signaling pathway from Ras that facilitates cellular transformation.* EMBO J, 1996. **15**(4): p. 810-6.
8. White, M.A., et al., *A role for the Ral guanine nucleotide dissociation stimulator in mediating Ras-induced transformation.* J Biol Chem, 1996. **271**(28): p. 16439-42.

9. Cowley, S., et al., *Activation of MAP kinase kinase is necessary and sufficient for PC12 differentiation and for transformation of NIH 3T3 cells.* Cell, 1994. **77**(6): p. 841-52.

10. Cox, A.D. and C.J. Der, *The dark side of Ras: regulation of apoptosis.* Oncogene, 2003. **22**(56): p. 8999-9006.

11. Wilson, C.Y. and P. Tolias, *Recent advances in cancer drug discovery targeting RAS.* Drug Discov Today, 2016. **21**(12): p. 1915-1919.

12. Kaelin, W.G., Jr., *The concept of synthetic lethality in the context of anticancer therapy.* Nat Rev Cancer, 2005. **5**(9): p. 689-98.

13. Ramji, D.P. and P. Foka, *CCAAT/enhancer-binding proteins: structure, function and regulation.* Biochem J, 2002. **365**(Pt 3): p. 561-75.

14. Tsukada, J., et al., *The CCAAT/enhancer (C/EBP) family of basic-leucine zipper (bZIP) transcription factors is a multifaceted highly-regulated system for gene regulation.* Cytokine. **54**(1): p. 6-19.

15. House, J.S., et al., *C/EBPalpha and C/EBPbeta are required for Sebocyte differentiation and stratified squamous differentiation in adult mouse skin.* PLoS One, 2010. **5**(3): p. e9837.

16. Matsusaka, T., et al., *Transcription factors NF-IL6 and NF-kB synergistically activate transcription of the inflammatory cytokine interleukin 6 and interleukin 8.* PNAS, 1993. **90**: p. 10193-10197.

17. Akagi, T., et al., *Impaired response to GM-CSF and G-CSF, and enhanced apoptosis in C/EBPbeta-deficient hematopoietic cells.* Blood, 2008. **111**(6): p. 2999-3004.

18. Armstrong, D.A., L.N. Phelps, and M.P. Vincenti, *CCAAT enhancer binding protein-beta regulates matrix metalloproteinase-1 expression in interleukin-1beta-stimulated A549 lung carcinoma cells.* Mol Cancer Res, 2009. **7**(9): p. 1517-24.

19. Nakajima, T., et al., *Phosphorylaton at threonine-235 by a ras dependent mitogen-activated protein kinase cascade is essential for transcription factor NF-IL6.* Proc. Natl. Acad. Sci. USA, 1993. **90**: p. 2207-2211.

20. Zhu, S., et al., *CCAAT/enhancer binding protein-beta is a mediator of keratinocyte survival and skin tumorigenesis involving oncogenic Ras signaling.* Proc Natl Acad Sci U S A, 2002. **99**(1): p. 207-12.

21. Buck, M., et al., *Phosphorylation of rat serine 105 or mouse threonine 217 in C/EBPbeta is required for hepatocyte proliferation induced by TGFalpha.* Molecular Cell, 1999. **4**: p. 1087-1092.

22. Cho, I.J., N.R. Woo, and S.G. Kim, *The identification of C/EBPbeta as a transcription factor necessary for the induction of MAPK phosphatase-1 by toll-like receptor-4 ligand.* Arch Biochem Biophys, 2008. **479**(1): p. 88-96.

23. Lu, Y.C., et al., *Differential role for c-Rel and C/EBPbeta/delta in TLR-mediated induction of proinflammatory cytokines.* J Immunol, 2009. **182**(11): p. 7212-21.

24. Cloutier, A., et al., *Inflammatory cytokine production by human neutrophils involves C/EBP transcription factors.* J Immunol, 2009. **182**(1): p. 563-71.

25. Pope, R.M., A. Leutz, and S.A. Ness, *C/EBP beta regulation of the tumor necrosis factor alpha gene.* J Clin Invest, 1994. **94**(4): p. 1449-55.

26. Shirakawa, F., et al., *The human prointerleukin 1 beta gene requires DNA sequences both proximal and distal to the transcription start site for tissue-specific induction.* Mol Cell Biol, 1993. **13**(3): p. 1332-44.

27. Dunn, S.M., et al., *Requirement for nuclear factor (NF)-kappa B p65 and NF-interleukin-6 binding elements in the tumor necrosis factor response region of the granulocyte colony-stimulating factor promoter.* Blood, 1994. **83**(9): p. 2469-79.

28. Kunsch, C., et al., *Synergistic transcriptional activation of the IL-8 gene by NF-kappa B p65 (RelA) and NF-IL-6.* J Immunol, 1994. **153**(1): p. 153-64.

29. Xia, C., et al., *Cross-talk between transcription factors NF-kappa B and C/EBP in the transcriptional regulation of genes.* Int J Biochem Cell Biol, 1997. **29**(12): p. 1525-39.

30. Aguilar-Morante, D., et al., *Decreased CCAAT/enhancer binding protein beta expression inhibits the growth of glioblastoma cells.* Neuroscience. **176**: p. 110-9.

31. Anastasov, N., et al., *C/EBPbeta expression in ALK-positive anaplastic large cell lymphomas is required for cell proliferation and is induced by the STAT3 signaling pathway.* Haematologica. **95**(5): p. 760-7.

32. Bundy, L.M. and L. Sealy, *CCAAT/enhancer binding protein beta (C/EBPbeta)-2 transforms normal mammary epithelial cells and induces epithelial to mesenchymal transition in culture.* Oncogene, 2003. **22**(6): p. 869-83.

33. Duprez, E., *A new role for C/EBPbeta in acute promyelocytic leukemia.* Cell Cycle, 2004. **3**(4): p. 389-90.

34. Homma, J., et al., *Increased expression of CCAAT/enhancer binding protein beta correlates with prognosis in glioma patients.* Oncol Rep, 2006. **15**(3): p. 595-601.

35. Kim, M.H., A.Z. Minton, and V. Agrawal, *C/EBPbeta regulates metastatic gene expression and confers TNF-alpha resistance to prostate cancer cells.* Prostate, 2009. **69**(13): p. 1435-47.

36. Li, W., et al., *A gene expression signature for relapse of primary wilms tumors.* Cancer Res, 2005. **65**(7): p. 2592-601.

37. Pal, R., et al., *C/EBPbeta regulates transcription factors critical for proliferation and survival of multiple myeloma cells.* Blood, 2009. **114**(18): p. 3890-8.

38. Rask, K., et al., *Increased expression of the transcription factors CCAAT-rnhancer binding brotein-beta and C/EBP-zeta correlate with invasiveness of human colorectal cancer.* International Journal of Cancer, 2000. **86**: p. 337-343.

39. Sundfeldt, K., et al., *The expression of CCAAT/enhancer binding protein in human ovary in vivo: specific increase in C/EBPbeta dering epithelial tumour progression.* British Journal of Cancer, 1999. **79**: p. 1240-1248.

40. Buck, M., et al., *C/EBPbeta phosphorylation by RSK creates a functional XEXD caspase inhibitory box critical for cell survival.* Mol Cell, 2001. **8**(4): p. 807-16.

41. Ewing, S.J., et al., *C/EBPbeta represses p53 to promote cell survival downstream of DNA damage independent of oncogenic Ras and p19(Arf).* Cell Death Differ, 2008. **15**(11): p. 1734-44.

42. Piva, R., et al., *Functional validation of the anaplastic lymphoma kinase signature identifies CEBPB and BCL2A1 as critical target genes.* J Clin Invest, 2006. **116**(12): p. 3171-82.

43. Wessells, J., S. Yakar, and P.F. Johnson, *Critical prosurvival roles for C/EBP beta and insulin-like growth factor I in macrophage tumor cells.* Mol Cell Biol, 2004. **24**(8): p. 3238-50.

44. Hanahan, D. and R.A. Weinberg, *Hallmarks of cancer: the next generation.* Cell, 2011. **144**(5): p. 646-74.

45. Luo, J., N.L. Solimini, and S.J. Elledge, *Principles of cancer therapy: oncogene and non-oncogene addiction.* Cell, 2009. **136**(5): p. 823-37.

46. Downward, J., *RAS Synthetic Lethal Screens Revisited: Still Seeking the Elusive Prize?* Clin Cancer Res, 2015. **21**(8): p. 1802-9.

47. O'Neil, N.J., M.L. Bailey, and P. Hieter, *Synthetic lethality and cancer.* Nat Rev Genet, 2017.

48. Weinstein, I.B., et al., *Disorders in cell circuitry associated with multistage carcinogenesis: exploitable targets for cancer prevention and therapy.* Clin Cancer Res, 1997. **3**(12 Pt 2): p. 2696-702.

49. Yoon, K., et al., *Decreased survival of C/EBP beta-deficient keratinocytes is due to aberrant regulation of p53 levels and function.* Oncogene, 2007. **26**(3): p. 360-7.

50. Vasioukhin, V., et al., *The magical touch: genome targeting in epidermal stem cells induced by tamoxifen application to mouse skin.* Proc Natl Acad Sci U S A, 1999. **96**(15): p. 8551-6.

51. Sterneck, E., et al., *Conditional ablation of C/EBP beta demonstrates its keratinocyte-specific requirement for cell survival and mouse skin tumorigenesis.* Oncogene, 2006. **25**(8): p. 1272-1276.

52. Jonkers, J., et al., *Synergistic tumor suppressor activity of BRCA2 and p53 in a conditional mouse model for breast cancer.* Nat Genet, 2001. **29**(4): p. 418-25.

53. Kramata, P., et al., *Patches of mutant p53-immunoreactive epidermal cells induced by chronic UVB Irradiation harbor the same p53 mutations as squamous cell carcinomas in the skin of hairless SKH-1 mice.* Cancer Res, 2005. **65**(9): p. 3577-85.

54. Thompson, E.A., et al., *C/EBPalpha expression is downregulated in human nonmelanoma skin cancers and inactivation of C/EBPalpha confers susceptibility to UVB-induced skin squamous cell carcinomas.* J Invest Dermatol, 2011. **131**(6): p. 1339-46.

55. Schneider, C.A., W.S. Rasband, and K.W. Eliceiri, *NIH Image to ImageJ: 25 years of image analysis.* Nat Methods, 2012. **9**(7): p. 671-5.

56. Kugelberg, E., et al., *Establishment of a superficial skin infection model in mice by using Staphylococcus aureus and Streptococcus pyogenes.* Antimicrob Agents Chemother, 2005. **49**(8): p. 3435-41.

57. Dobin, A., et al., *STAR: ultrafast universal RNA-seq aligner.* Bioinformatics, 2013. **29**(1): p. 15-21.

58. Love, M.I., W. Huber, and S. Anders, *Moderated estimation of fold change and dispersion for RNA-seq data with DESeq2.* Genome Biol, 2014. **15**(12): p. 550.

59. Benjamini, Y. and Y. Hochberg, *Controlling the false discovery rate: a practical and powerful approach to multiple testing.* Journal of the royal statistical society. Series B (Methodological), 1995: p. 289-300.

60. Subramanian, A., et al., *Gene set enrichment analysis: a knowledge-based approach for interpreting genome-wide expression profiles.* Proc Natl Acad Sci U S A, 2005. **102**(43): p. 15545-50.

61. Quintanilla, M., et al., *Carcinogen-specific mutation and amplification of Ha-ras during mouse skin carcinogenesis.* Nature, 1986. **322**(6074): p. 78-80.

62. Kuo, L.J. and L.X. Yang, *Gamma-H2AX - a novel biomarker for DNA double-strand breaks.* In Vivo, 2008. **22**(3): p. 305-9.

63. Munoz-Fontela, C., et al., *Emerging roles of p53 and other tumour-suppressor genes in immune regulation.* Nat Rev Immunol, 2016. **16**(12): p. 741-750.

64. Zhang, F. and S. Sriram, *Identification and characterization of the interferon-beta-mediated p53 signal pathway in human peripheral blood mononuclear cells.* Immunology, 2009. **128**(1 Suppl): p. e905-18.

65. Zou, B., et al., *XIAP-associated factor 1 (XAF1), a novel target of p53, enhances p53-mediated apoptosis via post-translational modification.* Mol Carcinog, 2012. **51**(5): p. 422-32.

66. Micali, O.C., et al., *Silencing of the XAF1 gene by promoter hypermethylation in cancer cells and reactivation to TRAIL-sensitization by IFN-beta.* BMC Cancer, 2007. **7**: p. 52.

67. Ashkenazi, A. and V.M. Dixit, *Death receptors: signaling and modulation.* Science, 1998. **281**(5381): p. 1305-8.

68. Gaillard, H., T. Garcia-Muse, and A. Aguilera, *Replication stress and cancer.* Nat Rev Cancer, 2015. **15**(5): p. 276-89.

69. Miciak, J. and F. Bunz, *Long story short: p53 mediates innate immunity.* Biochim Biophys Acta, 2016. **1865**(2): p. 220-7.

70. Liston, P., et al., *Identification of XAF1 as an antagonist of XIAP anti-Caspase activity.* Nat Cell Biol, 2001. **3**(2): p. 128-33.

FIGURE LEGENDS

Figure 1: **Spatial and temporal regulation of C/EBPβ in epidermis and in pre-existing oncogenic Ras skin tumors.** (A) Immunohistochemical (IHC) staining for C/EBPβ in a DMBA/TPA induced mouse squamous papilloma. (B) Schematic of the *K14*-CreER^{tam};*C/ebpβ*$^{flox/flox}$ (IKOβ) transgenic mouse model system. (C) IHC staining for C/EBPβ in IKOβ mouse epidermis and dermis following vehicle and tamoxifen dosing. (D) Western blot analysis for C/EBPβ in epidermal lysates from tamoxifen treated Cre and IKOβ mice. (E) H&E and C/EBPβ IHC staining in DMBA/TPA induced mouse squamous papilloma following vehicle and tamoxifen dosing. (F) DNA sequence alignment of the 61st codon of Ha-Ras in mouse tail and DMBA/TPA induced squamous papilloma.

Figure 2: Oncogenic Ras skin tumors depend on C/EBPβ for survival. (A) Tumor multiplicity in Cre and IKOβ before and after Tamoxifen treatment, (B) tumor incidence, and (C) tumor volume remaining (Cre N=10, IKOβ N=11). (D) Representative photographs of skin tumors before and after tamoxifen on the same mouse. (E) Tumor multiplicity in Cre and IKOβ before and after mice were dosed with Tamoxifen at a more progressed state, and (F) tumor incidence (Cre N=15, IKOβ N=18). N=# of mice *indicates significantly different from controls $p<0.05$ via the Student's t test.

Figure 3: Regressing C/EBPβ-deficient tumors display elevated levels of apoptosis and p53 protein while adjacent C/EBPβ-depleted skin is unaffected. Tumors from IKOβ mice dosed with either vehicle control or tamoxifen were collected two weeks after the initial

vehicle or tamoxifen dose. (A) Deletion of C/EBPβ was confirmed by IHC staining. (B) Quantification of apoptosis in H&E stained tumors (vehicle n=18, tamoxifen n=10). (C) Quantification of IHC staining for p53 (vehicle n=15, tamoxifen n=12). (D) Photomicrograph depicting increases in p53 staining following Tamoxifen treatment. (E) Quantification of apoptosis in H&E stained adjacent normal epidermis (vehicle N=5, tamoxifen N=8). (F) Quantification of IHC staining for p53 in adjacent normal epidermis (vehicle N=5, tamoxifen N=8). N=# of mice, n=# of tumors, *indicates significantly different from controls $p<0.05$ via the Student's t test.

Figure 4: Skin tumors exhibit DNA damage and regressing C/EBPβ-deficient tumors do not display differences, in proliferation, senescence, differentiation or inflammation. Tumors from IKOβ mice dosed with either vehicle control or tamoxifen were collected two weeks after the initial vehicle or tamoxifen dose. (A) Quantification of IHC staining for Phospho-Histone H2A.X (γH2AX) in adjacent normal epidermis (vehicle N=4, tamoxifen N=4). (B) Quantification of γH2AX in tumor (vehicle n=13, tamoxifen n=8). (C) Quantification of IHC staining for BrdU incorporation in tumors (vehicle n=17, tamoxifen n=9). (D) Quantification of IHC staining for Ki67 in tumors (vehicle n=13, tamoxifen n=9). (E) IHC staining for Keratin 5 and Keratin 10. Quantification of (F) neutrophil infiltration (G) mononuclear leukocyte infiltration, and (H) total inflammation (vehicle n=18, tamoxifen n=18) from H&E stained tumor sections. (I) Quantification of CD4 IHC staining in tumor parenchyma and stroma (vehicle n=7, tamoxifen n=7). (J) Quantification of CD8 IHC staining in tumor parenchyma and stroma (vehicle n=10, tamoxifen n=9). (K) Quantification

of F4/80 IHC staining in tumor parenchyma and stroma (vehicle n=11, tamoxifen n=9). N=# of mice, n=# of tumors, *indicates significantly different from controls $p<0.05$ via the Student's t test.

Figure 5: Oncogenic Ras tumor regression following deletion of C/EBPβ is dependent on p53. (A) Schematic of the *K14*-CreER^{tam};*C/ebpβ*$^{flox/flox}$;*p53*$^{flox/flox}$ (DIKO) transgenic mouse model system. (B) Western blot analysis of C/EBPβ and p53 in epidermal lysates of tamoxifen treated Cre, IKOβ, IKOp53, and DIKO mice. (C) IHC staining for C/EBPβ and p53 in normal DIKO mouse epidermis following vehicle and tamoxifen treatment. (D) H&E and IHC staining for C/EBPβ and p53 in DMBA/TPA induced mouse squamous papillomas following tamoxifen dosing. (E) Tumor multiplicity in DMBA/TPA induced skin squamous papilloma in Cre and DIKO mice dosed with tamoxifen following 19 weeks of skin tumor promotion (Cre N=10, DIKO N=11). (F) Tumor incidence in Cre and DIKO mice. (G) Tumor volume in Cre and DIKO mice. (H) Quantification of apoptosis in H&E stained tumors collected two weeks after the initial tamoxifen dose (Cre n=9, IKOβ n=3, IKOp53 n=7, DIKO n=7). (I) Quantification of γH2AX IHC staining. N=# of mice, n=# of tumors, *indicates significantly different from controls $p<0.05$ via the Student's t test.

Figure 6: Regressing tumors display enrichment of type I interferon response, p53 and TNF/death receptor signaling networks. Total RNA from 3 Cre and 3 IKOβ tumors from separate mice were subjected to RNA sequencing. (A) Heatmap showing total gene expression. (B) Geneset Enrichment Analysis showing top 20 positively and negatively

enriched pathways from the Broad Institute. (C) Taqman qRT-PCR analysis of Infβ1 transcript levels normalized to gapdh (Cre n=3, IKOβ n=3). (D) Heatmap of genes in the MSigDB interferon gene sets (combined the databases INTERFERON-GAMMA SIGNALING PATHWAY%PANTHER PATHWAY%P00035, INTERFERON GAMMA SIGNALING%REACTOME%R-HSA-877300.1, INTERFERON SIGNALING%REACTOME%R-HSA-913531.1, and INTERFERON ALPHA BETA SIGNALING%REACTOME%R-HSA-909733.1). (E) Heatmap of genes in the MSigDB HALLMARK_P53_PATHWAY%MSIGDB_C2%HALLMARK_P53_PATHWAY (F). Heatmap of genes in the MSigDB BIOCARTA_DEATH_PATHWAY%MSIGDB_C2%BIOCARTA_DEATH_PATHWAY and DEATH RECEPTOR SIGNALLING%REACTOME DATABASE ID RELEASE 59%73887. (G) Heatmap of genes in the MSigDB HALLMARK_TNFA_SIGNALING_VIA_NFKB%MSIGDB_C2%HALLMARK_TNFA_SIGNALING_VIA_NFKB. (H) Quantification of IHC staining for cleaved Caspase 8 (vehicle n=8, tamoxifen n=8). (I) Proposed models depicting the relationship of oncogenic Ras, C/EBPβ, p53, DNA damage, and the innate immune response. n=# of tumors, *indicates significantly different from controls $p<0.05$ via the Student's t test.

FIGURES

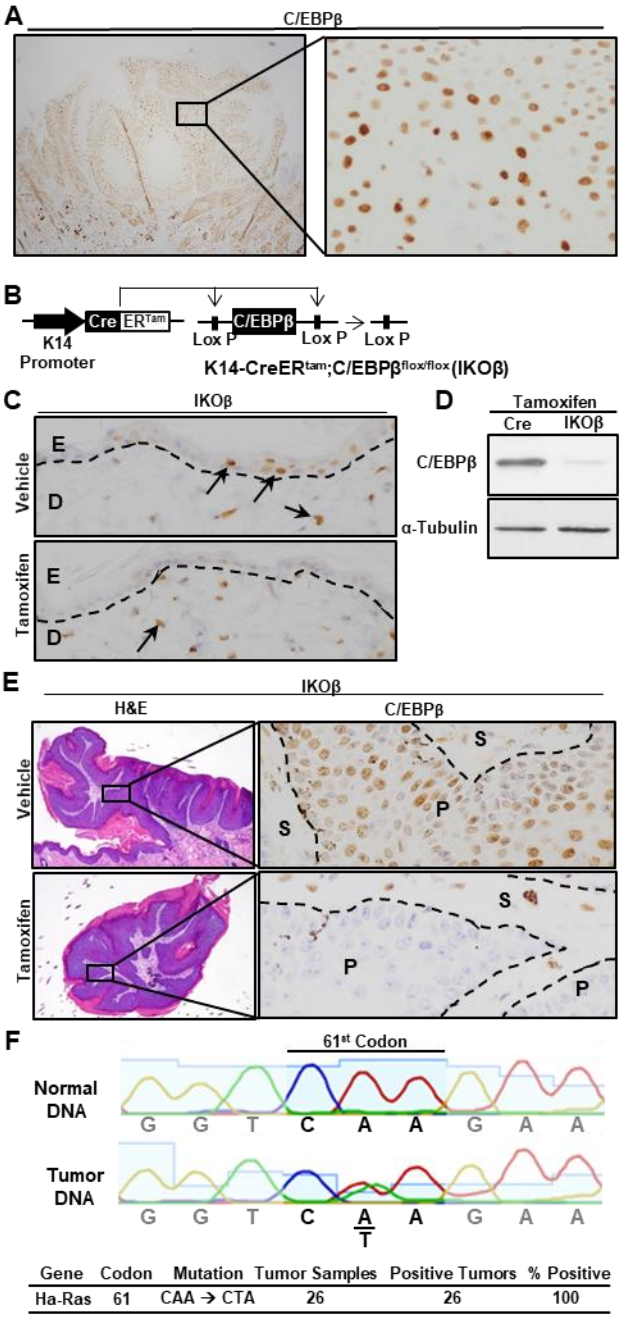

Gene	Codon	Mutation	Tumor Samples	Positive Tumors	% Positive
Ha-Ras	61	CAA → CTA	26	26	100

Figure 1: Spatial and temporal regulation of C/EBPβ in epidermis and in pre-existing oncogenic Ras skin tumors

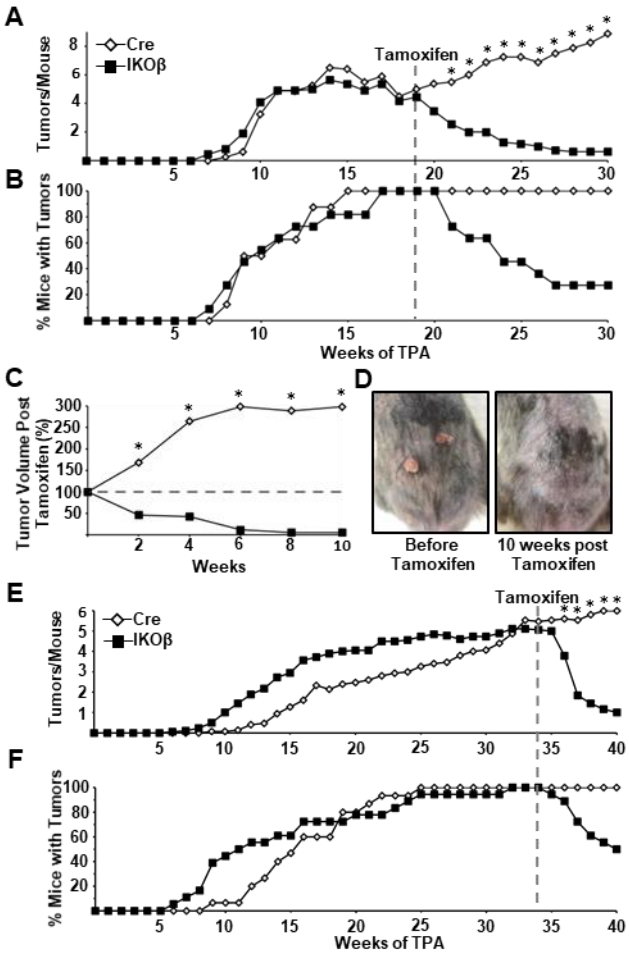

Figure 2: Oncogenic Ras skin tumors depend on C/EBPβ for survival

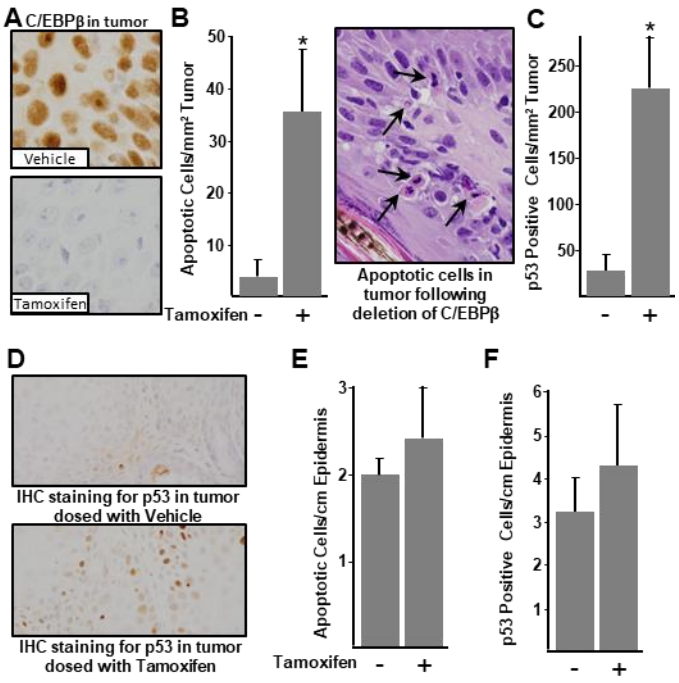

Figure 3: Regressing C/EBPβ-deficient tumors display elevated levels of apoptosis and p53 protein while adjacent C/EBPβ-depleted skin is unaffected

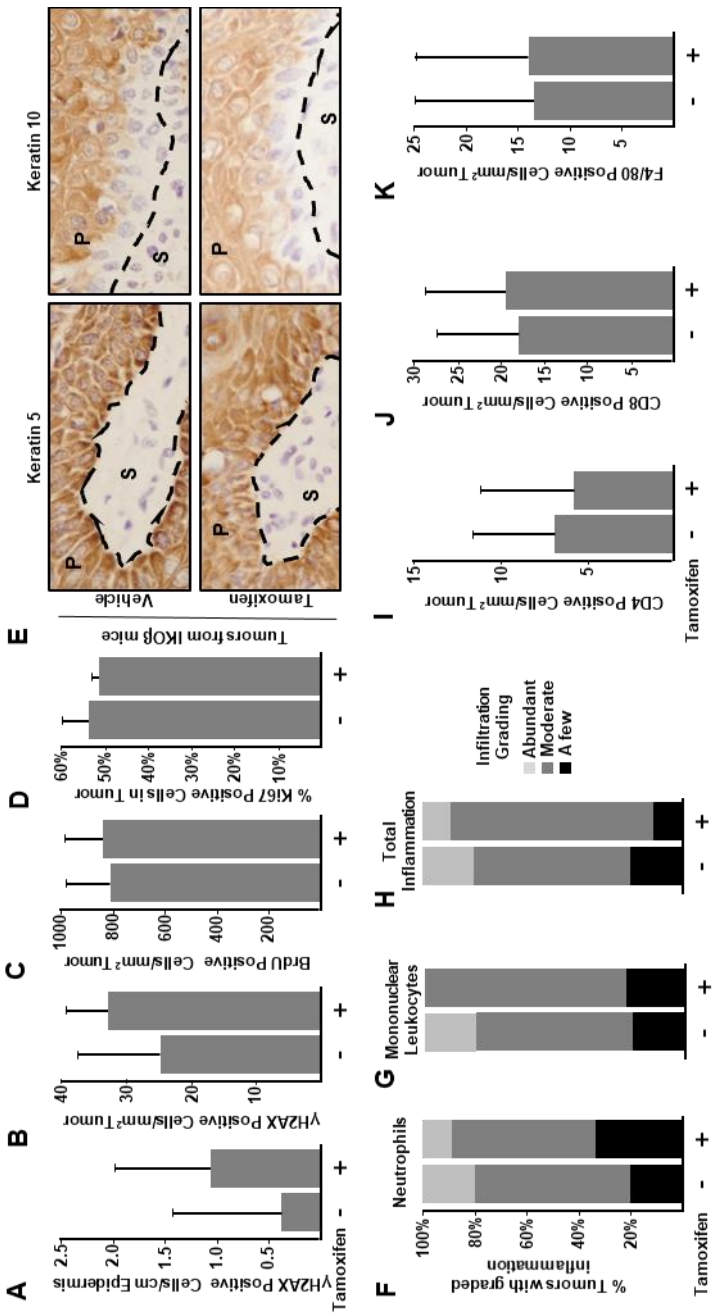

Figure 4: Skin tumors exhibit DNA damage and regressing C/EBPβ-deficient tumors do not display differences, in proliferation, senescence, differentiation or inflammation

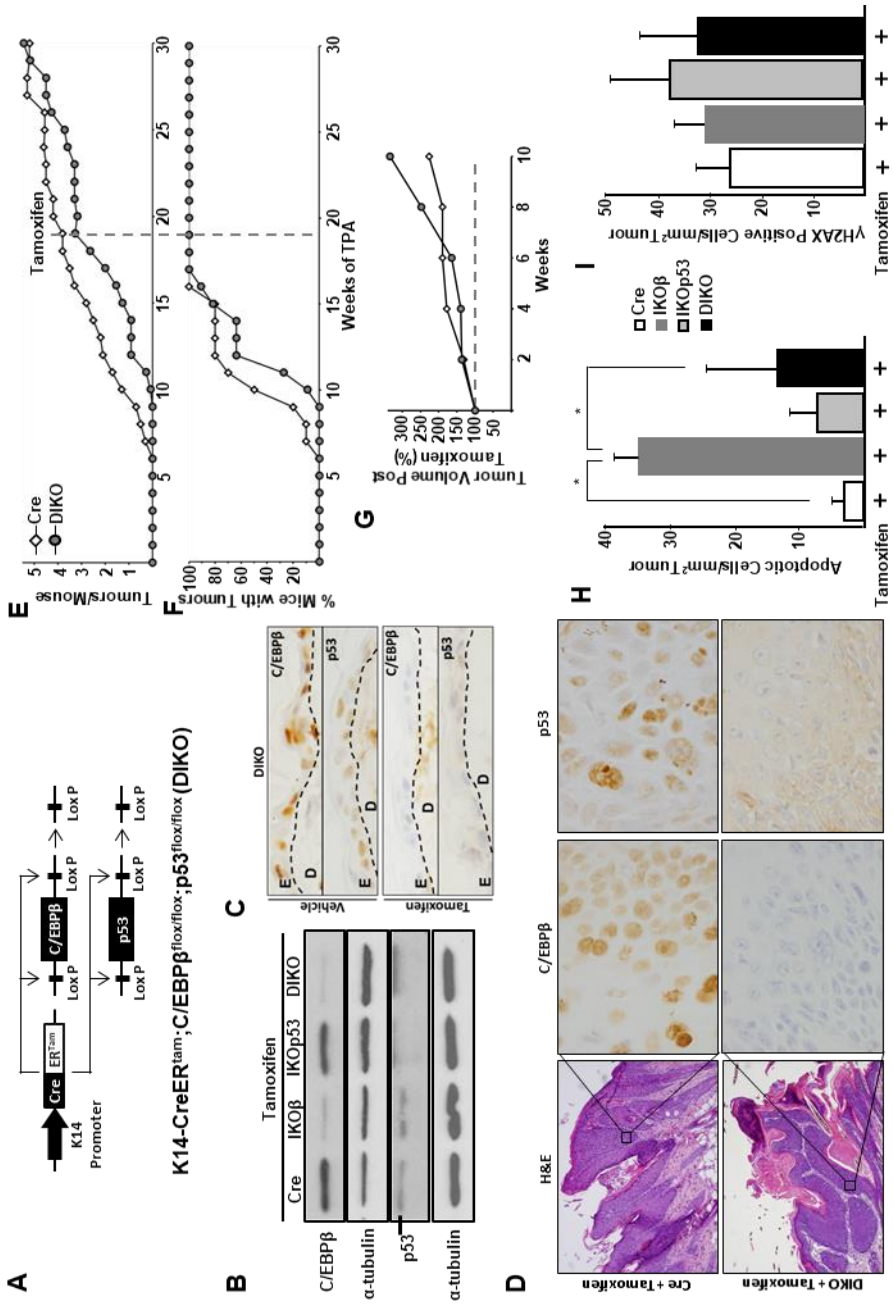

Figure 5: Oncogenic Ras tumor regression following deletion of C/EBPβ is dependent on p53

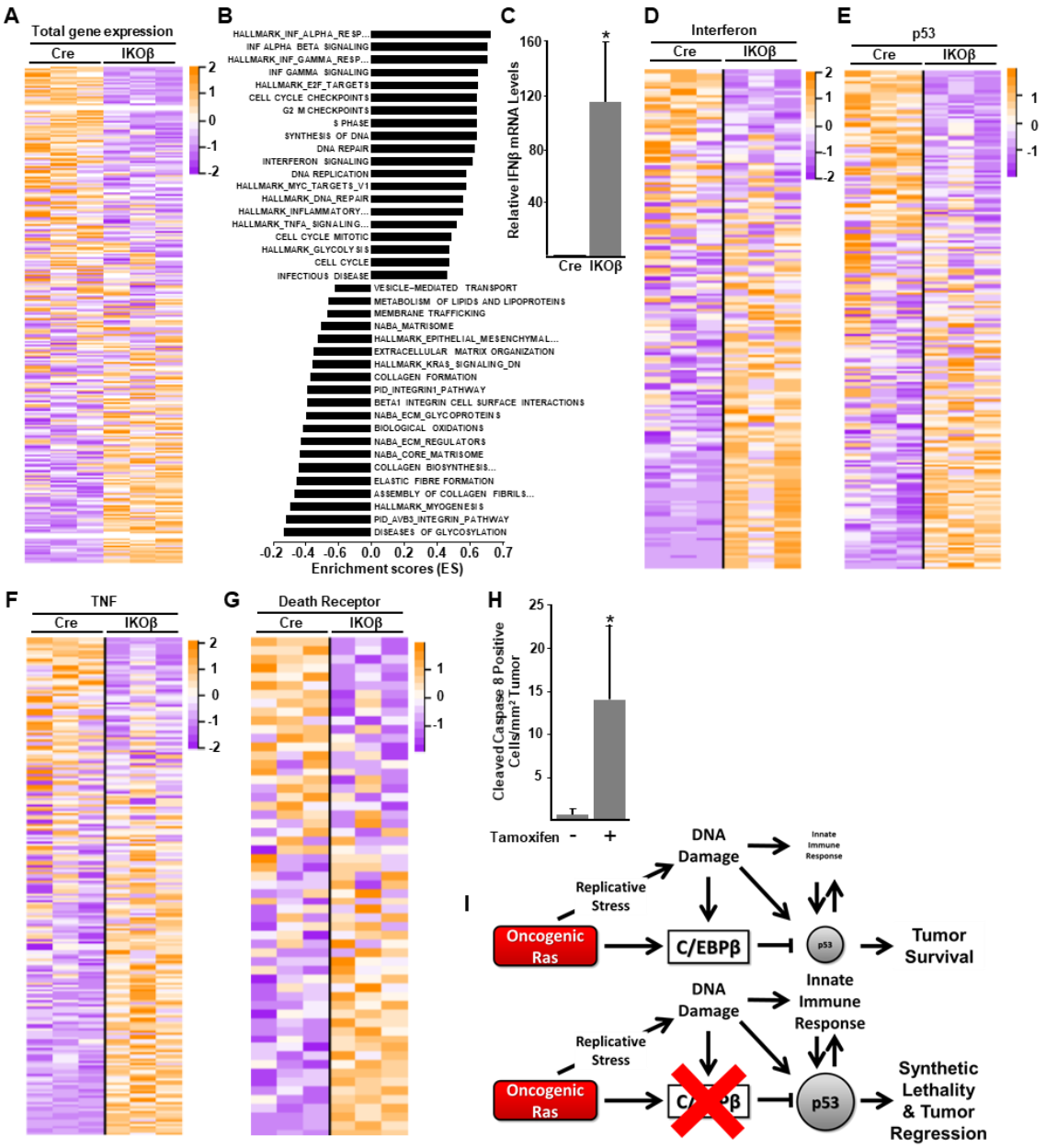

Figure 6: Regressing tumors display enrichment of type I interferon response, p53 and TNF/death receptor signaling networks

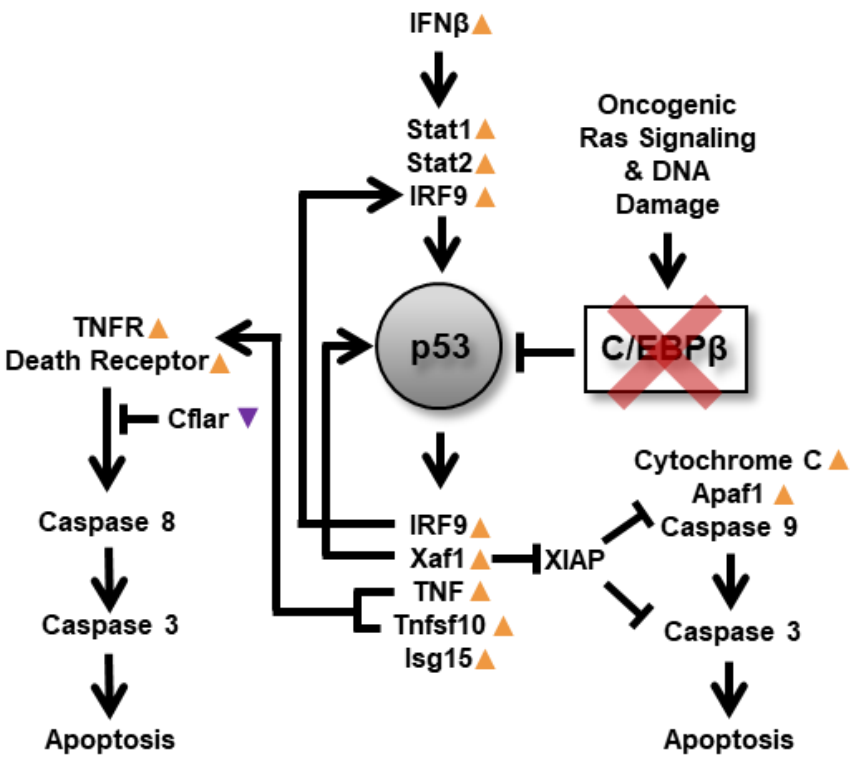

Figure 7: Model of type 1 interferon and p53 feedback loop inducing apoptosis in the absence of C/EBPβ

SUPPLEMENTAL TABLES

Supplemental Table 1: GSEA Pathway List

ENRICHED IN IKOβ (UPREGULATED IN REGRESSING TUMOR)						
NAME	SIZE	ES	NES	NOM p-val	FDR q-val	FWER p-val
HALLMARK_INTERFERON_GAMMA_RESPONSE%MSIGDB_C2%HALLMARK_INTERFERON_GAMMA_RESPONSE	57	0.710	6.196	0.000	0.000	0
HALLMARK_INTERFERON_ALPHA_RESPONSE%MSIGDB_C2%HALLMARK_INTERFERON_ALPHA_RESPONSE	41	0.727	5.311	0.000	0.000	0
HALLMARK_INFLAMMATORY_RESPONSE%MSIGDB_C2%HALLMARK_INFLAMMATORY_RESPONSE	43	0.560	4.352	0.000	0.000	0
INTERFERON SIGNALING%REACTOME%R-HSA-913531.1	31	0.617	4.112	0.000	0.000	0
HALLMARK_TNFA_SIGNALING_VIA_NFKB%MSIGDB_C2%HALLMARK_TNFA_SIGNALING_VIA_NFKB	44	0.522	4.065	0.000	0.000	0
CYTOKINE SIGNALING IN IMMUNE SYSTEM%REACTOME DATABASE ID RELEASE 59%1280215	101	0.348	3.963	0.000	0.000	0
GENE EXPRESSION%REACTOME DATABASE ID RELEASE 59%74160	86	0.356	3.718	0.000	0.000	0
INTERFERON ALPHA BETA SIGNALING%REACTOME%R-HSA-909733.1	16	0.711	3.474	0.000	0.000	0
HALLMARK_E2F_TARGETS%MSIGDB_C2%HALLMARK_E2F_TARGETS	19	0.646	3.351	0.000	0.000	0
IMMUNE SYSTEM%REACTOME DATABASE ID RELEASE 59%168256	234	0.204	3.321	0.000	0.000	0
CELL CYCLE%REACTOME DATABASE ID RELEASE 59%1640170	33	0.477	3.272	0.000	0.000	0
INTERFERON GAMMA SIGNALING%REACTOME%R-HSA-877300.1	18	0.646	3.272	0.000	0.000	0
CELL CYCLE, MITOTIC%REACTOME%R-HSA-69278.1	28	0.490	3.067	0.000	0.000	0
CELL CYCLE CHECKPOINTS%REACTOME DATABASE ID RELEASE 59%69620	16	0.643	3.039	0.000	0.000	0
EGFR1%IOB%EGFR1	68	0.318	3.027	0.000	0.000	0
G2 M CHECKPOINTS%REACTOME DATABASE ID RELEASE 59%69481	15	0.643	3.024	0.000	0.000	0
DNA REPAIR%REACTOME DATABASE ID RELEASE 59%73894	15	0.634	2.997	0.000	0.000	0
SYNTHESIS OF DNA%REACTOME DATABASE ID RELEASE 59%69239	15	0.643	2.996	0.000	0.000	0
EGFR1%NETPATH%EGFR1	67	0.317	2.975	0.000	0.000	0
S PHASE%REACTOME DATABASE ID RELEASE 59%69242	15	0.643	2.967	0.000	0.000	0
DNA REPLICATION%REACTOME DATABASE ID RELEASE 59%69306	17	0.584	2.899	0.000	0.000	0
HALLMARK_MYC_TARGETS_V1%MSIGDB_C2%HALLMARK_MYC_TARGETS_V1	17	0.584	2.865	0.000	0.000	0
HALLMARK_HYPOXIA%MSIGDB_C2%HALLMARK_HYPOXIA	42	0.371	2.830	0.000	0.000	0
HALLMARK_GLYCOLYSIS%MSIGDB_C2%HALLMARK_GLYCOLYSIS	25	0.477	2.796	0.000	0.000	0
INFECTIOUS DISEASE%REACTOME DATABASE ID RELEASE 59%5663205	23	0.464	2.699	0.000	0.000	0
HALLMARK_DNA_REPAIR%MSIGDB_C2%HALLMARK_DNA_REPAIR	15	0.563	2.655	0.000	0.000	0
GENERIC TRANSCRIPTION PATHWAY%REACTOME DATABASE ID RELEASE 59%212436	50	0.302	2.490	0.000	0.001	0.02
TRANSCRIPTIONAL REGULATION BY TP53%REACTOME%R-HSA-3700989.5	31	0.363	2.387	0.004	0.002	0.03
SIGNALING BY INTERLEUKINS%REACTOME DATABASE ID RELEASE 59%449147	69	0.242	2.336	0.000	0.002	0.05
GLUCOCORTICOID RECEPTOR REGULATORY NETWORK%PATHWAY INTERACTION DATABASE NCI-NATURE CURATED DATA%GLUCOCORTICOID RECEPTOR REGULATORY NETWORK	16	0.462	2.282	0.002	0.004	0.08
ANTIGEN PROCESSING: UBIQUITINATION & PROTEASOME DEGRADATION%REACTOME DATABASE ID RELEASE 59%983168	30	0.350	2.221	0.000	0.005	0.12
PID_REG_GR_PATHWAY%MSIGDB_C2%PID_REG_GR_PATHWAY	16	0.462	2.219	0.000	0.005	0.12
CLASS I MHC MEDIATED ANTIGEN PROCESSING & PRESENTATION%REACTOME%R-HSA-983169.3	36	0.312	2.206	0.000	0.006	0.13
RIG-I MDA5 MEDIATED INDUCTION OF IFN-ALPHA BETA PATHWAYS%REACTOME%R-HSA-168928.1	16	0.456	2.199	0.000	0.006	0.14
UB-SPECIFIC PROCESSING PROTEASES%REACTOME%R-HSA-5689880.2	17	0.448	2.189	0.000	0.006	0.15
HIV INFECTION%REACTOME%R-HSA-162906.1	15	0.462	2.164	0.000	0.007	0.17
C-TYPE LECTIN RECEPTORS (CLRS)%REACTOME DATABASE ID RELEASE 59%5621481	15	0.441	2.035	0.010	0.016	0.34
APOPTOSIS SIGNALING PATHWAY%PANTHER PATHWAY%P00006	17	0.398	2.033	0.006	0.015	0.34
HALLMARK_P53_PATHWAY%MSIGDB_C2%HALLMARK_P53_PATHWAY	37	0.285	2.020	0.012	0.016	0.36
HALLMARK_IL6_JAK_STAT3_SIGNALING%MSIGDB_C2%HALLMARK_IL6_JAK_STAT3_SIGNALING	17	0.408	2.013	0.006	0.016	0.37

Supplemental Table 1: Continued

HALLMARK_MTORC1_SIGNALING%MSIGDB_C2%HALLMARK_MTORC1_SIGNALING	24	0.342	1.998	0.008	0.017	0.4
SIGNALING BY MET%REACTOME%R-HSA-6806834.2	17	0.387	1.958	0.008	0.021	0.47
DEUBIQUITINATION%REACTOME%R-HSA-5688426.3	26	0.320	1.956	0.012	0.021	0.48
TNFALPHA%IOB%TNFALPHA	23	0.351	1.941	0.006	0.023	0.51
PROGRAMMED CELL DEATH%REACTOME%R-HSA-5357801.1	17	0.391	1.919	0.008	0.025	0.55
APOPTOSIS%REACTOME DATABASE ID RELEASE 59%109581	17	0.391	1.886	0.008	0.030	0.64
BCR%NETPATH%BCR	16	0.375	1.806	0.027	0.046	0.8
HALLMARK_ALLOGRAFT_REJECTION%MSIGDB_C2%HALLMARK_ALLOGRAFT_REJECTION	27	0.291	1.771	0.012	0.054	0.86
ORGANELLE BIOGENESIS AND MAINTENANCE%REACTOME DATABASE ID RELEASE 59%1852241	16	0.368	1.765	0.022	0.054	0.87
METABOLISM OF PROTEINS%REACTOME%R-HSA-392499.3	113	0.145	1.765	0.013	0.053	0.87
NABA_SECRETED_FACTORS%MSIGDB_C2%NABA_SECRETED_FACTORS	50	0.213	1.746	0.019	0.058	0.9
ADAPTIVE IMMUNE SYSTEM%REACTOME%R-HSA-1280218.3	77	0.171	1.713	0.027	0.068	0.94
PDGFR-BETA SIGNALING PATHWAY%PATHWAY INTERACTION DATABASE NCI-NATURE CURATED DATA%PDGFR-BETA SIGNALING PATHWAY	20	0.308	1.689	0.033	0.075	0.95
TNFALPHA%NETPATH%TNFALPHA	30	0.255	1.663	0.038	0.083	0.97
INNATE IMMUNE SYSTEM%REACTOME%R-HSA-168249.5	145	0.123	1.662	0.044	0.082	0.97
PID_PDGFRB_PATHWAY%MSIGDB_C2%PID_PDGFRB_PATHWAY	20	0.308	1.655	0.043	0.083	0.97
DIRECT P53 EFFECTORS%PATHWAY INTERACTION DATABASE NCI-NATURE CURATED DATA%DIRECT P53 EFFECTORS	25	0.274	1.643	0.035	0.087	0.98
HALLMARK_UV_RESPONSE_UP%MSIGDB_C2%HALLMARK_UV_RESPONSE_UP	22	0.294	1.632	0.034	0.089	0.99
TCR%NETPATH%TCR	24	0.273	1.618	0.031	0.093	0.99
ACTIVATED TLR4 SIGNALLING%REACTOME%R-HSA-166054.1	16	0.331	1.599	0.034	0.100	0.99
PID_P53_DOWNSTREAM_PATHWAY%MSIGDB_C2%PID_P53_DOWNSTREAM_PATHWAY	25	0.274	1.582	0.047	0.107	0.99
HALLMARK_KRAS_SIGNALING_UP%MSIGDB_C2%HALLMARK_KRAS_SIGNALING_UP	36	0.220	1.543	0.059	0.126	1
TOLL LIKE RECEPTOR 4 (TLR4) CASCADE%REACTOME%R-HSA-166016.1	18	0.296	1.503	0.083	0.148	1
POST-TRANSLATIONAL PROTEIN MODIFICATION%REACTOME DATABASE ID RELEASE 59%597592	79	0.143	1.480	0.087	0.161	1
CELLULAR RESPONSES TO STRESS%REACTOME DATABASE ID RELEASE 59%2262752	30	0.229	1.480	0.060	0.159	1
EGF RECEPTOR SIGNALING PATHWAY%PANTHER PATHWAY%P00018	16	0.302	1.477	0.065	0.158	1
NUCLEOTIDE METABOLISM%REACTOME DATABASE ID RELEASE 59%15869	15	0.289	1.352	0.133	0.262	1
HALLMARK_COMPLEMENT%MSIGDB_C2%HALLMARK_COMPLEMENT	20	0.249	1.336	0.132	0.275	1
DISEASES OF SIGNAL TRANSDUCTION%REACTOME%R-HSA-5663202.4	35	0.190	1.335	0.133	0.272	1
TGF_BETA_RECEPTOR%IOB%TGF_BETA_RECEPTOR	15	0.271	1.277	0.178	0.335	1
HALLMARK_IL2_STAT5_SIGNALING%MSIGDB_C2%HALLMARK_IL2_STAT5_SIGNALING	25	0.212	1.272	0.191	0.338	1
CARBOHYDRATE METABOLISM%REACTOME DATABASE ID RELEASE 59%71387	24	0.216	1.248	0.205	0.363	1
TOLL-LIKE RECEPTORS CASCADES%REACTOME%R-HSA-168898.3	20	0.236	1.244	0.196	0.363	1
PEPTIDE LIGAND-BINDING RECEPTORS%REACTOME%R-HSA-375276.4	15	0.260	1.237	0.205	0.369	1
TGF_BETA_RECEPTOR%NETPATH%TGF_BETA_RECEPTOR	17	0.241	1.220	0.228	0.387	1
B CELL ACTIVATION%REACTOME%R-HSA-983705.1	28	0.193	1.201	0.224	0.409	1
HALLMARK_ESTROGEN_RESPONSE_EARLY%MSIGDB_C2%HALLMARK_ESTROGEN_RESPONSE_EARLY	35	0.169	1.151	0.290	0.479	1
INFLAMMATION MEDIATED BY CHEMOKINE AND CYTOKINE SIGNALING PATHWAY%PANTHER PATHWAY%P00031	24	0.190	1.137	0.289	0.494	1
DISEASE%REACTOME%R-HSA-1643685.3	75	0.113	1.110	0.326	0.535	1
TRANSMEMBRANE TRANSPORT OF SMALL MOLECULES%REACTOME%R-HSA-382551.1	72	0.111	1.074	0.361	0.593	1
SIGNALING BY INSULIN RECEPTOR%REACTOME DATABASE ID RELEASE 59%74752	36	0.153	1.054	0.359	0.621	1
FATTY ACID, TRIACYLGLYCEROL, AND KETONE BODY METABOLISM%REACTOME DATABASE ID RELEASE 59%535734	22	0.186	1.043	0.402	0.634	1
SIGNALING BY SCF-KIT%REACTOME DATABASE ID RELEASE 59%1433557	35	0.152	1.040	0.387	0.631	1
FCERI MEDIATED MAPK ACTIVATION%REACTOME%R-HSA-2871796.1	33	0.150	1.036	0.391	0.631	1
IRS-MEDIATED SIGNALLING%REACTOME DATABASE ID RELEASE 59%112399	32	0.149	1.019	0.415	0.656	1

Supplemental Table 1: Continued

NGF SIGNALLING VIA TRKA FROM THE PLASMA MEMBRANE%REACTOME%R-HSA-187037.1	42	0.133	1.003	0.458	0.677	1
SIGNALING BY EGFR%REACTOME%R-HSA-177929.1	41	0.132	1.001	0.408	0.674	1
SIGNALLING TO RAS%REACTOME%R-HSA-167044.2	32	0.149	0.997	0.441	0.674	1
IGF1R SIGNALING CASCADE%REACTOME DATABASE ID RELEASE 59%2428924	32	0.149	0.996	0.466	0.668	1
INSULIN RECEPTOR SIGNALLING CASCADE%REACTOME%R-HSA-74751.3	32	0.149	0.996	0.445	0.661	1
SIGNALLING TO ERKS%REACTOME%R-HSA-187687.1	32	0.149	0.987	0.475	0.671	1
PDGF SIGNALING PATHWAY%PANTHER PATHWAY%P00047	17	0.202	0.979	0.462	0.678	1
IRS-RELATED EVENTS TRIGGERED BY IGF1R%REACTOME DATABASE ID RELEASE 59%2428928	32	0.149	0.978	0.483	0.673	1
INTERLEUKIN-2 SIGNALING%REACTOME%R-HSA-451927.2	30	0.147	0.974	0.472	0.673	1
INTERLEUKIN-3, 5 AND GM-CSF SIGNALING%REACTOME DATABASE ID RELEASE 59%512988	30	0.147	0.966	0.504	0.681	1
RET SIGNALING%REACTOME%R-HSA-8853659.3	31	0.148	0.965	0.492	0.674	1
FRS2-MEDIATED ACTIVATION%REACTOME%R-HSA-170968.1	30	0.147	0.960	0.504	0.677	1
DOWNSTREAM SIGNALING EVENTS OF B CELL RECEPTOR (BCR)%REACTOME DATABASE ID RELEASE 59%1168372	24	0.166	0.959	0.470	0.672	1
MAPK1 MAPK3 SIGNALING%REACTOME DATABASE ID RELEASE 59%5684996	29	0.146	0.956	0.503	0.671	1
SIGNALING BY LEPTIN%REACTOME DATABASE ID RELEASE 59%2586552	30	0.147	0.954	0.510	0.667	1
SIGNALLING TO P38 VIA RIT AND RIN%REACTOME DATABASE ID RELEASE 59%187706	30	0.147	0.954	0.484	0.660	1
INTERLEUKIN RECEPTOR SHC SIGNALING%REACTOME%R-HSA-912526.3	30	0.147	0.953	0.493	0.655	1
ARMS-MEDIATED ACTIVATION%REACTOME%R-HSA-170984.1	30	0.147	0.953	0.504	0.649	1
MAPK FAMILY SIGNALING CASCADES%REACTOME%R-HSA-5683057.2	30	0.147	0.951	0.533	0.645	1
PROLONGED ERK ACTIVATION EVENTS%REACTOME%R-HSA-169893.1	30	0.147	0.947	0.497	0.647	1
VEGFR2 MEDIATED CELL PROLIFERATION%REACTOME DATABASE ID RELEASE 59%5218921	30	0.147	0.940	0.524	0.651	1
HALLMARK_APOPTOSIS%MSIGDB_C2%HALLMARK_APOPTOSIS	32	0.141	0.931	0.486	0.659	1
SOS-MEDIATED SIGNALLING%REACTOME DATABASE ID RELEASE 59%112412	29	0.146	0.929	0.528	0.658	1
HALLMARK_ESTROGEN_RESPONSE_LATE%MSIGDB_C2%HALLMARK_ESTROGEN_RESPONSE_LATE	32	0.137	0.924	0.538	0.660	1
SHC1 EVENTS IN EGFR SIGNALING%REACTOME%R-HSA-180336.1	29	0.146	0.920	0.550	0.661	1
DAP12 INTERACTIONS%REACTOME DATABASE ID RELEASE 59%2172127	38	0.128	0.920	0.566	0.656	1
GRB2 EVENTS IN EGFR SIGNALING%REACTOME DATABASE ID RELEASE 59%179812	29	0.146	0.917	0.558	0.653	1
RAF MAP KINASE CASCADE%REACTOME DATABASE ID RELEASE 59%5673001	29	0.146	0.916	0.555	0.649	1
ASPARAGINE N-LINKED GLYCOSYLATION%REACTOME DATABASE ID RELEASE 59%446203	18	0.180	0.913	0.562	0.649	1
RHO GTPASE CYCLE%REACTOME%R-HSA-194840.2	17	0.187	0.913	0.533	0.643	1
DAP12 SIGNALING%REACTOME DATABASE ID RELEASE 59%2424491	37	0.126	0.898	0.588	0.661	1
GLYCOSAMINOGLYCAN METABOLISM%REACTOME%R-HSA-1630316.2	16	0.184	0.881	0.603	0.683	1
L1CAM INTERACTIONS%REACTOME%R-HSA-373760.2	15	0.188	0.879	0.601	0.680	1
SIGNALING BY NGF%REACTOME DATABASE ID RELEASE 59%166520	52	0.104	0.876	0.595	0.680	1
VEGFA-VEGFR2 PATHWAY%REACTOME%R-HSA-4420097.2	36	0.125	0.870	0.601	0.683	1
DOWNSTREAM SIGNAL TRANSDUCTION%REACTOME%R-HSA-186763.1	36	0.125	0.870	0.622	0.678	1
SIGNALING BY VEGF%REACTOME DATABASE ID RELEASE 59%194138	36	0.125	0.860	0.614	0.688	1
NEUTROPHIL DEGRANULATION%REACTOME%R-HSA-6798695.2	51	0.101	0.857	0.609	0.688	1
HALLMARK_FATTY_ACID_METABOLISM%MSIGDB_C2%HALLMARK_FATTY_ACID_METABOLISM	22	0.154	0.856	0.645	0.683	1
SIGNALING BY TYPE 1 INSULIN-LIKE GROWTH FACTOR 1 RECEPTOR (IGF1R)%REACTOME%R-HSA-2404192.2	33	0.119	0.808	0.726	0.750	1
ANGIOGENESIS%PANTHER PATHWAY%P00005	21	0.142	0.785	0.739	0.779	1
FC EPSILON RECEPTOR (FCERI) SIGNALING%REACTOME%R-HSA-2454202.1	45	0.099	0.764	0.748	0.804	1
TCF DEPENDENT SIGNALING IN RESPONSE TO WNT%REACTOME%R-HSA-201681.1	15	0.163	0.764	0.742	0.798	1
AMINO ACID AND DERIVATIVE METABOLISM%REACTOME DATABASE ID RELEASE 59%71291	24	0.125	0.728	0.782	0.841	1
GASTRIN-CREB SIGNALLING PATHWAY VIA PKC AND MAPK%REACTOME%R-HSA-881907.1	44	0.089	0.693	0.846	0.879	1
NEURONAL SYSTEM%REACTOME DATABASE ID RELEASE 59%112316	27	0.113	0.688	0.850	0.878	1
SIGNALING BY WNT%REACTOME%R-HSA-195721.3	25	0.115	0.682	0.873	0.879	1

Supplemental Table 1: Continued

GASTRIN_CCK2R_240212%PANTHER PATHWAY%P06959	16	0.128	0.613	0.939	0.939	1
SLC-MEDIATED TRANSMEMBRANE TRANSPORT%REACTOME DATABASE ID RELEASE 59%425407	28	0.078	0.497	0.992	0.990	1

ENRICHED IN CRE (DOWN-REGULATED IN REGRESSING TUMOR)						
NAME	**SIZE**	**ES**	**NES**	**NOM p-val**	**FDR q-val**	**FWER p-val**
NABA_MATRISOME%MSIGDB_C2%NABA_MATRISOME	173	-0.304	-4.402	0.000	0.000	0
NABA_CORE_MATRISOME%MSIGDB_C2%NABA_CORE_MATRISOME	61	-0.439	-4.051	0.000	0.000	0
NABA_ECM_REGULATORS%MSIGDB_C2%NABA_ECM_REGULATORS	45	-0.429	-3.369	0.000	0.000	0
EXTRACELLULAR MATRIX ORGANIZATION%REACTOME DATABASE ID RELEASE 59%1474244	68	-0.346	-3.305	0.000	0.000	0
HALLMARK_EPITHELIAL_MESENCHYMAL_TRANSITION%MSIGDB_C2%HALLMARK_EPITHELIAL_MESENCHYMAL_TRANSITION	67	-0.321	-3.015	0.000	0.000	0
METABOLISM OF LIPIDS AND LIPOPROTEINS%REACTOME%R-HSA-556833.3	102	-0.261	-2.997	0.000	0.000	0
NABA_ECM_GLYCOPROTEINS%MSIGDB_C2%NABA_ECM_GLYCOPROTEINS	41	-0.395	-2.921	0.000	0.000	0
HALLMARK_MYOGENESIS%MSIGDB_C2%HALLMARK_MYOGENESIS	20	-0.494	-2.672	0.000	0.000	0
DISEASES OF GLYCOSYLATION%REACTOME%R-HSA-3781865.1	17	-0.532	-2.610	0.000	0.001	0.01
NABA_MATRISOME_ASSOCIATED%MSIGDB_C2%NABA_MATRISOME_ASSOCIATED	112	-0.213	-2.606	0.000	0.000	0.01
ASSEMBLY OF COLLAGEN FIBRILS AND OTHER MULTIMERIC STRUCTURES%REACTOME DATABASE ID RELEASE 59%2022090	20	-0.467	-2.493	0.002	0.001	0.02
PID_AVB3_INTEGRIN_PATHWAY%MSIGDB_C2%PID_AVB3_INTEGRIN_PATHWAY	15	-0.522	-2.436	0.000	0.002	0.03
COLLAGEN FORMATION%REACTOME DATABASE ID RELEASE 59%1474290	27	-0.371	-2.277	0.000	0.004	0.08
COLLAGEN BIOSYNTHESIS AND MODIFYING ENZYMES%REACTOME DATABASE ID RELEASE 59%1650814	18	-0.444	-2.264	0.000	0.004	0.09
BIOLOGICAL OXIDATIONS%REACTOME%R-HSA-211859.1	19	-0.415	-2.235	0.002	0.005	0.11
BETA1 INTEGRIN CELL SURFACE INTERACTIONS%PATHWAY INTERACTION DATABASE NCI-NATURE CURATED DATA%BETA1 INTEGRIN CELL SURFACE INTERACTIONS	22	-0.390	-2.154	0.002	0.009	0.2
PID_INTEGRIN1_PATHWAY%MSIGDB_C2%PID_INTEGRIN1_PATHWAY	22	-0.390	-2.139	0.000	0.009	0.22
ELASTIC FIBRE FORMATION%REACTOME DATABASE ID RELEASE 59%1566948	15	-0.454	-2.130	0.002	0.009	0.23
MEMBRANE TRAFFICKING%REACTOME DATABASE ID RELEASE 59%199991	43	-0.269	-2.047	0.006	0.014	0.35
VESICLE-MEDIATED TRANSPORT%REACTOME%R-HSA-5653656.1	54	-0.223	-1.926	0.008	0.027	0.57
HALLMARK_KRAS_SIGNALING_DN%MSIGDB_C2%HALLMARK_KRAS_SIGNALING_DN	19	-0.357	-1.858	0.012	0.038	0.71
SPHINGOLIPID METABOLISM%REACTOME DATABASE ID RELEASE 59%428157	22	-0.307	-1.751	0.026	0.062	0.88
HALLMARK_XENOBIOTIC_METABOLISM%MSIGDB_C2%HALLMARK_XENOBIOTIC_METABOLISM	28	-0.262	-1.645	0.035	0.101	0.98
MUSCLE CONTRACTION%REACTOME DATABASE ID RELEASE 59%397014	20	-0.313	-1.626	0.045	0.106	0.99
PHOSPHOLIPID METABOLISM%REACTOME DATABASE ID RELEASE 59%1483257	20	-0.289	-1.552	0.043	0.144	1
INTEGRIN SIGNALLING PATHWAY%PANTHER PATHWAY%P00034	28	-0.248	-1.541	0.060	0.146	1
CLASS A 1 (RHODOPSIN-LIKE RECEPTORS)%REACTOME DATABASE ID RELEASE 59%373076	23	-0.274	-1.532	0.052	0.146	1
WNT%NETPATH%WNT	17	-0.313	-1.530	0.062	0.142	1
RESPONSE TO ELEVATED PLATELET CYTOSOLIC CA2+%REACTOME DATABASE ID RELEASE 59%76005	19	-0.288	-1.487	0.077	0.165	1
METABOLISM%REACTOME DATABASE ID RELEASE 59%1430728	210	-0.093	-1.480	0.077	0.165	1
WNT%IOB%WNT	16	-0.306	-1.480	0.064	0.160	1
PLATELET DEGRANULATION%REACTOME DATABASE ID RELEASE 59%114608	19	-0.288	-1.471	0.081	0.161	1
FORMATION OF THE CORNIFIED ENVELOPE%REACTOME%R-HSA-6809371.2	18	-0.275	-1.407	0.101	0.204	1
ALZHEIMER DISEASE-PRESENILIN PATHWAY%PANTHER PATHWAY%P00004	16	-0.280	-1.357	0.133	0.242	1
G ALPHA (I) SIGNALLING EVENTS%REACTOME DATABASE ID RELEASE 59%418594	20	-0.246	-1.346	0.130	0.246	1
PLATELET ACTIVATION, SIGNALING AND AGGREGATION%REACTOME DATABASE ID RELEASE 59%76002	32	-0.202	-1.330	0.150	0.253	1
O-LINKED GLYCOSYLATION%REACTOME%R-HSA-5173105.3	16	-0.268	-1.294	0.151	0.283	1

Supplemental Table 1: Continued

TRANSMISSION ACROSS CHEMICAL SYNAPSES%REACTOME%R-HSA-112315.3	17	-0.255	-1.269	0.181	0.303	1
SIGNALING BY GPCR%REACTOME%R-HSA-372790.2	80	-0.122	-1.255	0.179	0.310	1
GPCR LIGAND BINDING%REACTOME DATABASE ID RELEASE 59%500792	31	-0.193	-1.249	0.179	0.309	1
GPCR DOWNSTREAM SIGNALING%REACTOME%R-HSA-388396.2	41	-0.161	-1.187	0.234	0.377	1
HALLMARK_HEME_METABOLISM%MSIGDB_C2%HALLMARK_HEME_METABOLISM	20	-0.217	-1.165	0.261	0.397	1
KERATINIZATION%REACTOME%R-HSA-6805567.2	31	-0.175	-1.162	0.268	0.392	1
DEVELOPMENTAL BIOLOGY%REACTOME%R-HSA-1266738.3	108	-0.095	-1.137	0.285	0.414	1
SIGNALING BY RHO GTPASES%REACTOME DATABASE ID RELEASE 59%194315	29	-0.176	-1.095	0.343	0.466	1
HALLMARK_ADIPOGENESIS%MSIGDB_C2%HALLMARK_ADIPOGENESIS	26	-0.175	-1.069	0.349	0.495	1
NCAM SIGNALING FOR NEURITE OUT-GROWTH%REACTOME DATABASE ID RELEASE 59%375165	34	-0.154	-1.067	0.335	0.489	1
HALLMARK_APICAL_JUNCTION%MSIGDB_C2%HALLMARK_APICAL_JUNCTION	27	-0.164	-1.024	0.398	0.545	1
HALLMARK_COAGULATION%MSIGDB_C2%HALLMARK_COAGULATION	26	-0.170	-1.022	0.429	0.537	1
AXON GUIDANCE%REACTOME DATABASE ID RELEASE 59%422475	62	-0.113	-0.997	0.458	0.565	1
PI3K AKT SIGNALING%REACTOME DATABASE ID RELEASE 59%1257604	16	-0.203	-0.997	0.451	0.554	1
METABOLISM OF VITAMINS AND COFACTORS%REACTOME DATABASE ID RELEASE 59%196854	18	-0.196	-0.983	0.480	0.565	1
GAB1 SIGNALOSOME%REACTOME DATABASE ID RELEASE 59%180292	16	-0.203	-0.981	0.477	0.559	1
ROLE OF LAT2 NTAL LAB ON CALCIUM MOBILIZATION%REACTOME%R-HSA-2730905.1	16	-0.203	-0.980	0.468	0.549	1
WNT SIGNALING PATHWAY%PANTHER PATHWAY%P00057	25	-0.149	-0.885	0.599	0.689	1
ION CHANNEL TRANSPORT%REACTOME%R-HSA-983712.1	24	-0.136	-0.825	0.677	0.773	1
WNT_SIGNALING%MSIGDB_C2%WNT_SIGNALING	18	-0.152	-0.774	0.765	0.840	1
HEMOSTASIS%REACTOME%R-HSA-109582.1	65	-0.083	-0.768	0.754	0.836	1
PI3K AKT ACTIVATION%REACTOME DATABASE ID RELEASE 59%198203	17	-0.155	-0.764	0.757	0.827	1
SIGNALING PATHWAYS%REACTOME%R-HSA-162582.4	208	-0.048	-0.747	0.772	0.838	1
SIGNALING BY PDGF%REACTOME DATABASE ID RELEASE 59%186797	43	-0.099	-0.747	0.796	0.824	1
DEGRADATION OF THE EXTRACELLULAR MATRIX%REACTOME DATABASE ID RELEASE 59%1474228	21	-0.127	-0.709	0.836	0.861	1
NABA_ECM_AFFILIATED%MSIGDB_C2%NABA_ECM_AFFILIATED	17	-0.129	-0.632	0.907	0.930	1
HALLMARK_UV_RESPONSE_DN%MSIGDB_C2%HALLMARK_UV_RESPONSE_DN	35	-0.080	-0.558	0.956	0.967	1

Supplemental Table 2: Interferon Signaling Heatmap Gene List

Molecular Signature Database (MSigDB) gene lists combined ** = padj < 0.1					
[1] "INTERFERON-GAMMA SIGNALING PATHWAY%PANTHER PATHWAY%P00035"					
[2] "INTERFERON GAMMA SIGNALING%REACTOME%R-HSA-877300.1"					
[3] "INTERFERON SIGNALING%REACTOME%R-HSA-913531.1"					
[4] "INTERFERON ALPHA BETA SIGNALING%REACTOME%R-HSA-909733.1"					
Also included are 10 additional OAS genes which were identified in RNAseq data: Oas1c, Oasl2, Oas1b, Oas2, Oasl1, Oas1a, Oas1f, Oas1g, Oas1e					
	Name	**Description**	**log2 F.C.**	**stat**	**padj**
**	Oas1f	2'-5' oligoadenylate synthetase 1F [Source:MGI Symbol;Acc:MGI:2180855]	-1.42	-5.035	0
**	Cish	cytokine inducible SH2-containing protein [Source:MGI Symbol;Acc:MGI:103159]	-0.62	-4.303	5.00E-04
**	Trim62	tripartite motif-containing 62 [Source:MGI Symbol;Acc:MGI:1914775]	-0.61	-3.877	0.0024
**	Mapk13	mitogen-activated protein kinase 13 [Source:MGI Symbol;Acc:MGI:1346864]	-0.43	-3.860	0.0026
**	Mapk3	mitogen-activated protein kinase 3 [Source:MGI Symbol;Acc:MGI:1346859]	-0.49	-3.382	0.0109
**	Mapk14	mitogen-activated protein kinase 14 [Source:MGI Symbol;Acc:MGI:1346865]	-0.23	-2.573	0.0774
**	Camk2a	calcium/calmodulin-dependent protein kinase II alpha [Source:MGI Symbol;Acc:MGI:88256]	-0.84	-2.503	0.0901
**	Trim2	tripartite motif-containing 2 [Source:MGI Symbol;Acc:MGI:1933163]	-0.34	-2.455	0.0988
	Trim68	tripartite motif-containing 68 [Source:MGI Symbol;Acc:MGI:2142077]	-0.34	-2.322	0.1255
	Ubc	ubiquitin C [Source:MGI Symbol;Acc:MGI:98889]	-0.27	-2.124	0.1756
	Pias1	protein inhibitor of activated STAT 1 [Source:MGI Symbol;Acc:MGI:1913125]	-0.24	-2.055	0.1949
	Eif4g1	eukaryotic translation initiation factor 4, gamma 1 [Source:MGI Symbol;Acc:MGI:2384784]	-0.19	-1.971	0.2212
	Ncam1	neural cell adhesion molecule 1 [Source:MGI Symbol;Acc:MGI:97281]	-0.43	-1.958	0.2258
	Ciita	class II transactivator [Source:MGI Symbol;Acc:MGI:108445]	-0.41	-1.795	0.2826
	Pias3	protein inhibitor of activated STAT 3 [Source:MGI Symbol;Acc:MGI:1913126]	-0.21	-1.708	0.3201
	Plcg1	phospholipase C, gamma 1 [Source:MGI Symbol;Acc:MGI:97615]	-0.16	-1.513	0.3987
	Socs2	suppressor of cytokine signaling 2 [Source:MGI Symbol;Acc:MGI:1201787]	-0.31	-1.320	0.4849
	Nup62	nucleoporin 62 [Source:MGI Symbol;Acc:MGI:1351500]	-0.41	-1.256	0.5146
	Eif4g3	eukaryotic translation initiation factor 4 gamma, 3 [Source:MGI Symbol;Acc:MGI:1923935]	-0.11	-1.073	0.5975
	Trim46	tripartite motif-containing 46 [Source:MGI Symbol;Acc:MGI:2673000]	-0.29	-1.021	0.6192
	Ifi30	interferon gamma inducible protein 30 [Source:MGI Symbol;Acc:MGI:2137648]	-0.15	-1.004	0.6277
	H2-Q10	histocompatibility 2, Q region locus 10 [Source:MGI Symbol;Acc:MGI:95929]	-0.31	-0.928	0.663
	H2-Q1	histocompatibility 2, Q region locus 1 [Source:MGI Symbol;Acc:MGI:95928]	-0.21	-0.868	0.691
	Egr1	early growth response 1 [Source:MGI Symbol;Acc:MGI:95295]	-0.24	-0.856	0.6969
	Eif4e	eukaryotic translation initiation factor 4E [Source:MGI Symbol;Acc:MGI:95305]	-0.1	-0.762	0.7371
	Mid1	midline 1 [Source:MGI Symbol;Acc:MGI:1100537]	-0.15	-0.742	0.7468
	Socs6	suppressor of cytokine signaling 6 [Source:MGI Symbol;Acc:MGI:1924885]	-0.09	-0.701	0.766
	Mapk15	mitogen-activated protein kinase 15 [Source:MGI Symbol;Acc:MGI:2652894]	-0.17	-0.693	0.7698
	Nup214	nucleoporin 214 [Source:MGI Symbol;Acc:MGI:1095411]	-0.08	-0.658	0.7856
	Nedd4	neural precursor cell expressed, developmentally down-regulated 4 [Source:MGI Symbol;Acc:MGI:97297]	-0.1	-0.653	0.788
	Arih1	ariadne RBR E3 ubiquitin protein ligase 1 [Source:MGI Symbol;Acc:MGI:1344363]	-0.06	-0.614	0.8032
	Ip6k2	inositol hexaphosphate kinase 2 [Source:MGI Symbol;Acc:MGI:1923750]	-0.07	-0.595	0.811
	Eif4g2	eukaryotic translation initiation factor 4, gamma 2 [Source:MGI Symbol;Acc:MGI:109207]	-0.07	-0.558	0.824
	Ube2n	ubiquitin-conjugating enzyme E2N [Source:MGI Symbol;Acc:MGI:1934835]	-0.06	-0.528	0.835
	Coasy	Coenzyme A synthase [Source:MGI Symbol;Acc:MGI:1918993]	-0.08	-0.517	0.8401
	Camk2b	calcium/calmodulin-dependent protein kinase II, beta [Source:MGI Symbol;Acc:MGI:88257]	-0.17	-0.501	0.8461
	Kpna1	karyopherin (importin) alpha 1 [Source:MGI Symbol;Acc:MGI:103560]	-0.05	-0.498	0.8467

Supplemental Table 2: Continued

	H2-Aa	histocompatibility 2, class II antigen A, alpha [Source:MGI Symbol;Acc:MGI:95895]	-0.11	-0.440	0.8658
	Kpna7	karyopherin alpha 7 (importin alpha 8) [Source:MGI Symbol;Acc:MGI:2141165]	-0.1	-0.404	1
	H2-M5	histocompatibility 2, M region locus 5 [Source:MGI Symbol;Acc:MGI:95917]	-0.08	-0.232	0.9344
	Trim26	tripartite motif-containing 26 [Source:MGI Symbol;Acc:MGI:1337056]	-0.02	-0.210	0.9416
	Ptpn11	protein tyrosine phosphatase, non-receptor type 11 [Source:MGI Symbol;Acc:MGI:99511]	-0.02	-0.158	0.957
	Mapk12	mitogen-activated protein kinase 12 [Source:MGI Symbol;Acc:MGI:1353438]	-0.02	-0.112	0.9692
	Ifngr2	interferon gamma receptor 2 [Source:MGI Symbol;Acc:MGI:107654]	-0.01	-0.056	0.986
	Nupl2	nucleoporin like 2 [Source:MGI Symbol;Acc:MGI:2387631]	-0.01	-0.044	0.9894
	Irf3	interferon regulatory factor 3 [Source:MGI Symbol;Acc:MGI:1859179]	0	-0.004	0.9989
	Ptpn6	protein tyrosine phosphatase, non-receptor type 6 [Source:MGI Symbol;Acc:MGI:96055]	0	0.005	0.9987
	Trim10	tripartite motif-containing 10 [Source:MGI Symbol;Acc:MGI:1338757]	0	0.009	1
	Socs5	suppressor of cytokine signaling 5 [Source:MGI Symbol;Acc:MGI:2385459]	0	0.011	0.9972
	Kpna4	karyopherin (importin) alpha 4 [Source:MGI Symbol;Acc:MGI:1100848]	0	0.020	0.994
	Ifitm2	interferon induced transmembrane protein 2 [Source:MGI Symbol;Acc:MGI:1933382]	0.01	0.075	0.9803
	Nup88	nucleoporin 88 [Source:MGI Symbol;Acc:MGI:104900]	0.01	0.102	0.972
	Nup133	nucleoporin 133 [Source:MGI Symbol;Acc:MGI:2442620]	0.02	0.111	0.9694
	Nup35	nucleoporin 35 [Source:MGI Symbol;Acc:MGI:1916732]	0.02	0.161	0.9561
	H2-M3	histocompatibility 2, M region locus 3 [Source:MGI Symbol;Acc:MGI:95915]	0.04	0.177	0.9517
	Nup188	nucleoporin 188 [Source:MGI Symbol;Acc:MGI:2446190]	0.03	0.180	0.9504
	Mapk8	mitogen-activated protein kinase 8 [Source:MGI Symbol;Acc:MGI:1346861]	0.03	0.272	0.9239
	Trim25	tripartite motif-containing 25 [Source:MGI Symbol;Acc:MGI:102749]	0.04	0.311	0.9099
	Mapk1	mitogen-activated protein kinase 1 [Source:MGI Symbol;Acc:MGI:1346858]	0.03	0.313	0.9088
	Pom121	nuclear pore membrane protein 121 [Source:MGI Symbol;Acc:MGI:2137624]	0.05	0.377	0.8889
	Nup205	nucleoporin 205 [Source:MGI Symbol;Acc:MGI:2141625]	0.06	0.429	0.8681
	Pias4	protein inhibitor of activated STAT 4 [Source:MGI Symbol;Acc:MGI:2136940]	0.05	0.454	0.8603
	Fcgr1	Fc receptor, IgG, high affinity I [Source:MGI Symbol;Acc:MGI:95498]	0.16	0.475	0.8528
	Irf5	interferon regulatory factor 5 [Source:MGI Symbol;Acc:MGI:1350924]	0.07	0.487	0.8493
	Mapk9	mitogen-activated protein kinase 9 [Source:MGI Symbol;Acc:MGI:1346862]	0.08	0.487	0.8493
	Trim35	tripartite motif-containing 35 [Source:MGI Symbol;Acc:MGI:1914104]	0.08	0.526	0.836
	Socs7	suppressor of cytokine signaling 7 [Source:MGI Symbol;Acc:MGI:2651588]	0.07	0.540	0.8312
	Ube2e1	ubiquitin-conjugating enzyme E2E 1 [Source:MGI Symbol;Acc:MGI:107411]	0.06	0.550	0.8279
	Trim6	tripartite motif-containing 6 [Source:MGI Symbol;Acc:MGI:2137352]	0.17	0.551	0.8273
	Tyk2	tyrosine kinase 2 [Source:MGI Symbol;Acc:MGI:1929470]	0.06	0.562	0.823
	Ifnar1	interferon (alpha and beta) receptor 1 [Source:MGI Symbol;Acc:MGI:107658]	0.06	0.564	0.8224
	Rnasel	ribonuclease L (2', 5'-oligoisoadenylate synthetase-dependent) [Source:MGI Symbol;Acc:MGI:1098272]	0.13	0.593	0.8116
	Irf2	interferon regulatory factor 2 [Source:MGI Symbol;Acc:MGI:96591]	0.07	0.606	0.8065
	Eif4a1	eukaryotic translation initiation factor 4A1 [Source:MGI Symbol;Acc:MGI:95303]	0.06	0.641	0.7921
	Ndc1	NDC1 transmembrane nucleoporin [Source:MGI Symbol;Acc:MGI:1920037]	0.14	0.666	0.7827
	Trim45	tripartite motif-containing 45 [Source:MGI Symbol;Acc:MGI:1918187]	0.16	0.768	0.7348
	Prkcd	protein kinase C, delta [Source:MGI Symbol;Acc:MGI:97598]	0.08	0.791	0.726
	Camk2g	calcium/calmodulin-dependent protein kinase II gamma [Source:MGI Symbol;Acc:MGI:88259]	0.11	0.890	0.6823
	Vcam1	vascular cell adhesion molecule 1 [Source:MGI Symbol;Acc:MGI:98926]	0.28	0.905	0.6754
	Eif4a2	eukaryotic translation initiation factor 4A2 [Source:MGI Symbol;Acc:MGI:106906]	0.11	0.945	0.6543
	Socs4	suppressor of cytokine signaling 4 [Source:MGI Symbol;Acc:MGI:1914546]	0.12	0.967	0.6444
	Nup155	nucleoporin 155 [Source:MGI Symbol;Acc:MGI:2181182]	0.13	0.972	0.6423

Supplemental Table 2: Continued

	Tpr	translocated promoter region, nuclear basket protein [Source:MGI Symbol;Acc:MGI:1922066]	0.11	0.988	0.6352
	Trim3	tripartite motif-containing 3 [Source:MGI Symbol;Acc:MGI:1860040]	0.14	1.017	0.6208
	Irf4	interferon regulatory factor 4 [Source:MGI Symbol;Acc:MGI:1096873]	0.32	1.022	0.6184
	Pin1	protein (peptidyl-prolyl cis/trans isomerase) NIMA-interacting 1 [Source:MGI Symbol;Acc:MGI:1346036]	0.13	1.054	0.6056
	Trim17	tripartite motif-containing 17 [Source:MGI Symbol;Acc:MGI:1861440]	0.36	1.071	0.5986
	Isg20	interferon-stimulated protein [Source:MGI Symbol;Acc:MGI:1928895]	0.22	1.093	0.5878
	Ptafr	platelet-activating factor receptor [Source:MGI Symbol;Acc:MGI:106066]	0.37	1.172	0.5529
	Nup160	nucleoporin 160 [Source:MGI Symbol;Acc:MGI:1926227]	0.17	1.199	0.5408
	Trim8	tripartite motif-containing 8 [Source:MGI Symbol;Acc:MGI:1933302]	0.12	1.220	0.5309
	Trim14	tripartite motif-containing 14 [Source:MGI Symbol;Acc:MGI:1921985]	0.35	1.230	0.5269
	Ranbp2	RAN binding protein 2 [Source:MGI Symbol;Acc:MGI:894323]	0.14	1.237	0.5233
	Nup153	nucleoporin 153 [Source:MGI Symbol;Acc:MGI:2385621]	0.15	1.250	0.5165
	Pias2	protein inhibitor of activated STAT 2 [Source:MGI Symbol;Acc:MGI:1096566]	0.16	1.272	0.5076
	Jak1	Janus kinase 1 [Source:MGI Symbol;Acc:MGI:96628]	0.13	1.304	0.4924
	Jak2	Janus kinase 2 [Source:MGI Symbol;Acc:MGI:96629]	0.16	1.332	0.4797
	Kpnb1	karyopherin (importin) beta 1 [Source:MGI Symbol;Acc:MGI:107532]	0.17	1.339	0.4765
	Ppm1b	protein phosphatase 1B, magnesium dependent, beta isoform [Source:MGI Symbol;Acc:MGI:101841]	0.14	1.348	0.4727
	Nup50	nucleoporin 50 [Source:MGI Symbol;Acc:MGI:1351502]	0.15	1.398	0.4501
	Nup93	nucleoporin 93 [Source:MGI Symbol;Acc:MGI:1919055]	0.19	1.435	0.4329
	Uba7	ubiquitin-like modifier activating enzyme 7 [Source:MGI Symbol;Acc:MGI:1349462]	0.41	1.489	0.4095
	Ifitm3	interferon induced transmembrane protein 3 [Source:MGI Symbol;Acc:MGI:1913391]	0.35	1.490	0.4091
	Oasl1	2'-5' oligoadenylate synthetase-like 1 [Source:MGI Symbol;Acc:MGI:2180849]	0.5	1.514	0.3985
	Nup37	nucleoporin 37 [Source:MGI Symbol;Acc:MGI:1919964]	0.23	1.517	0.397
	Aaas	achalasia, adrenocortical insufficiency, alacrimia [Source:MGI Symbol;Acc:MGI:2443767]	0.27	1.596	0.3641
	Nup107	nucleoporin 107 [Source:MGI Symbol;Acc:MGI:2143854]	0.23	1.636	0.3462
	Camk2d	calcium/calmodulin-dependent protein kinase II, delta [Source:MGI Symbol;Acc:MGI:1341265]	0.22	1.652	0.3407
	Nup54	nucleoporin 54 [Source:MGI Symbol;Acc:MGI:1920460]	0.23	1.700	0.3231
	Eif4a3	eukaryotic translation initiation factor 4A3 [Source:MGI Symbol;Acc:MGI:1923731]	0.2	1.739	0.3068
	Ifngr1	interferon gamma receptor 1 [Source:MGI Symbol;Acc:MGI:107655]	0.2	1.771	0.2928
	Samhd1	SAM domain and HD domain, 1 [Source:MGI Symbol;Acc:MGI:1927468]	0.3	1.808	0.278
	Irf6	interferon regulatory factor 6 [Source:MGI Symbol;Acc:MGI:1859211]	0.3	1.855	0.2613
	Kpna3	karyopherin (importin) alpha 3 [Source:MGI Symbol;Acc:MGI:1100863]	0.21	1.863	0.2577
	Nup210	nucleoporin 210 [Source:MGI Symbol;Acc:MGI:1859555]	0.47	1.872	0.2549
	Nup85	nucleoporin 85 [Source:MGI Symbol;Acc:MGI:3046173]	0.24	1.881	0.2516
	Flnb	filamin, beta [Source:MGI Symbol;Acc:MGI:2446089]	0.29	2.006	0.21
	Ifi27	interferon, alpha-inducible protein 27 [Source:MGI Symbol;Acc:MGI:1277180]	0.45	2.094	0.1841
	Gbp5	guanylate binding protein 5 [Source:MGI Symbol;Acc:MGI:2429943]	0.77	2.331	0.1237
	Oas1c	2'-5' oligoadenylate synthetase 1C [Source:MGI Symbol;Acc:MGI:2149633]	0.56	2.410	0.1075
**	H2-Eb1	histocompatibility 2, class II antigen E beta [Source:MGI Symbol;Acc:MGI:95901]	0.61	2.458	0.0984
**	Rae1	ribonucleic acid export 1 [Source:MGI Symbol;Acc:MGI:1913929]	0.29	2.576	0.0772
**	Socs1	suppressor of cytokine signaling 1 [Source:MGI Symbol;Acc:MGI:1354910]	0.51	2.579	0.0766
**	Adar	adenosine deaminase, RNA-specific [Source:MGI Symbol;Acc:MGI:1889575]	0.47	2.597	0.0741
**	Pml	promyelocytic leukemia [Source:MGI Symbol;Acc:MGI:104662]	0.5	2.615	0.0714
**	Ifit2	interferon-induced protein with tetratricopeptide repeats 2 [Source:MGI Symbol;Acc:MGI:99449]	0.85	2.755	0.0533
**	Nup43	nucleoporin 43 [Source:MGI Symbol;Acc:MGI:1917162]	0.33	2.813	0.0468

Supplemental Table 2: Continued

**	Trim21	tripartite motif-containing 21 [Source:MGI Symbol;Acc:MGI:106657]	0.66	3.057	0.0262
**	Psmb8	proteasome (prosome, macropain) subunit, beta type 8 (large multifunctional peptidase 7) [Source:MGI Symbol;Acc:MGI:1346527]	0.81	3.334	0.0126
**	Oas1e	2'-5' oligoadenylate synthetase 1E [Source:MGI Symbol;Acc:MGI:2180856]	0.98	3.368	0.0113
**	Irf1	interferon regulatory factor 1 [Source:MGI Symbol;Acc:MGI:96590]	0.53	3.529	0.0072
**	B2m	beta-2 microglobulin [Source:MGI Symbol;Acc:MGI:88127]	0.82	3.627	0.0054
**	Cd44	CD44 antigen [Source:MGI Symbol;Acc:MGI:88338]	0.4	3.702	0.0043
**	Ifi35	interferon-induced protein 35 [Source:MGI Symbol;Acc:MGI:1917360]	0.76	3.702	0.0043
**	Trim12c	tripartite motif-containing 12C [Source:MGI Symbol;Acc:MGI:4821183]	0.78	3.718	0.004
**	Eif2ak2	eukaryotic translation initiation factor 2-alpha kinase 2 [Source:MGI Symbol;Acc:MGI:1353449]	0.78	3.819	0.0029
**	Oas3	2'-5' oligoadenylate synthetase 3 [Source:MGI Symbol;Acc:MGI:2180850]	1.32	3.954	0.0019
**	Oas2	2'-5' oligoadenylate synthetase 2 [Source:MGI Symbol;Acc:MGI:2180852]	1.32	4.019	0.0015
**	Rsad2	radical S-adenosyl methionine domain containing 2 [Source:MGI Symbol;Acc:MGI:1929628]	1.29	4.109	1
**	Stat1	signal transducer and activator of transcription 1 [Source:MGI Symbol;Acc:MGI:103063]	0.69	4.125	0.001
**	Ube2l6	ubiquitin-conjugating enzyme E2L 6 [Source:MGI Symbol;Acc:MGI:1914500]	1.09	4.202	8.00E-04
**	Stat2	signal transducer and activator of transcription 2 [Source:MGI Symbol;Acc:MGI:103039]	0.98	4.257	6.00E-04
**	Gbp7	guanylate binding protein 7 [Source:MGI Symbol;Acc:MGI:2444421]	1.13	4.385	4.00E-04
**	Irf9	interferon regulatory factor 9 [Source:MGI Symbol;Acc:MGI:107587]	0.85	4.401	4.00E-04
**	Gbp3	guanylate binding protein 3 [Source:MGI Symbol;Acc:MGI:1926263]	1.39	4.489	3.00E-04
**	Ptpn1	protein tyrosine phosphatase, non-receptor type 1 [Source:MGI Symbol;Acc:MGI:97805]	0.4	4.515	2.00E-04
**	Socs3	suppressor of cytokine signaling 3 [Source:MGI Symbol;Acc:MGI:1201791]	0.57	4.517	2.00E-04
**	Irf7	interferon regulatory factor 7 [Source:MGI Symbol;Acc:MGI:1859212]	1.52	4.524	2.00E-04
**	Mapk11	mitogen-activated protein kinase 11 [Source:MGI Symbol;Acc:MGI:1338024]	0.82	4.593	2.00E-04
**	Ddx58	DEAD (Asp-Glu-Ala-Asp) box polypeptide 58 [Source:MGI Symbol;Acc:MGI:2442858]	1.18	4.743	1.00E-04
**	Isg15	ISG15 ubiquitin-like modifier [Source:MGI Symbol;Acc:MGI:1855694]	1.58	4.767	1.00E-04
**	Icam1	intercellular adhesion molecule 1 [Source:MGI Symbol;Acc:MGI:96392]	0.55	4.782	1.00E-04
**	Oasl2	2'-5' oligoadenylate synthetase-like 2 [Source:MGI Symbol;Acc:MGI:1344390]	1.63	4.915	0
**	Gbp2	guanylate binding protein 2 [Source:MGI Symbol;Acc:MGI:102772]	1.46	5.243	0
**	Bst2	bone marrow stromal cell antigen 2 [Source:MGI Symbol;Acc:MGI:1916800]	1.62	5.348	0
**	Oas1b	2'-5' oligoadenylate synthetase 1B [Source:MGI Symbol;Acc:MGI:97430]	1.42	5.406	0
**	Ifit3b	interferon-induced protein with tetratricopeptide repeats 3B [Source:MGI Symbol;Acc:MGI:3698419]	2.1	6.261	0
**	Mt2	metallothionein 2 [Source:MGI Symbol;Acc:MGI:97172]	0.76	7.203	0
**	Oas1g	2'-5' oligoadenylate synthetase 1G [Source:MGI Symbol;Acc:MGI:97429]	2.35	7.609	0
**	Oas1a	2'-5' oligoadenylate synthetase 1A [Source:MGI Symbol;Acc:MGI:2180860]	2.36	8.004	0
**	Usp18	ubiquitin specific peptidase 18 [Source:MGI Symbol;Acc:MGI:1344364]	2.73	8.831	0

Supplemental Table 3: p53 Signaling Heatmap Gene List

Molecular Signature Database (MSigDB) gene list: ** = padj < 0.1					
"HALLMARK_P53_PATHWAY%MSIGDB_C2%HALLMARK_P53_PATHWAY"					
	Name	**Description**	**log2 F.C.**	**stat**	**padj**
**	Ctsd	cathepsin D [Source:MGI Symbol;Acc:MGI:88562]	-1.12	-7.316	0
**	Slc7a11	solute carrier family 7 (cationic amino acid transporter, y+ system), member 11 [Source:MGI Symbol;Acc:MGI:1347355]	-1.36	-6.953	0
**	Cyfip2	cytoplasmic FMR1 interacting protein 2 [Source:MGI Symbol;Acc:MGI:1924134]	-1.11	-5.856	0
**	Klk8	kallikrein related-peptidase 8 [Source:MGI Symbol;Acc:MGI:1343327]	-0.52	-5.317	0
**	Gm2a	GM2 ganglioside activator protein [Source:MGI Symbol;Acc:MGI:95762]	-0.97	-5.263	0
**	Inhbb	inhibin beta-B [Source:MGI Symbol;Acc:MGI:96571]	-0.72	-4.424	3.00E-04
**	App	amyloid beta (A4) precursor protein [Source:MGI Symbol;Acc:MGI:88059]	-0.41	-3.971	0.0018
**	Jun	jun proto-oncogene [Source:MGI Symbol;Acc:MGI:96646]	-0.44	-3.965	0.0018
**	Kif13b	kinesin family member 13B [Source:MGI Symbol;Acc:MGI:1098265]	-0.46	-3.845	0.0027
**	F2r	coagulation factor II (thrombin) receptor [Source:MGI Symbol;Acc:MGI:101802]	-0.9	-3.638	0.0052
**	Eps8l2	EPS8-like 2 [Source:MGI Symbol;Acc:MGI:2138828]	-0.42	-3.618	0.0055
**	Slc3a2	solute carrier family 3 (activators of dibasic and neutral amino acid transport), member 2 [Source:MGI Symbol;Acc:MGI:96955]	-0.52	-3.540	0.007
**	Plk3	polo-like kinase 3 [Source:MGI Symbol;Acc:MGI:109604]	-0.45	-3.430	0.0097
**	Steap3	STEAP family member 3 [Source:MGI Symbol;Acc:MGI:1915678]	-0.72	-3.119	0.0224
**	Gpx2	glutathione peroxidase 2 [Source:MGI Symbol;Acc:MGI:106609]	-1.05	-3.117	0.0225
**	Fdxr	ferredoxin reductase [Source:MGI Symbol;Acc:MGI:104724]	-0.39	-2.900	0.0383
**	Foxo3	forkhead box O3 [Source:MGI Symbol;Acc:MGI:1890081]	-0.41	-2.781	0.0503
**	Ldhb	lactate dehydrogenase B [Source:MGI Symbol;Acc:MGI:96763]	-0.82	-2.751	0.0538
**	Txnip	thioredoxin interacting protein [Source:MGI Symbol;Acc:MGI:1889549]	-0.58	-2.656	0.0654
**	Tob1	transducer of ErbB-2.1 [Source:MGI Symbol;Acc:MGI:1349721]	-0.31	-2.625	0.0699
**	Hmox1	heme oxygenase 1 [Source:MGI Symbol;Acc:MGI:96163]	-0.54	-2.547	0.082
**	Sesn1	sestrin 1 [Source:MGI Symbol;Acc:MGI:2155278]	-0.45	-2.537	0.0838
**	Fuca1	fucosidase, alpha-L- 1, tissue [Source:MGI Symbol;Acc:MGI:95593]	-0.42	-2.532	0.0848
**	Ctsf	cathepsin F [Source:MGI Symbol;Acc:MGI:1861434]	-0.56	-2.482	0.0938
	Btg1	B cell translocation gene 1, anti-proliferative [Source:MGI Symbol;Acc:MGI:88215]	-0.41	-2.415	0.1066
	Ptpn14	protein tyrosine phosphatase, non-receptor type 14 [Source:MGI Symbol;Acc:MGI:102467]	-0.3	-2.358	0.1178
	Sphk1	sphingosine kinase 1 [Source:MGI Symbol;Acc:MGI:1316649]	-0.45	-2.326	0.1249
	Acvr1b	activin A receptor, type 1B [Source:MGI Symbol;Acc:MGI:1338944]	-0.32	-2.238	0.1457
	Hist1h1c	histone cluster 1, H1c [Source:MGI Symbol;Acc:MGI:1931526]	-0.38	-2.222	0.1495
	Lif	leukemia inhibitory factor [Source:MGI Symbol;Acc:MGI:96787]	-0.5	-2.085	0.1866
	Tcn2	transcobalamin 2 [Source:MGI Symbol;Acc:MGI:98534]	-0.44	-2.030	0.2032
	Gadd45a	growth arrest and DNA-damage-inducible 45 alpha [Source:MGI Symbol;Acc:MGI:107799]	-0.28	-1.958	0.226
	Trib3	tribbles pseudokinase 3 [Source:MGI Symbol;Acc:MGI:1345675]	-0.31	-1.939	0.2321
	Xpc	xeroderma pigmentosum, complementation group C [Source:MGI Symbol;Acc:MGI:103557]	-0.23	-1.897	0.2456
	Cgrrf1	cell growth regulator with ring finger domain 1 [Source:MGI Symbol;Acc:MGI:1916368]	-0.37	-1.821	0.2733
	Mxd4	Max dimerization protein 4 [Source:MGI Symbol;Acc:MGI:104991]	-0.29	-1.667	0.3352
	Zfp36l1	zinc finger protein 36, C3H type-like 1 [Source:MGI Symbol;Acc:MGI:107946]	-0.22	-1.551	0.3836
	Sec61a1	Sec61 alpha 1 subunit (S. cerevisiae) [Source:MGI Symbol;Acc:MGI:1858417]	-0.18	-1.542	0.3876
	Ralgds	ral guanine nucleotide dissociation stimulator [Source:MGI Symbol;Acc:MGI:107485]	-0.14	-1.422	0.438
	Csrnp2	cysteine-serine-rich nuclear protein 2 [Source:MGI Symbol;Acc:MGI:2386852]	-0.34	-1.313	0.4883

Supplemental Table 3: Continued

	Btg2	B cell translocation gene 2, anti-proliferative [Source:MGI Symbol;Acc:MGI:108384]	-0.17	-1.173	0.5522
	Alox8	arachidonate 8-lipoxygenase [Source:MGI Symbol;Acc:MGI:1098228]	-0.39	-1.168	0.5543
	Ppm1d	protein phosphatase 1D magnesium-dependent, delta isoform [Source:MGI Symbol;Acc:MGI:1858214]	-0.18	-1.148	0.5632
	H2afj	H2A histone family, member J [Source:MGI Symbol;Acc:MGI:3606192]	-0.14	-1.145	0.5641
	Sp1	trans-acting transcription factor 1 [Source:MGI Symbol;Acc:MGI:98372]	-0.13	-1.066	0.601
	Lrmp	lymphoid-restricted membrane protein [Source:MGI Symbol;Acc:MGI:108424]	-0.28	-1.006	0.6263
	Ifi30	interferon gamma inducible protein 30 [Source:MGI Symbol;Acc:MGI:2137648]	-0.15	-1.004	0.6277
	Irak1	interleukin-1 receptor-associated kinase 1 [Source:MGI Symbol;Acc:MGI:107420]	-0.1	-0.996	0.6318
	Zbtb16	zinc finger and BTB domain containing 16 [Source:MGI Symbol;Acc:MGI:103222]	-0.33	-0.991	0.6337
	Cdkn2aip	CDKN2A interacting protein [Source:MGI Symbol;Acc:MGI:1918175]	-0.16	-0.961	0.647
	Rhbdf2	rhomboid 5 homolog 2 [Source:MGI Symbol;Acc:MGI:2442473]	-0.11	-0.910	0.6732
	Mxd1	MAX dimerization protein 1 [Source:MGI Symbol;Acc:MGI:96908]	-0.15	-0.852	0.6992
	Hexim1	hexamethylene bis-acetamide inducible 1 [Source:MGI Symbol;Acc:MGI:2385923]	-0.11	-0.847	0.7015
	Rxra	retinoid X receptor alpha [Source:MGI Symbol;Acc:MGI:98214]	-0.08	-0.813	0.7175
	Sertad3	SERTA domain containing 3 [Source:MGI Symbol;Acc:MGI:2180697]	-0.11	-0.759	0.7388
	Ier5	immediate early response 5 [Source:MGI Symbol;Acc:MGI:1337072]	-0.08	-0.757	0.7399
	Rb1	RB transcriptional corepressor 1 [Source:MGI Symbol;Acc:MGI:97874]	-0.08	-0.738	0.7487
	Cdkn2b	cyclin-dependent kinase inhibitor 2B (p15, inhibits CDK4) [Source:MGI Symbol;Acc:MGI:104737]	-0.12	-0.630	0.7969
	Ip6k2	inositol hexaphosphate kinase 2 [Source:MGI Symbol;Acc:MGI:1923750]	-0.07	-0.595	0.811
	Vdr	vitamin D receptor [Source:MGI Symbol;Acc:MGI:103076]	-0.08	-0.560	0.8233
	Plxnb2	plexin B2 [Source:MGI Symbol;Acc:MGI:2154239]	-0.06	-0.550	0.8276
	Vamp8	vesicle-associated membrane protein 8 [Source:MGI Symbol;Acc:MGI:1336882]	-0.07	-0.543	0.8299
	Tm7sf3	transmembrane 7 superfamily member 3 [Source:MGI Symbol;Acc:MGI:1914873]	-0.11	-0.517	0.8402
	Notch1	notch 1 [Source:MGI Symbol;Acc:MGI:97363]	-0.07	-0.511	0.8417
	Tm4sf1	transmembrane 4 superfamily member 1 [Source:MGI Symbol;Acc:MGI:104678]	-0.12	-0.487	0.8495
	Baiap2	brain-specific angiogenesis inhibitor 1-associated protein 2 [Source:MGI Symbol;Acc:MGI:2137336]	-0.06	-0.479	0.8515
	Cdh13	cadherin 13 [Source:MGI Symbol;Acc:MGI:99551]	-0.06	-0.454	0.8603
	Ppp1r15a	protein phosphatase 1, regulatory (inhibitor) subunit 15A [Source:MGI Symbol;Acc:MGI:1927072]	-0.07	-0.442	0.8649
	Osgin1	oxidative stress induced growth inhibitor 1 [Source:MGI Symbol;Acc:MGI:1919089]	-0.09	-0.430	0.868
	Mknk2	MAP kinase-interacting serine/threonine kinase 2 [Source:MGI Symbol;Acc:MGI:894279]	-0.07	-0.404	0.8785
	Retsat	retinol saturase (all trans retinol 13,14 reductase) [Source:MGI Symbol;Acc:MGI:1914692]	-0.05	-0.359	0.8957
	Klf4	Kruppel-like factor 4 (gut) [Source:MGI Symbol;Acc:MGI:1342287]	-0.05	-0.350	0.8981
	Tpd52l1	tumor protein D52-like 1 [Source:MGI Symbol;Acc:MGI:1298386]	-0.07	-0.332	0.9027
	Ccnd2	cyclin D2 [Source:MGI Symbol;Acc:MGI:88314]	-0.1	-0.310	0.9104
	Nudt15	nudix (nucleoside diphosphate linked moiety X)-type motif 15 [Source:MGI Symbol;Acc:MGI:2443366]	-0.09	-0.303	0.913
	Krt17	keratin 17 [Source:MGI Symbol;Acc:MGI:96691]	-0.1	-0.298	0.9145
	Perp	PERP, TP53 apoptosis effector [Source:MGI Symbol;Acc:MGI:1929938]	-0.02	-0.208	0.9424
	Prmt2	protein arginine N-methyltransferase 2 [Source:MGI Symbol;Acc:MGI:1316652]	-0.03	-0.189	0.9471
	Rpl18	ribosomal protein L18 [Source:MGI Symbol;Acc:MGI:98003]	-0.02	-0.166	0.9548
	Rgs16	regulator of G-protein signaling 16 [Source:MGI Symbol;Acc:MGI:108407]	-0.03	-0.096	0.9737
	Ak1	adenylate kinase 1 [Source:MGI Symbol;Acc:MGI:87977]	-0.02	-0.092	0.9747
	Ddb2	damage specific DNA binding protein 2 [Source:MGI Symbol;Acc:MGI:1355314]	0	-0.020	0.9941
	Hdac3	histone deacetylase 3 [Source:MGI Symbol;Acc:MGI:1343091]	0	-0.013	0.997
	Ddit3	DNA-damage inducible transcript 3 [Source:MGI Symbol;Acc:MGI:109247]	0	-0.012	0.9971
	Fgf13	fibroblast growth factor 13 [Source:MGI Symbol;Acc:MGI:109178]	0	0.004	0.999

Supplemental Table 3: Continued

	Casp1	caspase 1 [Source:MGI Symbol;Acc:MGI:96544]	0.02	0.116	0.9675
	Abat	4-aminobutyrate aminotransferase [Source:MGI Symbol;Acc:MGI:2443582]	0.03	0.122	0.9659
	Ier3	immediate early response 3 [Source:MGI Symbol;Acc:MGI:104814]	0.03	0.142	0.9601
	Clca2	chloride channel accessory 2 [Source:MGI Symbol;Acc:MGI:2139758]	0.02	0.158	0.957
	Cd81	CD81 antigen [Source:MGI Symbol;Acc:MGI:1096398]	0.03	0.160	0.9563
	Cdkn2a	cyclin-dependent kinase inhibitor 2A [Source:MGI Symbol;Acc:MGI:104738]	0.05	0.193	0.9461
	Sat1	spermidine/spermine N1-acetyl transferase 1 [Source:MGI Symbol;Acc:MGI:98233]	0.03	0.207	0.9427
	Rrp8	ribosomal RNA processing 8, methyltransferase, homolog (yeast) [Source:MGI Symbol;Acc:MGI:1914251]	0.04	0.230	0.9346
	Triap1	TP53 regulated inhibitor of apoptosis 1 [Source:MGI Symbol;Acc:MGI:1916326]	0.03	0.232	0.934
	St14	suppression of tumorigenicity 14 (colon carcinoma) [Source:MGI Symbol;Acc:MGI:1338881]	0.03	0.243	0.9319
	Trp53	transformation related protein 53 [Source:MGI Symbol;Acc:MGI:98834]	0.04	0.302	0.9135
	Slc35d1	solute carrier family 35 (UDP-glucuronic acid/UDP-N-acetylgalactosamine dual transporter), member D1 [Source:MGI Symbol;Acc:MGI:2140361]	0.06	0.317	0.9079
	Wwp1	WW domain containing E3 ubiquitin protein ligase 1 [Source:MGI Symbol;Acc:MGI:1861728]	0.05	0.342	0.8994
	Rad9a	RAD9 checkpoint clamp component A [Source:MGI Symbol;Acc:MGI:1328356]	0.07	0.356	0.8966
	Pom121	nuclear pore membrane protein 121 [Source:MGI Symbol;Acc:MGI:2137624]	0.05	0.377	0.8889
	Ccp110	centriolar coiled coil protein 110 [Source:MGI Symbol;Acc:MGI:2141942]	0.08	0.420	0.8721
	Mapkapk3	mitogen-activated protein kinase-activated protein kinase 3 [Source:MGI Symbol;Acc:MGI:2143163]	0.07	0.462	0.8582
	Ephx1	epoxide hydrolase 1, microsomal [Source:MGI Symbol;Acc:MGI:95405]	0.1	0.463	0.8577
	Ccnk	cyclin K [Source:MGI Symbol;Acc:MGI:1276106]	0.06	0.505	0.8442
	Aen	apoptosis enhancing nuclease [Source:MGI Symbol;Acc:MGI:1915298]	0.12	0.528	0.835
	Nupr1	nuclear protein transcription regulator 1 [Source:MGI Symbol;Acc:MGI:1891834]	0.08	0.537	0.8327
	Ikbkap	inhibitor of kappa light polypeptide enhancer in B cells, kinase complex-associated protein [Source:MGI Symbol;Acc:MGI:1914544]	0.08	0.555	0.8253
	Tspyl2	TSPY-like 2 [Source:MGI Symbol;Acc:MGI:106244]	0.09	0.573	0.8185
	Wrap73	WD repeat containing, antisense to Trp73 [Source:MGI Symbol;Acc:MGI:1891749]	0.1	0.583	0.8149
	Tprkb	Tp53rk binding protein [Source:MGI Symbol;Acc:MGI:1917036]	0.07	0.585	0.8143
	Rab40c	Rab40C, member RAS oncogene family [Source:MGI Symbol;Acc:MGI:2183454]	0.08	0.591	0.8125
	Ankra2	ankyrin repeat, family A (RFXANK-like), 2 [Source:MGI Symbol;Acc:MGI:1915808]	0.09	0.603	0.8079
	Trp63	transformation related protein 63 [Source:MGI Symbol;Acc:MGI:1330810]	0.09	0.619	0.8018
	Slc19a2	solute carrier family 19 (thiamine transporter), member 2 [Source:MGI Symbol;Acc:MGI:1928761]	0.08	0.632	0.7961
	Il1a	interleukin 1 alpha [Source:MGI Symbol;Acc:MGI:96542]	0.16	0.647	0.7898
	Zmat3	zinc finger matrin type 3 [Source:MGI Symbol;Acc:MGI:1195270]	0.1	0.679	0.7766
	Fbxw7	F-box and WD-40 domain protein 7 [Source:MGI Symbol;Acc:MGI:1354695]	0.12	0.704	0.7646
	Polh	polymerase (DNA directed), eta (RAD 30 related) [Source:MGI Symbol;Acc:MGI:1891457]	0.1	0.714	0.759
	Cebpa	CCAAT/enhancer binding protein (C/EBP), alpha [Source:MGI Symbol;Acc:MGI:99480]	0.14	0.858	0.696
	Epha2	Eph receptor A2 [Source:MGI Symbol;Acc:MGI:95278]	0.12	0.897	0.679
	Jag2	jagged 2 [Source:MGI Symbol;Acc:MGI:1098270]	0.17	0.904	0.676
	Fas	Fas (TNF receptor superfamily member 6) [Source:MGI Symbol;Acc:MGI:95484]	0.22	0.924	0.6656
	Itgb4	integrin beta 4 [Source:MGI Symbol;Acc:MGI:96613]	0.18	0.930	0.6625
	Upp1	uridine phosphorylase 1 [Source:MGI Symbol;Acc:MGI:1097668]	0.21	0.945	0.6542
	Ada	adenosine deaminase [Source:MGI Symbol;Acc:MGI:87916]	0.18	0.953	0.6509
	Ei24	etoposide induced 2.4 mRNA [Source:MGI Symbol;Acc:MGI:108090]	0.09	0.977	0.64
	Dgka	diacylglycerol kinase, alpha [Source:MGI Symbol;Acc:MGI:102952]	0.13	1.011	0.6243
	Serpinb5	serine (or cysteine) peptidase inhibitor, clade B, member 5 [Source:MGI Symbol;Acc:MGI:109579]	0.12	1.030	0.6159
	Cd82	CD82 antigen [Source:MGI Symbol;Acc:MGI:104651]	0.17	1.058	0.6046

Supplemental Table 3: Continued

	Cdk5r1	cyclin-dependent kinase 5, regulatory subunit 1 (p35) [Source:MGI Symbol;Acc:MGI:101764]	0.23	1.078	0.595
	Plk2	polo-like kinase 2 [Source:MGI Symbol;Acc:MGI:1099790]	0.15	1.081	0.5936
	Hras	Harvey rat sarcoma virus oncogene [Source:MGI Symbol;Acc:MGI:96224]	0.15	1.167	0.5545
	Rad51c	RAD51 paralog C [Source:MGI Symbol;Acc:MGI:2150020]	0.28	1.177	0.551
	Rchy1	ring finger and CHY zinc finger domain containing 1 [Source:MGI Symbol;Acc:MGI:1915348]	0.12	1.211	0.5352
	Nol8	nucleolar protein 8 [Source:MGI Symbol;Acc:MGI:1918180]	0.13	1.240	0.5216
	Hbegf	heparin-binding EGF-like growth factor [Source:MGI Symbol;Acc:MGI:96070]	0.33	1.262	0.512
	Tgfb1	transforming growth factor, beta 1 [Source:MGI Symbol;Acc:MGI:98725]	0.24	1.307	0.4907
	Bax	BCL2-associated X protein [Source:MGI Symbol;Acc:MGI:99702]	0.21	1.310	0.4891
	Vwa5a	von Willebrand factor A domain containing 5A [Source:MGI Symbol;Acc:MGI:1915026]	0.19	1.335	0.4785
	Dram1	DNA-damage regulated autophagy modulator 1 [Source:MGI Symbol;Acc:MGI:1918962]	0.21	1.347	0.473
	Trafd1	TRAF type zinc finger domain containing 1 [Source:MGI Symbol;Acc:MGI:1923551]	0.16	1.369	0.4624
	Rnf19b	ring finger protein 19B [Source:MGI Symbol;Acc:MGI:1922484]	0.22	1.396	0.4509
	Abhd4	abhydrolase domain containing 4 [Source:MGI Symbol;Acc:MGI:1915938]	0.18	1.398	0.4501
	Ptpre	protein tyrosine phosphatase, receptor type, E [Source:MGI Symbol;Acc:MGI:97813]	0.32	1.434	0.4333
	Iscu	iron-sulfur cluster assembly enzyme [Source:MGI Symbol;Acc:MGI:1913633]	0.17	1.446	0.4282
	Ccnd3	cyclin D3 [Source:MGI Symbol;Acc:MGI:88315]	0.17	1.453	0.4253
	Tnni1	troponin I, skeletal, slow 1 [Source:MGI Symbol;Acc:MGI:105073]	0.46	1.455	0.4246
	Pitpnc1	phosphatidylinositol transfer protein, cytoplasmic 1 [Source:MGI Symbol;Acc:MGI:1919045]	0.4	1.514	0.3984
	Bmp2	bone morphogenetic protein 2 [Source:MGI Symbol;Acc:MGI:88177]	0.34	1.653	0.3407
	Prkab1	protein kinase, AMP-activated, beta 1 non-catalytic subunit [Source:MGI Symbol;Acc:MGI:1336167]	0.24	1.686	0.3274
	Blcap	bladder cancer associated protein [Source:MGI Symbol;Acc:MGI:1858907]	0.18	1.702	0.3218
	Def6	differentially expressed in FDCP 6 [Source:MGI Symbol;Acc:MGI:1346328]	0.24	1.780	0.2889
	Tgfa	transforming growth factor alpha [Source:MGI Symbol;Acc:MGI:98724]	0.3	1.795	0.2826
	Hint1	histidine triad nucleotide binding protein 1 [Source:MGI Symbol;Acc:MGI:1321133]	0.22	1.823	0.2726
	Bak1	BCL2-antagonist/killer 1 [Source:MGI Symbol;Acc:MGI:1097161]	0.3	1.831	0.2694
	Tchh	trichohyalin [Source:MGI Symbol;Acc:MGI:2177944]	0.39	1.848	0.2634
	Phlda3	pleckstrin homology like domain, family A, member 3 [Source:MGI Symbol;Acc:MGI:1351485]	0.33	2.006	0.21
	Fam162a	family with sequence similarity 162, member A [Source:MGI Symbol;Acc:MGI:1917436]	0.24	2.014	0.2078
	Pidd1	p53 induced death domain protein 1 [Source:MGI Symbol;Acc:MGI:1889507]	0.41	2.149	0.168
	Abcc5	ATP-binding cassette, sub-family C (CFTR/MRP), member 5 [Source:MGI Symbol;Acc:MGI:1351644]	0.28	2.183	0.1591
	Traf4	TNF receptor associated factor 4 [Source:MGI Symbol;Acc:MGI:1202880]	0.47	2.207	0.153
	Hspa4l	heat shock protein 4 like [Source:MGI Symbol;Acc:MGI:107422]	0.35	2.219	0.1505
	Pmm1	phosphomannomutase 1 [Source:MGI Symbol;Acc:MGI:1353418]	0.34	2.297	0.1309
	Dnttip2	deoxynucleotidyltransferase, terminal, interacting protein 2 [Source:MGI Symbol;Acc:MGI:1923173]	0.23	2.333	0.1233
**	Ccng1	cyclin G1 [Source:MGI Symbol;Acc:MGI:102890]	0.48	2.512	0.0884
**	Ercc5	excision repair cross-complementing rodent repair deficiency, complementation group 5 [Source:MGI Symbol;Acc:MGI:103582]	0.32	2.554	0.0809
**	Sdc1	syndecan 1 [Source:MGI Symbol;Acc:MGI:1349162]	0.24	2.575	0.0772
**	Socs1	suppressor of cytokine signaling 1 [Source:MGI Symbol;Acc:MGI:1354910]	0.51	2.579	0.0766
**	Sfn	stratifin [Source:MGI Symbol;Acc:MGI:1891831]	0.41	2.691	0.0615
**	Cdkn1a	cyclin-dependent kinase inhibitor 1A (P21) [Source:MGI Symbol;Acc:MGI:104556]	0.39	2.714	0.0586
**	Zfp365	zinc finger protein 365 [Source:MGI Symbol;Acc:MGI:2143676]	0.8	2.828	0.045
**	Dcxr	dicarbonyl L-xylulose reductase [Source:MGI Symbol;Acc:MGI:1915130]	0.6	2.981	0.0313
**	Stom	stomatin [Source:MGI Symbol;Acc:MGI:95403]	0.33	3.012	0.0291

Supplemental Table 3: Continued

**	Apaf1	apoptotic peptidase activating factor 1 [Source:MGI Symbol;Acc:MGI:1306796]	0.55	3.038	0.0273
**	S100a4	S100 calcium binding protein A4 [Source:MGI Symbol;Acc:MGI:1330282]	0.66	3.107	0.0231
**	Tap1	transporter 1, ATP-binding cassette, sub-family B (MDR/TAP) [Source:MGI Symbol;Acc:MGI:98483]	0.64	3.239	0.0163
**	Ninj1	ninjurin 1 [Source:MGI Symbol;Acc:MGI:1196617]	0.44	3.502	0.0078
**	Rap2b	RAP2B, member of RAS oncogene family [Source:MGI Symbol;Acc:MGI:1921262]	0.57	3.572	0.0064
**	Fos	FBJ osteosarcoma oncogene [Source:MGI Symbol;Acc:MGI:95574]	0.97	3.674	0.0046
**	Mdm2	transformed mouse 3T3 cell double minute 2 [Source:MGI Symbol;Acc:MGI:96952]	0.54	3.685	0.0045
**	Pcna	proliferating cell nuclear antigen [Source:MGI Symbol;Acc:MGI:97503]	0.41	3.781	0.0033
**	Ndrg1	N-myc downstream regulated gene 1 [Source:MGI Symbol;Acc:MGI:1341799]	0.94	3.807	0.003
**	Pdgfa	platelet derived growth factor, alpha [Source:MGI Symbol;Acc:MGI:97527]	0.63	3.811	0.003
**	Procr	protein C receptor, endothelial [Source:MGI Symbol;Acc:MGI:104596]	1.11	3.940	0.0019
**	Gls2	glutaminase 2 (liver, mitochondrial) [Source:MGI Symbol;Acc:MGI:2143539]	0.64	4.139	0.001
**	Tsc22d1	TSC22 domain family, member 1 [Source:MGI Symbol;Acc:MGI:109127]	0.66	4.328	5.00E-04
**	Rps27l	ribosomal protein S27-like [Source:MGI Symbol;Acc:MGI:1915191]	0.4	4.426	3.00E-04
**	S100a10	S100 calcium binding protein A10 (calpactin) [Source:MGI Symbol;Acc:MGI:1339468]	0.64	4.521	2.00E-04
**	Atf3	activating transcription factor 3 [Source:MGI Symbol;Acc:MGI:109384]	1.36	5.123	0
**	Rrad	Ras-related associated with diabetes [Source:MGI Symbol;Acc:MGI:1930943]	1.72	5.764	0
**	Ddit4	DNA-damage-inducible transcript 4 [Source:MGI Symbol;Acc:MGI:1921997]	0.78	6.699	0

Supplemental Table 4: TNF Signaling Heatmap Gene List

Molecular Signature Database (MSigDB) gene list: ** = padj < 0.1					
"HALLMARK_TNFA_SIGNALING_VIA_NFKB%MSIGDB_C2%HALLMARK_TNFA_SIGNALING_VIA_NFKB)"					
	Name	**Description**	**log2 F.C.**	**stat**	**padj**
**	Cebpb	CCAAT/enhancer binding protein (C/EBP), beta [Source:MGI Symbol;Acc:MGI:88373]	-3.07	-12.700	0
**	Abca1	ATP-binding cassette, sub-family A (ABC1), member 1 [Source:MGI Symbol;Acc:MGI:99607]	-0.95	-5.942	0
**	Serpinb8	serine (or cysteine) peptidase inhibitor, clade B, member 8 [Source:MGI Symbol;Acc:MGI:894657]	-0.68	-5.590	0
**	Il18	interleukin 18 [Source:MGI Symbol;Acc:MGI:107936]	-0.79	-4.760	1.00E-04
**	Dusp5	dual specificity phosphatase 5 [Source:MGI Symbol;Acc:MGI:2685183]	-0.78	-4.108	0.0011
**	Jun	jun proto-oncogene [Source:MGI Symbol;Acc:MGI:96646]	-0.44	-3.965	0.0018
**	Egr3	early growth response 3 [Source:MGI Symbol;Acc:MGI:1306780]	-0.67	-3.848	0.0027
**	Cflar	CASP8 and FADD-like apoptosis regulator [Source:MGI Symbol;Acc:MGI:1336166]	-0.37	-2.711	0.059
**	Tubb2a	tubulin, beta 2A class IIA [Source:MGI Symbol;Acc:MGI:107861]	-0.44	-2.587	0.0755
	Btg1	B cell translocation gene 1, anti-proliferative [Source:MGI Symbol;Acc:MGI:88215]	-0.41	-2.415	0.1066
	Sphk1	sphingosine kinase 1 [Source:MGI Symbol;Acc:MGI:1316649]	-0.45	-2.326	0.1249
	Lif	leukemia inhibitory factor [Source:MGI Symbol;Acc:MGI:96787]	-0.5	-2.085	0.1866
	Ripk2	receptor (TNFRSF)-interacting serine-threonine kinase 2 [Source:MGI Symbol;Acc:MGI:1891456]	-0.36	-2.075	0.1892
	Gadd45a	growth arrest and DNA-damage-inducible 45 alpha [Source:MGI Symbol;Acc:MGI:107799]	-0.28	-1.958	0.226
	Egr2	early growth response 2 [Source:MGI Symbol;Acc:MGI:95296]	-0.56	-1.834	0.2684
	Il6	interleukin 6 [Source:MGI Symbol;Acc:MGI:96559]	-0.61	-1.827	0.2707
	Maff	v-maf musculoaponeurotic fibrosarcoma oncogene family, protein F (avian) [Source:MGI Symbol;Acc:MGI:96910]	-0.23	-1.700	0.3231
	Ccl12	chemokine (C-C motif) ligand 12 [Source:MGI Symbol;Acc:MGI:108224]	-0.56	-1.689	0.3266
	Tank	TRAF family member-associated Nf-kappa B activator [Source:MGI Symbol;Acc:MGI:107676]	-0.21	-1.668	0.3352
	Edn1	endothelin 1 [Source:MGI Symbol;Acc:MGI:95283]	-0.49	-1.538	0.3889
	Map2k3	mitogen-activated protein kinase kinase 3 [Source:MGI Symbol;Acc:MGI:1346868]	-0.15	-1.499	0.4058
	Map3k8	mitogen-activated protein kinase kinase kinase 8 [Source:MGI Symbol;Acc:MGI:1346878]	-0.27	-1.406	0.446
	Ptger4	prostaglandin E receptor 4 (subtype EP4) [Source:MGI Symbol;Acc:MGI:104311]	-0.33	-1.389	0.4541
	Nfe2l2	nuclear factor, erythroid derived 2, like 2 [Source:MGI Symbol;Acc:MGI:108420]	-0.27	-1.377	0.4593
	Zbtb10	zinc finger and BTB domain containing 10 [Source:MGI Symbol;Acc:MGI:2139883]	-0.4	-1.295	0.4963
	Sgk1	serum/glucocorticoid regulated kinase 1 [Source:MGI Symbol;Acc:MGI:1340062]	-0.16	-1.222	0.5303
	Btg2	B cell translocation gene 2, anti-proliferative [Source:MGI Symbol;Acc:MGI:108384]	-0.17	-1.173	0.5522
	Csf1	colony stimulating factor 1 (macrophage) [Source:MGI Symbol;Acc:MGI:1339753]	-0.15	-1.073	0.5975
	Phlda2	pleckstrin homology like domain, family A, member 2 [Source:MGI Symbol;Acc:MGI:1202307]	-0.22	-1.010	0.6245
	Irs2	insulin receptor substrate 2 [Source:MGI Symbol;Acc:MGI:109334]	-0.2	-0.967	0.6441
	Gadd45b	growth arrest and DNA-damage-inducible 45 beta [Source:MGI Symbol;Acc:MGI:107776]	-0.14	-0.914	0.6709
	Pde4b	phosphodiesterase 4B, cAMP specific [Source:MGI Symbol;Acc:MGI:99557]	-0.2	-0.897	0.6792
	Hes1	hairy and enhancer of split 1 (Drosophila) [Source:MGI Symbol;Acc:MGI:104853]	-0.11	-0.872	0.6896
	Egr1	early growth response 1 [Source:MGI Symbol;Acc:MGI:95295]	-0.24	-0.856	0.6969
	Mxd1	MAX dimerization protein 1 [Source:MGI Symbol;Acc:MGI:96908]	-0.15	-0.852	0.6992
	Pdlim5	PDZ and LIM domain 5 [Source:MGI Symbol;Acc:MGI:1927489]	-0.08	-0.822	0.7136
	Bcl6	B cell leukemia/lymphoma 6 [Source:MGI Symbol;Acc:MGI:107187]	-0.14	-0.817	0.7155
	Zfp36	zinc finger protein 36 [Source:MGI Symbol;Acc:MGI:99180]	-0.15	-0.786	0.7281
	Jag1	jagged 1 [Source:MGI Symbol;Acc:MGI:1095416]	-0.1	-0.764	0.7364
	Ier5	immediate early response 5 [Source:MGI Symbol;Acc:MGI:1337072]	-0.08	-0.757	0.7399

Supplemental Table 4: Continued

	Marcks	myristoylated alanine rich protein kinase C substrate [Source:MGI Symbol;Acc:MGI:96907]	-0.1	-0.733	0.7509
	Btg3	B cell translocation gene 3 [Source:MGI Symbol;Acc:MGI:109532]	-0.16	-0.697	0.7681
	Cxcl1	chemokine (C-X-C motif) ligand 1 [Source:MGI Symbol;Acc:MGI:108068]	-0.17	-0.679	0.7766
	Il6st	interleukin 6 signal transducer [Source:MGI Symbol;Acc:MGI:96560]	-0.09	-0.659	0.7852
	Sik1	salt inducible kinase 1 [Source:MGI Symbol;Acc:MGI:104754]	-0.09	-0.635	0.7955
	Fosl2	fos-like antigen 2 [Source:MGI Symbol;Acc:MGI:102858]	-0.08	-0.602	0.8083
	Tnfaip6	tumor necrosis factor alpha induced protein 6 [Source:MGI Symbol;Acc:MGI:1195266]	-0.18	-0.602	0.8083
	Slc16a6	solute carrier family 16 (monocarboxylic acid transporters), member 6 [Source:MGI Symbol;Acc:MGI:2144585]	-0.06	-0.555	0.8254
	Klf2	Kruppel-like factor 2 (lung) [Source:MGI Symbol;Acc:MGI:1342772]	-0.13	-0.509	0.8422
	Klf9	Kruppel-like factor 9 [Source:MGI Symbol;Acc:MGI:1333856]	-0.08	-0.490	0.8491
	Ppp1r15a	protein phosphatase 1, regulatory (inhibitor) subunit 15A [Source:MGI Symbol;Acc:MGI:1927072]	-0.07	-0.442	0.8649
	Myc	myelocytomatosis oncogene [Source:MGI Symbol;Acc:MGI:97250]	-0.05	-0.413	0.8749
	Ccnd1	cyclin D1 [Source:MGI Symbol;Acc:MGI:88313]	-0.14	-0.410	0.8761
	Kynu	kynureninase (L-kynurenine hydrolase) [Source:MGI Symbol;Acc:MGI:1918039]	-0.12	-0.402	0.879
	Klf4	Kruppel-like factor 4 (gut) [Source:MGI Symbol;Acc:MGI:1342287]	-0.05	-0.350	0.8981
	Dennd5a	DENN/MADD domain containing 5A [Source:MGI Symbol;Acc:MGI:1201681]	-0.06	-0.349	0.8983
	Gch1	GTP cyclohydrolase 1 [Source:MGI Symbol;Acc:MGI:95675]	-0.05	-0.187	0.9474
	Il15ra	interleukin 15 receptor, alpha chain [Source:MGI Symbol;Acc:MGI:104644]	-0.04	-0.177	0.9515
	Ehd1	EH-domain containing 1 [Source:MGI Symbol;Acc:MGI:1341878]	-0.02	-0.167	0.9546
	Serpinb2	serine (or cysteine) peptidase inhibitor, clade B, member 2 [Source:MGI Symbol;Acc:MGI:97609]	-0.02	-0.088	0.9758
	Tnip2	TNFAIP3 interacting protein 2 [Source:MGI Symbol;Acc:MGI:2386643]	-0.01	-0.087	0.976
	Ifngr2	interferon gamma receptor 2 [Source:MGI Symbol;Acc:MGI:107654]	-0.01	-0.056	0.986
	Ier2	immediate early response 2 [Source:MGI Symbol;Acc:MGI:104815]	0	-0.041	0.9898
	B4galt5	UDP-Gal:betaGlcNAc beta 1,4-galactosyltransferase, polypeptide 5 [Source:MGI Symbol;Acc:MGI:1927169]	-0.01	-0.034	0.9915
	Ptx3	pentraxin related gene [Source:MGI Symbol;Acc:MGI:104641]	0	-0.009	0.9976
	Sod2	superoxide dismutase 2, mitochondrial [Source:MGI Symbol;Acc:MGI:98352]	0.01	0.076	0.9802
	Dusp1	dual specificity phosphatase 1 [Source:MGI Symbol;Acc:MGI:105120]	0.03	0.125	0.965
	Ier3	immediate early response 3 [Source:MGI Symbol;Acc:MGI:104814]	0.03	0.142	0.9601
	Sat1	spermidine/spermine N1-acetyl transferase 1 [Source:MGI Symbol;Acc:MGI:98233]	0.03	0.207	0.9427
	Bcl2a1d	B cell leukemia/lymphoma 2 related protein A1d [Source:MGI Symbol;Acc:MGI:1278325]	0.07	0.215	0.939
	Klf10	Kruppel-like factor 10 [Source:MGI Symbol;Acc:MGI:1101353]	0.03	0.239	0.9327
	Id2	inhibitor of DNA binding 2 [Source:MGI Symbol;Acc:MGI:96397]	0.04	0.250	0.9307
	Litaf	LPS-induced TN factor [Source:MGI Symbol;Acc:MGI:1929512]	0.04	0.259	0.9271
	Trib1	tribbles pseudokinase 1 [Source:MGI Symbol;Acc:MGI:2443397]	0.05	0.268	0.9244
	Fut4	fucosyltransferase 4 [Source:MGI Symbol;Acc:MGI:95594]	0.09	0.268	0.9244
	Junb	jun B proto-oncogene [Source:MGI Symbol;Acc:MGI:96647]	0.04	0.298	0.9145
	Bhlhe40	basic helix-loop-helix family, member e40 [Source:MGI Symbol;Acc:MGI:1097714]	0.06	0.344	0.8991
	Ackr3	atypical chemokine receptor 3 [Source:MGI Symbol;Acc:MGI:109562]	0.06	0.434	0.8675
	Cxcl11	chemokine (C-X-C motif) ligand 11 [Source:MGI Symbol;Acc:MGI:1860203]	0.11	0.452	1
	Sqstm1	sequestosome 1 [Source:MGI Symbol;Acc:MGI:107931]	0.07	0.488	0.8493
	Ccl20	chemokine (C-C motif) ligand 20 [Source:MGI Symbol;Acc:MGI:1329031]	0.15	0.512	0.8414
	Nfat5	nuclear factor of activated T cells 5 [Source:MGI Symbol;Acc:MGI:1859333]	0.08	0.531	0.8344
	Atp2b1	ATPase, Ca++ transporting, plasma membrane 1 [Source:MGI Symbol;Acc:MGI:104653]	0.1	0.563	0.8225
	Il23a	interleukin 23, alpha subunit p19 [Source:MGI Symbol;Acc:MGI:1932410]	0.19	0.581	0.8159
	Rhob	ras homolog family member B [Source:MGI Symbol;Acc:MGI:107949]	0.09	0.634	0.7958

Supplemental Table 4: Continued

	Olr1	oxidized low density lipoprotein (lectin-like) receptor 1 [Source:MGI Symbol;Acc:MGI:1261434]	0.21	0.634	0.7956
	Rel	reticuloendotheliosis oncogene [Source:MGI Symbol;Acc:MGI:97897]	0.11	0.638	0.7936
	Il1a	interleukin 1 alpha [Source:MGI Symbol;Acc:MGI:96542]	0.16	0.647	0.7898
	Tgif1	TGFB-induced factor homeobox 1 [Source:MGI Symbol;Acc:MGI:1194497]	0.15	0.652	0.7884
	Zc3h12a	zinc finger CCCH type containing 12A [Source:MGI Symbol;Acc:MGI:2385891]	0.14	0.667	0.7823
	Dusp4	dual specificity phosphatase 4 [Source:MGI Symbol;Acc:MGI:2442191]	0.23	0.713	0.7603
	Birc2	baculoviral IAP repeat-containing 2 [Source:MGI Symbol;Acc:MGI:1197009]	0.12	0.729	0.7528
	Dnajb4	DnaJ heat shock protein family (Hsp40) member B4 [Source:MGI Symbol;Acc:MGI:1914285]	0.12	0.730	0.7523
	Nfil3	nuclear factor, interleukin 3, regulated [Source:MGI Symbol;Acc:MGI:109495]	0.12	0.738	0.7487
	Tnfaip2	tumor necrosis factor, alpha-induced protein 2 [Source:MGI Symbol;Acc:MGI:104960]	0.13	0.779	0.7315
	Tnc	tenascin C [Source:MGI Symbol;Acc:MGI:101922]	0.13	0.823	0.7129
	Tnip1	TNFAIP3 interacting protein 1 [Source:MGI Symbol;Acc:MGI:1926194]	0.11	0.894	0.6805
	Tlr2	toll-like receptor 2 [Source:MGI Symbol;Acc:MGI:1346060]	0.24	0.986	0.636
	Cd69	CD69 antigen [Source:MGI Symbol;Acc:MGI:88343]	0.33	0.991	0.6336
	Icosl	icos ligand [Source:MGI Symbol;Acc:MGI:1354701]	0.14	1.030	0.6159
	Plk2	polo-like kinase 2 [Source:MGI Symbol;Acc:MGI:1099790]	0.15	1.081	0.5936
	Ccl5	chemokine (C-C motif) ligand 5 [Source:MGI Symbol;Acc:MGI:98262]	0.31	1.124	0.574
	Ccnl1	cyclin L1 [Source:MGI Symbol;Acc:MGI:1922664]	0.15	1.158	0.5589
	Dusp2	dual specificity phosphatase 2 [Source:MGI Symbol;Acc:MGI:101911]	0.33	1.191	0.5442
	Efna1	ephrin A1 [Source:MGI Symbol;Acc:MGI:103236]	0.16	1.229	0.5273
	Hbegf	heparin-binding EGF-like growth factor [Source:MGI Symbol;Acc:MGI:96070]	0.33	1.262	0.512
	Ldlr	low density lipoprotein receptor [Source:MGI Symbol;Acc:MGI:96765]	0.18	1.319	0.4854
	Fosl1	fos-like antigen 1 [Source:MGI Symbol;Acc:MGI:107179]	0.45	1.339	0.4765
	Dram1	DNA-damage regulated autophagy modulator 1 [Source:MGI Symbol;Acc:MGI:1918962]	0.21	1.347	0.473
	Clcf1	cardiotrophin-like cytokine factor 1 [Source:MGI Symbol;Acc:MGI:1930088]	0.43	1.350	0.4715
	Rnf19b	ring finger protein 19B [Source:MGI Symbol;Acc:MGI:1922484]	0.22	1.396	0.4509
	Gem	GTP binding protein (gene overexpressed in skeletal muscle) [Source:MGI Symbol;Acc:MGI:99844]	0.39	1.417	0.4404
	Slc2a6	solute carrier family 2 (facilitated glucose transporter), member 6 [Source:MGI Symbol;Acc:MGI:2443286]	0.41	1.421	0.4383
	Ptpre	protein tyrosine phosphatase, receptor type, E [Source:MGI Symbol;Acc:MGI:97813]	0.32	1.434	0.4333
	Fjx1	four jointed box 1 (Drosophila) [Source:MGI Symbol;Acc:MGI:1341907]	0.35	1.472	0.4178
	Klf6	Kruppel-like factor 6 [Source:MGI Symbol;Acc:MGI:1346318]	0.15	1.479	0.4143
	Snn	stannin [Source:MGI Symbol;Acc:MGI:1276549]	0.23	1.502	0.4045
	Cd80	CD80 antigen [Source:MGI Symbol;Acc:MGI:101775]	0.41	1.504	0.4041
	Gpr183	G protein-coupled receptor 183 [Source:MGI Symbol;Acc:MGI:2442034]	0.35	1.539	0.3887
	Cyr61	cysteine rich protein 61 [Source:MGI Symbol;Acc:MGI:88613]	0.36	1.572	0.3748
	Tnfaip8	tumor necrosis factor, alpha-induced protein 8 [Source:MGI Symbol;Acc:MGI:2147191]	0.2	1.572	0.3747
	B4galt1	UDP-Gal:betaGlcNAc beta 1,4- galactosyltransferase, polypeptide 1 [Source:MGI Symbol;Acc:MGI:95705]	0.21	1.582	0.3699
	Birc3	baculoviral IAP repeat-containing 3 [Source:MGI Symbol;Acc:MGI:1197007]	0.32	1.630	0.3491
	Cd83	CD83 antigen [Source:MGI Symbol;Acc:MGI:1328316]	0.47	1.646	0.3422
	Bmp2	bone morphogenetic protein 2 [Source:MGI Symbol;Acc:MGI:88177]	0.34	1.653	0.3407
	Yrdc	yrdC domain containing (E.coli) [Source:MGI Symbol;Acc:MGI:2387201]	0.22	1.665	0.3359
	Areg	amphiregulin [Source:MGI Symbol;Acc:MGI:88068]	0.46	1.681	0.3294
	Il12b	interleukin 12b [Source:MGI Symbol;Acc:MGI:96540]	0.5	1.687	1
	Pmepa1	prostate transmembrane protein, androgen induced 1 [Source:MGI Symbol;Acc:MGI:1929600]	0.27	1.688	0.3268
	F2rl1	coagulation factor II (thrombin) receptor-like 1 [Source:MGI Symbol;Acc:MGI:101910]	0.29	1.724	0.313

Supplemental Table 4: Continued

	Eif1	eukaryotic translation initiation factor 1 [Source:MGI Symbol;Acc:MGI:105125]	0.15	1.760	0.2984
	Kdm6b	KDM1 lysine (K)-specific demethylase 6B [Source:MGI Symbol;Acc:MGI:2448492]	0.28	1.824	0.272
	Il7r	interleukin 7 receptor [Source:MGI Symbol;Acc:MGI:96562]	0.47	1.834	0.2686
	Ccrl2	chemokine (C-C motif) receptor-like 2 [Source:MGI Symbol;Acc:MGI:1920904]	0.62	1.880	0.252
	Rela	v-rel reticuloendotheliosis viral oncogene homolog A (avian) [Source:MGI Symbol;Acc:MGI:103290]	0.2	1.999	0.2118
	Smad3	SMAD family member 3 [Source:MGI Symbol;Acc:MGI:1201674]	0.44	2.003	0.2109
	Nfkbie	nuclear factor of kappa light polypeptide gene enhancer in B cells inhibitor, epsilon [Source:MGI Symbol;Acc:MGI:1194908]	0.42	2.081	0.1876
	Sdc4	syndecan 4 [Source:MGI Symbol;Acc:MGI:1349164]	0.2	2.103	0.1816
	Stat5a	signal transducer and activator of transcription 5A [Source:MGI Symbol;Acc:MGI:103036]	0.36	2.130	0.1738
	Vegfa	vascular endothelial growth factor A [Source:MGI Symbol;Acc:MGI:103178]	0.37	2.132	0.1733
	Mcl1	myeloid cell leukemia sequence 1 [Source:MGI Symbol;Acc:MGI:101769]	0.18	2.160	0.1654
	Spsb1	splA/ryanodine receptor domain and SOCS box containing 1 [Source:MGI Symbol;Acc:MGI:1921896]	0.49	2.162	0.1651
	Traf1	TNF receptor-associated factor 1 [Source:MGI Symbol;Acc:MGI:101836]	0.53	2.174	0.1616
	Nr4a2	nuclear receptor subfamily 4, group A, member 2 [Source:MGI Symbol;Acc:MGI:1352456]	0.59	2.202	0.1543
	Phlda1	pleckstrin homology like domain, family A, member 1 [Source:MGI Symbol;Acc:MGI:1096880]	0.49	2.284	0.1344
	Plau	plasminogen activator, urokinase [Source:MGI Symbol;Acc:MGI:97611]	0.43	2.306	0.129
	Slc2a3	solute carrier family 2 (facilitated glucose transporter), member 3 [Source:MGI Symbol;Acc:MGI:95757]	0.76	2.312	0.1281
	Ets2	E26 avian leukemia oncogene 2, 3' domain [Source:MGI Symbol;Acc:MGI:95456]	0.22	2.341	0.1213
	Bcl3	B cell leukemia/lymphoma 3 [Source:MGI Symbol;Acc:MGI:88140]	0.29	2.353	0.1189
	Plek	pleckstrin [Source:MGI Symbol;Acc:MGI:1860485]	0.66	2.441	0.1017
	Ccl4	chemokine (C-C motif) ligand 4 [Source:MGI Symbol;Acc:MGI:98261]	0.86	2.612	1
**	Tiparp	TCDD-inducible poly(ADP-ribose) polymerase [Source:MGI Symbol;Acc:MGI:2159210]	0.37	2.658	0.0652
**	Nfkb1	nuclear factor of kappa light polypeptide gene enhancer in B cells 1, p105 [Source:MGI Symbol;Acc:MGI:97312]	0.26	2.683	0.0623
**	Cdkn1a	cyclin-dependent kinase inhibitor 1A (P21) [Source:MGI Symbol;Acc:MGI:104556]	0.39	2.714	0.0586
**	Inhba	inhibin beta-A [Source:MGI Symbol;Acc:MGI:96570]	0.91	2.737	0.0556
**	Ifit2	interferon-induced protein with tetratricopeptide repeats 2 [Source:MGI Symbol;Acc:MGI:99449]	0.85	2.755	0.0533
**	F3	coagulation factor III [Source:MGI Symbol;Acc:MGI:88381]	0.77	2.851	0.0428
**	Gfpt2	glutamine fructose-6-phosphate transaminase 2 [Source:MGI Symbol;Acc:MGI:1338883]	0.96	2.917	0.0369
**	Cxcl5	chemokine (C-X-C motif) ligand 5 [Source:MGI Symbol;Acc:MGI:1096868]	0.82	2.934	0.0353
**	Per1	period circadian clock 1 [Source:MGI Symbol;Acc:MGI:1098283]	0.32	3.051	0.0264
**	Il1b	interleukin 1 beta [Source:MGI Symbol;Acc:MGI:96543]	1.03	3.067	1
**	Rcan1	regulator of calcineurin 1 [Source:MGI Symbol;Acc:MGI:1890564]	0.5	3.075	0.0252
**	Trip10	thyroid hormone receptor interactor 10 [Source:MGI Symbol;Acc:MGI:2146901]	0.39	3.213	0.0174
**	Cxcl2	chemokine (C-X-C motif) ligand 2 [Source:MGI Symbol;Acc:MGI:1340094]	1.08	3.237	1
**	Tap1	transporter 1, ATP-binding cassette, sub-family B (MDR/TAP) [Source:MGI Symbol;Acc:MGI:98483]	0.64	3.239	0.0163
**	Pnrc1	proline-rich nuclear receptor coactivator 1 [Source:MGI Symbol;Acc:MGI:1917838]	0.53	3.242	0.0162
**	Nfkb2	nuclear factor of kappa light polypeptide gene enhancer in B cells 2, p49/p100 [Source:MGI Symbol;Acc:MGI:1099800]	0.52	3.329	0.0127
**	G0s2	G0/G1 switch gene 2 [Source:MGI Symbol;Acc:MGI:1316737]	1.12	3.420	0.0099
**	Relb	avian reticuloendotheliosis viral (v-rel) oncogene related B [Source:MGI Symbol;Acc:MGI:103289]	0.64	3.423	0.0099
**	Panx1	pannexin 1 [Source:MGI Symbol;Acc:MGI:1860055]	0.46	3.465	0.0087
**	Ninj1	ninjurin 1 [Source:MGI Symbol;Acc:MGI:1196617]	0.44	3.502	0.0078
**	Irf1	interferon regulatory factor 1 [Source:MGI Symbol;Acc:MGI:96590]	0.53	3.529	0.0072
**	Ptgs2	prostaglandin-endoperoxide synthase 2 [Source:MGI Symbol;Acc:MGI:97798]	1.18	3.559	0.0066
**	Fos	FBJ osteosarcoma oncogene [Source:MGI Symbol;Acc:MGI:95574]	0.97	3.674	0.0046

Supplemental Table 4: Continued

**	Cd44	CD44 antigen [Source:MGI Symbol;Acc:MGI:88338]	0.4	3.702	0.0043
**	Ifih1	interferon induced with helicase C domain 1 [Source:MGI Symbol;Acc:MGI:1918836]	1.12	4.300	5.00E-04
**	Lamb3	laminin, beta 3 [Source:MGI Symbol;Acc:MGI:99915]	0.83	4.309	5.00E-04
**	Cxcl3	chemokine (C-X-C motif) ligand 3 [Source:MGI Symbol;Acc:MGI:3037818]	1.26	4.320	5.00E-04
**	Plaur	plasminogen activator, urokinase receptor [Source:MGI Symbol;Acc:MGI:97612]	1.24	4.328	5.00E-04
**	Tsc22d1	TSC22 domain family, member 1 [Source:MGI Symbol;Acc:MGI:109127]	0.66	4.328	5.00E-04
**	Socs3	suppressor of cytokine signaling 3 [Source:MGI Symbol;Acc:MGI:1201791]	0.57	4.517	2.00E-04
**	Serpine1	serine (or cysteine) peptidase inhibitor, clade E, member 1 [Source:MGI Symbol;Acc:MGI:97608]	1.25	4.556	2.00E-04
**	Ddx58	DEAD (Asp-Glu-Ala-Asp) box polypeptide 58 [Source:MGI Symbol;Acc:MGI:2442858]	1.18	4.743	1.00E-04
**	Pfkfb3	6-phosphofructo-2-kinase/fructose-2,6-biphosphatase 3 [Source:MGI Symbol;Acc:MGI:2181202]	0.71	4.765	1.00E-04
**	Icam1	intercellular adhesion molecule 1 [Source:MGI Symbol;Acc:MGI:96392]	0.55	4.782	1.00E-04
**	Atf3	activating transcription factor 3 [Source:MGI Symbol;Acc:MGI:109384]	1.36	5.123	0
**	Tnfrsf9	tumor necrosis factor receptor superfamily, member 9 [Source:MGI Symbol;Acc:MGI:1101059]	1.46	5.184	0
**	Nampt	nicotinamide phosphoribosyltransferase [Source:MGI Symbol;Acc:MGI:1929865]	0.58	5.679	0
**	Nfkbia	nuclear factor of kappa light polypeptide gene enhancer in B cells inhibitor, alpha [Source:MGI Symbol;Acc:MGI:104741]	0.65	5.767	0
**	Cxcl10	chemokine (C-X-C motif) ligand 10 [Source:MGI Symbol;Acc:MGI:1352450]	1.99	5.978	0
**	Nr4a3	nuclear receptor subfamily 4, group A, member 3 [Source:MGI Symbol;Acc:MGI:1352457]	1.84	6.613	0
**	Nr4a1	nuclear receptor subfamily 4, group A, member 1 [Source:MGI Symbol;Acc:MGI:1352454]	1.42	6.791	0
**	Tnf	tumor necrosis factor [Source:MGI Symbol;Acc:MGI:104798]	1.74	7.699	0
**	Tnfaip3	tumor necrosis factor, alpha-induced protein 3 [Source:MGI Symbol;Acc:MGI:1196377]	1.16	7.716	0
**	Fosb	FBJ osteosarcoma oncogene B [Source:MGI Symbol;Acc:MGI:95575]	2.56	9.053	0

Supplemental Table 5: Death Receptor Signaling Heatmap Gene List

Molecular Signature Database (MSigDB) gene lists combined: ** = padj < 0.1					
[1] "BIOCARTA_DEATH_PATHWAY%MSIGDB_C2%BIOCARTA_DEATH_PATHWAY"					
[2] "DEATH RECEPTOR SIGNALLING%REACTOME DATABASE ID RELEASE 59%73887"					
	Name	**Description**	**Log2 F.C.**	**stat**	**padj**
**	Usp2	ubiquitin specific peptidase 2 [Source:MGI Symbol;Acc:MGI:1858178]	-0.75	-4.800	1.00E-04
**	Cflar	CASP8 and FADD-like apoptosis regulator [Source:MGI Symbol;Acc:MGI:1336166]	-0.37	-2.711	0.059
	Clip3	CAP-GLY domain containing linker protein 3 [Source:MGI Symbol;Acc:MGI:1923936]	-0.73	-2.201	0.1546
	Ubc	ubiquitin C [Source:MGI Symbol;Acc:MGI:98889]	-0.27	-2.124	0.1756
	Tab2	TGF-beta activated kinase 1/MAP3K7 binding protein 2 [Source:MGI Symbol;Acc:MGI:1915902]	-0.23	-2.033	0.2026
	Gas2	growth arrest specific 2 [Source:MGI Symbol;Acc:MGI:95657]	-0.31	-1.849	0.2634
	Xiap	X-linked inhibitor of apoptosis [Source:MGI Symbol;Acc:MGI:107572]	-0.26	-1.839	0.2671
	Bag4	BCL2-associated athanogene 4 [Source:MGI Symbol;Acc:MGI:1914634]	-0.28	-1.537	0.3895
	Tab3	TGF-beta activated kinase 1/MAP3K7 binding protein 3 [Source:MGI Symbol;Acc:MGI:1913974]	-0.18	-1.528	0.3928
	Bid	BH3 interacting domain death agonist [Source:MGI Symbol;Acc:MGI:108093]	-0.26	-1.473	0.4177
	Sppl2a	signal peptide peptidase like 2A [Source:MGI Symbol;Acc:MGI:1913802]	-0.16	-1.354	0.4695
	Smpd2	sphingomyelin phosphodiesterase 2, neutral [Source:MGI Symbol;Acc:MGI:1278330]	-0.23	-1.290	0.4986
	Tnfrsf1a	tumor necrosis factor receptor superfamily, member 1a [Source:MGI Symbol;Acc:MGI:1314884]	-0.09	-0.949	0.6525
	Usp4	ubiquitin specific peptidase 4 (proto-oncogene) [Source:MGI Symbol;Acc:MGI:98905]	-0.09	-0.913	0.6712
	Fadd	Fas (TNFRSF6)-associated via death domain [Source:MGI Symbol;Acc:MGI:109324]	-0.14	-0.824	0.712
	Sptan1	spectrin alpha, non-erythrocytic 1 [Source:MGI Symbol;Acc:MGI:98386]	-0.09	-0.800	0.7233
	Tnfrsf25	tumor necrosis factor receptor superfamily, member 25 [Source:MGI Symbol;Acc:MGI:1934667]	-0.18	-0.796	0.724
	Adam17	a disintegrin and metallopeptidase domain 17 [Source:MGI Symbol;Acc:MGI:1096335]	-0.11	-0.778	0.7318
	Dffa	DNA fragmentation factor, alpha subunit [Source:MGI Symbol;Acc:MGI:1196227]	-0.09	-0.677	0.7771
	Nsmaf	neutral sphingomyelinase (N-SMase) activation associated factor [Source:MGI Symbol;Acc:MGI:1341864]	-0.06	-0.639	0.7934
	Cyld	CYLD lysine 63 deubiquitinase [Source:MGI Symbol;Acc:MGI:1921506]	-0.04	-0.287	0.9189
	Ikbkg	inhibitor of kappaB kinase gamma [Source:MGI Symbol;Acc:MGI:1338074]	-0.03	-0.200	0.9446
	Sharpin	SHANK-associated RH domain interacting protein [Source:MGI Symbol;Acc:MGI:1913331]	-0.02	-0.177	0.9515
	Bcl2	B cell leukemia/lymphoma 2 [Source:MGI Symbol;Acc:MGI:88138]	-0.01	-0.093	0.9742
	Casp9	caspase 9 [Source:MGI Symbol;Acc:MGI:1277950]	0	0.007	0.9983
	Map3k7	mitogen-activated protein kinase kinase kinase 7 [Source:MGI Symbol;Acc:MGI:1346877]	0.01	0.089	0.9756
	Ripk1	receptor (TNFRSF)-interacting serine-threonine kinase 1 [Source:MGI Symbol;Acc:MGI:108212]	0.04	0.328	0.9038
	Chuk	conserved helix-loop-helix ubiquitous kinase [Source:MGI Symbol;Acc:MGI:99484]	0.03	0.344	0.8991
	Sppl2b	signal peptide peptidase like 2B [Source:MGI Symbol;Acc:MGI:1920468]	0.04	0.362	0.8943
	Tax1bp1	Tax1 (human T cell leukemia virus type I) binding protein 1 [Source:MGI Symbol;Acc:MGI:1289308]	0.08	0.652	0.7884
	Tnfrsf10b	tumor necrosis factor receptor superfamily, member 10b [Source:MGI Symbol;Acc:MGI:1341090]	0.14	0.705	0.764
	Birc2	baculoviral IAP repeat-containing 2 [Source:MGI Symbol;Acc:MGI:1197009]	0.12	0.729	0.7528
	Rnf31	ring finger protein 31 [Source:MGI Symbol;Acc:MGI:1934704]	0.1	0.774	0.733
	Otulin	OTU deubiquitinase with linear linkage specificity [Source:MGI Symbol;Acc:MGI:3577015]	0.12	0.819	0.7151
	Usp21	ubiquitin specific peptidase 21 [Source:MGI Symbol;Acc:MGI:1353665]	0.12	0.893	0.6811
	Fas	Fas (TNF receptor superfamily member 6) [Source:MGI Symbol;Acc:MGI:95484]	0.22	0.924	0.6656
	Casp8	caspase 8 [Source:MGI Symbol;Acc:MGI:1261423]	0.13	1.043	0.6105
	Tab1	TGF-beta activated kinase 1/MAP3K7 binding protein 1 [Source:MGI Symbol;Acc:MGI:1913763]	0.15	1.152	0.5612
	Rbck1	RanBP-type and C3HC4-type zinc finger containing 1 [Source:MGI Symbol;Acc:MGI:1344372]	0.16	1.203	0.5387
	Casp7	caspase 7 [Source:MGI Symbol;Acc:MGI:109383]	0.16	1.228	0.5281

Supplemental Table 5: Continued

	Map3k14	mitogen-activated protein kinase kinase kinase 14 [Source:MGI Symbol;Acc:MGI:1858204]	0.22	1.412	0.4427
	Tradd	TNFRSF1A-associated via death domain [Source:MGI Symbol;Acc:MGI:109200]	0.15	1.416	0.4412
	Otud7b	OTU domain containing 7B [Source:MGI Symbol;Acc:MGI:2654703]	0.15	1.430	0.4345
	Birc3	baculoviral IAP repeat-containing 3 [Source:MGI Symbol;Acc:MGI:1197007]	0.32	1.630	0.3491
	Ikbkb	inhibitor of kappaB kinase beta [Source:MGI Symbol;Acc:MGI:1338071]	0.18	1.852	0.2622
	Rela	v-rel reticuloendotheliosis viral oncogene homolog A (avian) [Source:MGI Symbol;Acc:MGI:103290]	0.2	1.999	0.2118
	Traf1	TNF receptor-associated factor 1 [Source:MGI Symbol;Acc:MGI:101836]	0.53	2.174	0.1616
	Casp6	caspase 6 [Source:MGI Symbol;Acc:MGI:1312921]	0.39	2.362	0.1172
**	Lmna	lamin A [Source:MGI Symbol;Acc:MGI:96794]	0.35	2.487	0.0929
**	Casp3	caspase 3 [Source:MGI Symbol;Acc:MGI:107739]	0.47	2.544	0.0826
**	Nfkb1	nuclear factor of kappa light polypeptide gene enhancer in B cells 1, p105 [Source:MGI Symbol;Acc:MGI:97312]	0.26	2.683	0.0623
**	Traf2	TNF receptor-associated factor 2 [Source:MGI Symbol;Acc:MGI:101835]	0.4	2.922	0.0365
**	Tnfsf10	tumor necrosis factor (ligand) superfamily, member 10 [Source:MGI Symbol;Acc:MGI:107414]	0.76	3.034	0.0276
**	Apaf1	apoptotic peptidase activating factor 1 [Source:MGI Symbol;Acc:MGI:1306796]	0.55	3.038	0.0273
**	Dffb	DNA fragmentation factor, beta subunit [Source:MGI Symbol;Acc:MGI:1196287]	0.43	3.078	0.025
**	Nfkbia	nuclear factor of kappa light polypeptide gene enhancer in B cells inhibitor, alpha [Source:MGI Symbol;Acc:MGI:104741]	0.65	5.767	0
**	Tnf	tumor necrosis factor [Source:MGI Symbol;Acc:MGI:104798]	1.74	7.699	0
**	Tnfaip3	tumor necrosis factor, alpha-induced protein 3 [Source:MGI Symbol;Acc:MGI:1196377]	1.16	7.716	0

GENERAL DISCUSSION

For longer than the author of this dissertation has been alive, scientists have unsuccessfully attempted to target the one of the deadliest proteins in cancer biology, oncogenic Ras. With 30% of all human cancers containing an oncogenic Ras protein, and an estimated 1.7 million new cases of cancer being diagnosed, more than half a million people will have been introduced to this killer in 2017 [213]. Over 50,000 of these individuals will be diagnosed with pancreatic cancer. The overwhelming majority will harbor a mutation in the Ki-Ras protein. Less than 5,000 will survive 5 years.

Traditional chemotherapeutics work by targeting cells at different phases of the cell cycle with the goal of destroying the rapidly dividing cancerous cells. The downside to this approach is that the unbiased compounds cannot tell the difference between the rapidly dividing cancer cells and the dividing normal cells. This non-specific targeting leads to side effects that limit the amount of drug which can be dosed and the frequency at which it can be administered, which decreases the effectiveness of treatments. Another downside to traditional chemotherapeutics and radiation therapy is that the treatment itself can act as a carcinogen. Because of these limits in traditional therapies, world governments, non-profits, corporations, and scientists have aggressively pursued the "holy grail" of targeted, personalized anti-cancer medicines and treatments. A PubMed search just for "cancer immunotherapy" retrieves over 70,000 publications with close to half of them being published in the past 10 years.

Through the analysis of genetic and epigenetic signatures of a cancer, specific molecular alterations and pathways can be identified and targeted. An early successful

example of this is the targeting of the human epidermal growth factor receptor 2 (HER2) in certain breast cancers with the monoclonal-antibody trastuzumab (Herceptin®) [214]. This targeted therapeutic approach can be effective because of concepts known as oncogene and non-oncogene addiction [215], where even though a tumor has amassed a variety of genetic abnormalities due to the multistage process of tumorigenesis, inhibition of a single protein or pathway can be detrimental to tumor maintenance and survival [61]. Oncogene and non-oncogene addiction can be manifested through the related concepts of synthetic lethality [58] and induced essentiality [216]. In terms of cancer, synthetic lethality is revealed when mutation or deletion of single genes are tolerated by the tumor, however mutation or deletion of a combination of genes results in death of cancer cells. Induced essentiality describes a situation where mutation or deletion of a single gene causes the tumor to become dependent on a single protein or pathway which if deleted or mutated would cause death of cancer cells.

Tumor cells must overcome cellular stresses arising from a variety of sources including DNA damage, oncogenic signaling, and ROS in order to acquire the traits associated with the hallmarks of cancer [4]. Considering the concept of synthetic lethality, loss of one or more pathways that confer the ability of tumor cells to respond to these stress phenotypes could result in selective tumor killing, which would leave normal wildtype cells unharmed as they are not having to compensate for the added stress of the tumor microenvironment. Knowing that C/EBPβ is required for oncogenic Ras driven skin tumorigenesis [134, 163] and that C/EBPβ$^{-/-}$ mouse skin has an enhanced apoptotic response downstream of DNA damage [155, 164], we hypothesized that C/EBPβ was required by oncogenic Ras skin tumors for survival and that deletion of C/EBPβ would promote tumor

regression and apoptosis. Knockout of C/EBPβ did result in tumor regression, and the fact that the apoptotic phenotype was limited to the tumor and not the surrounding normal epidermis is an important finding that fits the narrative of synthetic lethality. This finding makes C/EBPβ an interesting and promising target for future potential anti-cancer therapies.

The observed tumor regression and apoptosis were accompanied by transcriptomic evidence of a non-canonical p53 response. Traditionally a p53 apoptotic response downstream of DNA damage involves regulation of several hallmarks of the intrinsic apoptotic pathway including Bax, Noxa, Bcl-2, and Puma [217]. Though we did not see altered regulation of these genes, we did observe regulation of other key genes that play roles in both extrinsic and intrinsic apoptotic pathways. Increases in TNF, IFN, and death receptor associated genes suggests an extrinsic apoptotic response; however, we still observed upregulation of C*ytochrome C*, *apaf1*, and x*af1* that are required for intrinsic apoptosis. Taking a step back from this binary (extrinsic vs intrinsic) view of apoptosis and utilizing a global systems approach we can see what looks like an innate immune response begin to take shape involving a combination of the two.

Though not observed in the RNAseq dataset, TaqMan real-time PCR was able to detect induction of the type 1 interferon *ifn-β*. The transcriptome analysis revealed increases in *Stat1*, *Stat2*, and *Irf9*; together, these factors can form the interferon-stimulated gene factor 3 (ISGF3) complex which can translocate to the nucleus, bind to an IFN-stimulated response element (ISRE), and induce transcription of OAS genes which we also see increased in the RNAseq dataset [218]. This is traditionally thought of as the intrinsic anti-viral response. We also see upregulation of *cgas* expression which can associate with Stat1 dimers downstream

of type 1 interferon signaling to induce an anti-proliferative/pro-apoptotic response [218]. cGAS can interact with Sting and activate Irf3 and NFκB which are then able to induce transcription of type 1 interferons [219]. Interferon stimulated genes (ISGs) are transcriptionally up-regulated by interferon signaling. p53 has an IFN-stimulated response element (ISRE) in its promotor making it an ISG [220]. It is also known that p53 can up-regulate Genes involved in the innate immunity response [208]. This feedback loop acts to amplify the type 1 interferon response [209, 221].

One of the genes upregulated in the regressing tumors was XIAP-Associated factor 1 (x*af1*). During an intrinsic apoptotic response Xaf1 directly inhibits X-linked inhibitor of apoptosis (XIAP) [190]. Another gene upregulated in the regressing tumor dataset is *tnfsf10* which encodes the tumor necrosis factor-related apoptosis-inducing ligand (TRAIL) which binds death receptor and activates the extrinsic apoptotic pathway [222]. XAF1, as well as p53, have been shown to sensitize cancer cells to TRAIL [223, 224]. The upregulation of *xaf1*in the regressing tumors could be key in mediating a combination of intrinsic and extrinsic apoptosis as part of an interferon response.

Previous findings as well as findings presented herein all point to C/EBPβ somehow acting to inhibit p53 signaling. Our lab showed an enhanced p53 apoptotic response following dosing with UVB radiation, a potent inducer of p53 cell cycle arrest and apoptosis in the skin [155]. Additionally, some of the genes associated with innate immunity/interferon signaling and the extrinsic apoptotic pathway that were up-regulated in regressing tumors are up-regulated in C/EBPβ$^{-/-}$ skin in the absence of any DNA damage. This phenotype could indicate a priming of keratinocytes to an apoptotic response in the absence of C/EBPβ. Taken

together, we would propose C/EBPβ as a pro-survival factor that acts to fine-tune the apoptotic response.

Even though p53 has been extensively studied and characterized, the mechanism by which a cell decides to undergo apoptosis as opposed to senescence or cell cycle arrest remains elusive. C/EBPβ may in some way act as an arbiter of p53 and cell fate. This newly uncovered synthetic lethal interaction opens up the door to potential future anti-tumor therapies. Whether the synthetic lethality is tissue- or Ha-Ras-specific is yet to be elucidated as well as the potential requirement for wildtype p53.

C/EBPβ levels are increased in numerous human cancers, and often associated with poor prognoses and invasive growth [144-153]. High levels of C/EBPβ suggest that the tumor may have developed a dependency on C/EBPβ and that, like in our model system, there may be a synthetic lethal interaction between C/EBPβ and the respective tumor's oncogenic environment. Future therapies aimed at decreasing levels of C/EBPβ in cancer cells either by RNAi or small molecule inhibitors would be an obvious option. Treatments aimed at increasing the dominant negative C/EBP family members, such as the alternatively translated C/EBPβ isoform LIP, could potentially be effective as well if C/EBPβ transcriptional activity is responsible for the survival of a tumor. Taking advantage of the type 1 interferon response elicited following deletion of C/EBPβ in this study could be another approach for future therapy. If the mechanism of regression hinges on the type 1 interferon response, adjunct therapy involving the inhibition of C/EBPβ as well as supplementing factors like INFβ could prove effective. In other words, if loss of C/EBPβ acts to prime cells to be sensitive to a type 1 interferon response, then pushing the balance

towards an apoptotic response could induce the synthetic lethal phenotype observed in the oncogenic Ras skin tumors.

In summary, we have shown that in addition to C/EBPβ being required for oncogenic Ras driven skin tumorigenesis: i) C/EBPβ is required for these survival of chemical carcinogen-induced, Ha-Ras^{Q61L} driven skin tumors, ii) loss of C/EBPβ is a synthetic lethal event in oncogenic Ha-Ras^{Q61L} driven skin tumors and results in tumor specific apoptosis, iii) synthetic lethality and tumor regression are dependent on the tumor suppressor p53, and iv) synthetic lethality and tumor regression in the absence of C/EBPβ are associated with an innate immune type 1 interferon response.

GENERAL REFERENCES

1. Kochanek, K.D., Murphy, S.L., Xu, J.Q., Tejada-Vera, B. , *Deaths: Final data for 2014*, in *National Vital Statistics Reports*. 2016, National Center for Health Statistics.
2. Group, U.C.S.W. *United States Cancer Statistics: 1999-2014 Incidence and Mortality Web-based Report*. 2017; Available from: www.cdc.gov/uscs.
3. Mariotto, A.B., et al., *Projections of the cost of cancer care in the United States: 2010-2020.* J Natl Cancer Inst, 2011. **103**(2): p. 117-28.
4. Hanahan, D. and R.A. Weinberg, *Hallmarks of cancer: the next generation.* Cell, 2011. **144**(5): p. 646-74.
5. Pott, P., et al., *Cancer scroti.* Chirurgical Observations,, 1775. **3**: p. 177-83.
6. Herr, H.W., *Percivall Pott, the environment and cancer.* BJU Int, 2011. **108**(4): p. 479-81.
7. *Cancer Facts & Figures 2017*. 2017, American Cancer Society: Atlanta.
8. Harvey, J.J., *An Unidentified Virus Which Causes the Rapid Production of Tumours in Mice.* Nature, 1964. **204**: p. 1104-5.
9. Kirsten, W.H. and L.A. Mayer, *Morphologic responses to a murine erythroblastosis virus.* J Natl Cancer Inst, 1967. **39**(2): p. 311-35.
10. Shih, T.Y., et al., *Identification of a sarcoma virus-coded phosphoprotein in nonproducer cells transformed by Kirsten or Harvey murine sarcoma virus.* Virology, 1979. **96**(1): p. 64-79.

11. Shimizu, K., et al., *Isolation and preliminary characterization of the transforming gene of a human neuroblastoma cell line.* Proc Natl Acad Sci U S A, 1983. **80**(2): p. 383-7.

12. Miao, W., et al., *p120 Ras GTPase-activating protein interacts with Ras-GTP through specific conserved residues.* J Biol Chem, 1996. **271**(26): p. 15322-9.

13. Pylayeva-Gupta, Y., E. Grabocka, and D. Bar-Sagi, *RAS oncogenes: weaving a tumorigenic web.* Nat Rev Cancer, 2011. **11**(11): p. 761-74.

14. Malumbres, M. and M. Barbacid, *RAS oncogenes: the first 30 years.* Nat Rev Cancer, 2003. **3**(6): p. 459-65.

15. Cox, A.D. and C.J. Der, *Ras history: The saga continues.* Small GTPases, 2010. **1**(1): p. 2-27.

16. Downward, J., *Cell biology: metabolism meets death.* Nature, 2003. **424**(6951): p. 896-7.

17. Slamon, D.J., et al., *Studies of the HER-2/neu proto-oncogene in human breast and ovarian cancer.* Science, 1989. **244**(4905): p. 707-12.

18. Bellacosa, A., et al., *Molecular alterations of the AKT2 oncogene in ovarian and breast carcinomas.* Int J Cancer, 1995. **64**(4): p. 280-5.

19. Simpson, L. and R. Parsons, *PTEN: life as a tumor suppressor.* Exp Cell Res, 2001. **264**(1): p. 29-41.

20. Bos, J.L., H. Rehmann, and A. Wittinghofer, *GEFs and GAPs: critical elements in the control of small G proteins.* Cell, 2007. **129**(5): p. 865-77.

21. Clark, R., et al., *Antibodies specific for amino acid 12 of the ras oncogene product inhibit GTP binding.* Proc Natl Acad Sci U S A, 1985. **82**(16): p. 5280-4.

22. Ahmadian, M.R., et al., *Guanosine triphosphatase stimulation of oncogenic Ras mutants.* Proc Natl Acad Sci U S A, 1999. **96**(12): p. 7065-70.

23. Lim, S.M., et al., *Therapeutic targeting of oncogenic K-Ras by a covalent catalytic site inhibitor.* Angew Chem Int Ed Engl, 2014. **53**(1): p. 199-204.

24. Becher, I., et al., *Affinity profiling of the cellular kinome for the nucleotide cofactors ATP, ADP, and GTP.* ACS Chem Biol, 2013. **8**(3): p. 599-607.

25. John, J., et al., *Kinetic and structural analysis of the Mg(2+)-binding site of the guanine nucleotide-binding protein p21H-ras.* J Biol Chem, 1993. **268**(2): p. 923-9.

26. Ahearn, I.M., et al., *Regulating the regulator: post-translational modification of RAS.* Nat Rev Mol Cell Biol, 2011. **13**(1): p. 39-51.

27. Rine, J. and S.H. Kim, *A role for isoprenoid lipids in the localization and function of an oncoprotein.* New Biol, 1990. **2**(3): p. 219-26.

28. Der, C.J. and A.D. Cox, *Isoprenoid modification and plasma membrane association: critical factors for ras oncogenicity.* Cancer Cells, 1991. **3**(9): p. 331-40.

29. Reiss, Y., et al., *Sequence requirement for peptide recognition by rat brain p21ras protein farnesyltransferase.* Proc Natl Acad Sci U S A, 1991. **88**(3): p. 732-6.

30. Sinensky, M. and R.J. Lutz, *The prenylation of proteins.* Bioessays, 1992. **14**(1): p. 25-31.

31. Barrington, R.E., et al., *A farnesyltransferase inhibitor induces tumor regression in transgenic mice harboring multiple oncogenic mutations by mediating alterations in both cell cycle control and apoptosis.* Mol Cell Biol, 1998. **18**(1): p. 85-92.

32. Kohl, N.E., et al., *Development of inhibitors of protein farnesylation as potential chemotherapeutic agents.* J Cell Biochem Suppl, 1995. **22**: p. 145-50.

33. Kohl, N.E., et al., *Inhibition of farnesyltransferase induces regression of mammary and salivary carcinomas in ras transgenic mice.* Nat Med, 1995. **1**(8): p. 792-7.

34. Kohl, N.E., et al., *Inhibition of Ras function in vitro and in vivo using inhibitors of farnesyl-protein transferase.* Methods Enzymol, 1995. **255**: p. 378-86.

35. Appels, N.M., J.H. Beijnen, and J.H. Schellens, *Development of farnesyl transferase inhibitors: a review.* Oncologist, 2005. **10**(8): p. 565-78.

36. Whyte, D.B., et al., *K- and N-Ras are geranylgeranylated in cells treated with farnesyl protein transferase inhibitors.* J Biol Chem, 1997. **272**(22): p. 14459-64.

37. Lobell, R.B., et al., *Evaluation of farnesyl:protein transferase and geranylgeranyl:protein transferase inhibitor combinations in preclinical models.* Cancer Res, 2001. **61**(24): p. 8758-68.

38. deSolms, S.J., et al., *Dual protein farnesyltransferase-geranylgeranyltransferase-I inhibitors as potential cancer chemotherapeutic agents.* J Med Chem, 2003. **46**(14): p. 2973-84.

39. Engelman, J.A., et al., *Effective use of PI3K and MEK inhibitors to treat mutant Kras G12D and PIK3CA H1047R murine lung cancers.* Nat Med, 2008. **14**(12): p. 1351-6.

40. Asati, V., D.K. Mahapatra, and S.K. Bharti, *PI3K/Akt/mTOR and Ras/Raf/MEK/ERK signaling pathways inhibitors as anticancer agents: Structural and pharmacological perspectives.* Eur J Med Chem, 2016. **109**: p. 314-41.

41. Bennouna, J., et al., *A Phase II, open-label, randomised study to assess the efficacy and safety of the MEK1/2 inhibitor AZD6244 (ARRY-142886) versus capecitabine monotherapy in patients with colorectal cancer who have failed one or two prior chemotherapeutic regimens.* Invest New Drugs, 2011. **29**(5): p. 1021-8.

42. Keating, G.M. and A. Santoro, *Sorafenib: a review of its use in advanced hepatocellular carcinoma.* Drugs, 2009. **69**(2): p. 223-40.

43. Troiani, T., et al., *Intrinsic resistance to selumetinib, a selective inhibitor of MEK1/2, by cAMP-dependent protein kinase A activation in human lung and colorectal cancer cells.* Br J Cancer, 2012. **106**(10): p. 1648-59.

44. Ryan, M.B., et al., *Targeting RAS-mutant cancers: is ERK the key?* Trends Cancer, 2015. **1**(3): p. 183-198.

45. Jha, S., et al., *Dissecting Therapeutic Resistance to ERK Inhibition.* Mol Cancer Ther, 2016. **15**(4): p. 548-59.

46. Kirouac, D.C., et al., *Clinical responses to ERK inhibition in BRAF(V600E)-mutant colorectal cancer predicted using a computational model.* NPJ Syst Biol Appl, 2017. **3**: p. 14.

47. Germann, U.A., et al., *Targeting the MAPK Signaling Pathway in Cancer: Promising Preclinical Activity with the Novel Selective ERK1/2 Inhibitor BVD-523 (Ulixertinib).* Mol Cancer Ther, 2017. **16**(11): p. 2351-2363.

48. Gupta, S., et al., *Binding of ras to phosphoinositide 3-kinase p110alpha is required for ras-driven tumorigenesis in mice.* Cell, 2007. **129**(5): p. 957-68.

49. Castellano, E., et al., *Requirement for interaction of PI3-kinase p110alpha with RAS in lung tumor maintenance.* Cancer Cell, 2013. **24**(5): p. 617-30.

50. Baselga, J., et al., *Buparlisib plus fulvestrant versus placebo plus fulvestrant in postmenopausal, hormone receptor-positive, HER2-negative, advanced breast cancer (BELLE-2): a randomised, double-blind, placebo-controlled, phase 3 trial.* Lancet Oncol, 2017. **18**(7): p. 904-916.

51. Elster, N., et al., *A preclinical evaluation of the PI3K alpha/delta dominant inhibitor BAY 80-6946 in HER2-positive breast cancer models with acquired resistance to the HER2-targeted therapies trastuzumab and lapatinib.* Breast Cancer Res Treat, 2015. **149**(2): p. 373-83.

52. Spencer, A., et al., *The novel AKT inhibitor afuresertib shows favorable safety, pharmacokinetics, and clinical activity in multiple myeloma.* Blood, 2014. **124**(14): p. 2190-5.

53. Motzer, R.J., et al., *Efficacy of everolimus in advanced renal cell carcinoma: a double-blind, randomised, placebo-controlled phase III trial.* Lancet, 2008. **372**(9637): p. 449-56.

54. Shin, S.Y., et al., *Positive- and negative-feedback regulations coordinate the dynamic behavior of the Ras-Raf-MEK-ERK signal transduction pathway.* J Cell Sci, 2009. **122**(Pt 3): p. 425-35.

55. Carracedo, A. and P.P. Pandolfi, *The PTEN-PI3K pathway: of feedbacks and cross-talks.* Oncogene, 2008. **27**(41): p. 5527-41.

56. Cox, A.D., et al., *Drugging the undruggable RAS: Mission possible?* Nat Rev Drug Discov, 2014. **13**(11): p. 828-51.

57. Dang, C.V., et al., *Drugging the 'undruggable' cancer targets.* Nat Rev Cancer, 2017. **17**(8): p. 502-508.

58. Kaelin, W.G., Jr., *The concept of synthetic lethality in the context of anticancer therapy.* Nat Rev Cancer, 2005. **5**(9): p. 689-98.

59. O'Neil, N.J., M.L. Bailey, and P. Hieter, *Synthetic lethality and cancer.* Nat Rev Genet, 2017.

60. Downward, J., *RAS Synthetic Lethal Screens Revisited: Still Seeking the Elusive Prize?* Clin Cancer Res, 2015. **21**(8): p. 1802-9.

61. Weinstein, I.B. and A. Joe, *Oncogene addiction.* Cancer Res, 2008. **68**(9): p. 3077-80.

62. Ashworth, A., C.J. Lord, and J.S. Reis-Filho, *Genetic interactions in cancer progression and treatment.* Cell, 2011. **145**(1): p. 30-8.

63. Scholl, C., et al., *Synthetic lethal interaction between oncogenic KRAS dependency and STK33 suppression in human cancer cells.* Cell, 2009. **137**(5): p. 821-34.

64. Barbie, D.A., et al., *Systematic RNA interference reveals that oncogenic KRAS-driven cancers require TBK1.* Nature, 2009. **462**(7269): p. 108-12.

65. Frenkel, K., L. Wei, and H. Wei, *7,12-dimethylbenz[a]anthracene induces oxidative DNA modification in vivo.* Free Radic Biol Med, 1995. **19**(3): p. 373-80.

66. Balmain, A., et al., *Activation of the mouse cellular Harvey-ras gene in chemically induced benign skin papillomas.* Nature, 1984. **307**(5952): p. 658-60.

67. Bailleul, B., et al., *Initiation of skin carcinogenesis can occur by induction of carcinogen-specific point mutations in the Harvey-ras gene.* Prog Clin Biol Res, 1989. **298**: p. 137-45.

68. Chakravarti, D., et al., *Relating aromatic hydrocarbon-induced DNA adducts and c-H-ras mutations in mouse skin papillomas: the role of apurinic sites.* Proc Natl Acad Sci U S A, 1995. **92**(22): p. 10422-6.

69. Kanitakis, J., *Anatomy, histology and immunohistochemistry of normal human skin.* Eur J Dermatol, 2002. **12**(4): p. 390-9; quiz 400-1.

70. Gailit, J. and R.A. Clark, *Wound repair in the context of extracellular matrix.* Curr Opin Cell Biol, 1994. **6**(5): p. 717-25.

71. Sherratt, J.A. and J.D. Murray, *Models of epidermal wound healing.* Proc Biol Sci, 1990. **241**(1300): p. 29-36.

72. Kolarsick, P.A.J., M.A. Kolarsick, and C. Goodwin, *Anatomy and Physiology of the Skin.* Journal of the Dermatology Nurses' Association, 2011. **3**(4): p. 203-213.

73. Ito, M., et al., *Stem cells in the hair follicle bulge contribute to wound repair but not to homeostasis of the epidermis.* Nat Med, 2005. **11**(12): p. 1351-4.

74. Levy, V., et al., *Distinct stem cell populations regenerate the follicle and interfollicular epidermis.* Dev Cell, 2005. **9**(6): p. 855-61.

75. Blanpain, C. and E. Fuchs, *Epidermal homeostasis: a balancing act of stem cells in the skin.* Nat Rev Mol Cell Biol, 2009. **10**(3): p. 207-17.

76. Hansen, L.A., et al., *The epidermal growth factor receptor is required to maintain the proliferative population in the basal compartment of epidermal tumors.* Cancer Res, 2000. **60**(13): p. 3328-32.

77. Watt, F.M. and P.H. Jones, *Expression and function of the keratinocyte integrins.* Dev Suppl, 1993: p. 185-92.

78. Menon, G.K., S. Grayson, and P.M. Elias, *Ionic calcium reservoirs in mammalian epidermis: ultrastructural localization by ion-capture cytochemistry.* J Invest Dermatol, 1985. **84**(6): p. 508-12.

79. Watt, F.M., et al., *Regulation of keratinocyte terminal differentiation by integrin-extracellular matrix interactions.* J Cell Sci, 1993. **106 (Pt 1)**: p. 175-82.

80. Fuchs, E. and H. Green, *Changes in keratin gene expression during terminal differentiation of the keratinocyte.* Cell, 1980. **19**(4): p. 1033-42.

81. Zhu, S., et al., *C/EBPbeta modulates the early events of keratinocyte differentiation involving growth arrest and keratin 1 and keratin 10 expression.* Mol Cell Biol, 1999. **19**(10): p. 7181-90.

82. Candi, E., R. Schmidt, and G. Melino, *The cornified envelope: a model of cell death in the skin.* Nat Rev Mol Cell Biol, 2005. **6**(4): p. 328-40.

83. Eckert, R.L., et al., *Transglutaminase function in epidermis.* J Invest Dermatol, 2005. **124**(3): p. 481-92.

84. Schauber, J. and R.L. Gallo, *Antimicrobial peptides and the skin immune defense system.* J Allergy Clin Immunol, 2009. **124**(3 Suppl 2): p. R13-8.

85. Nagy, I., et al., *Propionibacterium acnes and lipopolysaccharide induce the expression of antimicrobial peptides and proinflammatory cytokines/chemokines in human sebocytes.* Microbes Infect, 2006. **8**(8): p. 2195-205.

86. Fournier, B. and D.J. Philpott, *Recognition of Staphylococcus aureus by the innate immune system.* Clin Microbiol Rev, 2005. **18**(3): p. 521-40.

87. Merad, M., F. Ginhoux, and M. Collin, *Origin, homeostasis and function of Langerhans cells and other langerin-expressing dendritic cells.* Nat Rev Immunol, 2008. **8**(12): p. 935-47.

88. Zaid, A., et al., *Persistence of skin-resident memory T cells within an epidermal niche.* Proc Natl Acad Sci U S A, 2014. **111**(14): p. 5307-12.

89. Nestle, F.O., et al., *Skin immune sentinels in health and disease.* Nat Rev Immunol, 2009. **9**(10): p. 679-91.

90. Ismail, A. and N. Yusuf, *Type I interferons: key players in normal skin and select cutaneous malignancies.* Dermatol Res Pract, 2014. **2014**: p. 847545.

91. Hurst, H.C., *Transcription factors. 1: bZIP proteins.* Protein Profile, 1994. **1**(2): p. 123-68.

92. Ron, D. and J.F. Habener, *CHOP, a novel developmentally regulated nuclear protein that dimerizes with transcription factors C/EBP and LAP and functions as a dominant-negative inhibitor of gene transcription.* Genes Dev, 1992. **6**(3): p. 439-53.

93. Landschulz, W.H., et al., *Isolation of a recombinant copy of the gene encoding C/EBP.* Genes Dev, 1988. **2**(7): p. 786-800.

94. Akira, S., et al., *A nuclear factor for IL-6 expression (NF-IL6) is a member of a C/EBP family.* EMBO J, 1990. **9**(6): p. 1897-906.

95. Poli, V., F.P. Mancini, and R. Cortese, *IL-6DBP, a nuclear protein involved in interleukin-6 signal transduction, defines a new family of leucine zipper proteins related to C/EBP*. Cell, 1990. **63**(3): p. 643-53.

96. Descombes, P., et al., *LAP, a novel member of the C/EBP gene family, encodes a liver-enriched transcriptional activator protein.* Genes Dev, 1990. **4**(9): p. 1541-51.

97. Chang, C.J., et al., *Molecular cloning of a transcription factor, AGP/EBP, that belongs to members of the C/EBP family.* Mol Cell Biol, 1990. **10**(12): p. 6642-53.

98. Roman, C., et al., *Ig/EBP-1: a ubiquitously expressed immunoglobulin enhancer binding protein that is similar to C/EBP and heterodimerizes with C/EBP*. Genes Dev, 1990. **4**(8): p. 1404-15.

99. Cao, Z., R.M. Umek, and S.L. McKnight, *Regulated expression of three C/EBP isoforms during adipose conversion of 3T3-L1 cells.* Genes Dev, 1991. **5**(9): p. 1538-52.

100. Williams, S.C., C.A. Cantwell, and P.F. Johnson, *A family of C/EBP-related proteins capable of forming covalently linked leucine zipper dimers in vitro.* Genes Dev, 1991. **5**(9): p. 1553-67.

101. Osada, S., et al., *DNA binding specificity of the CCAAT/enhancer-binding protein transcription factor family.* J Biol Chem, 1996. **271**(7): p. 3891-6.

102. Tsukada, J., et al., *The CCAAT/enhancer (C/EBP) family of basic-leucine zipper (bZIP) transcription factors is a multifaceted highly-regulated system for gene regulation.* Cytokine, 2011. **54**(1): p. 6-19.

103. Chumakov, A.M., et al., *Cloning of the novel human myeloid-cell-specific C/EBP-epsilon transcription factor.* Mol Cell Biol, 1997. **17**(3): p. 1375-86.

104. Park, J.S., et al., *Isolation, characterization and chromosomal localization of the human GADD153 gene.* Gene, 1992. **116**(2): p. 259-67.

105. Lin, F.T., et al., *A 30-kDa alternative translation product of the CCAAT/enhancer binding protein alpha message: transcriptional activator lacking antimitotic activity.* Proc Natl Acad Sci U S A, 1993. **90**(20): p. 9606-10.

106. Descombes, P. and U. Schibler, *A liver-enriched transcriptional activator protein, LAP, and a transcriptional inhibitory protein, LIP, are translated from the same mRNA.* Cell, 1991. **67**(3): p. 569-79.

107. Ossipow, V., P. Descombes, and U. Schibler, *CCAAT/enhancer-binding protein mRNA is translated into multiple proteins with different transcription activation potentials.* Proc Natl Acad Sci U S A, 1993. **90**(17): p. 8219-23.

108. Yamanaka, R., et al., *CCAAT/enhancer binding protein epsilon is preferentially up-regulated during granulocytic differentiation and its functional versatility is determined by alternative use of promoters and differential splicing.* Proc Natl Acad Sci U S A, 1997. **94**(12): p. 6462-7.

109. Cooper, C., et al., *Ig/EBP (C/EBP gamma) is a transdominant negative inhibitor of C/EBP family transcriptional activators.* Nucleic Acids Res, 1995. **23**(21): p. 4371-7.

110. LeClair, K.P., M.A. Blanar, and P.A. Sharp, *The p50 subunit of NF-kappa B associates with the NF-IL6 transcription factor.* Proc Natl Acad Sci U S A, 1992. **89**(17): p. 8145-9.

111. Vallejo, M., et al., *C/ATF, a member of the activating transcription factor family of DNA-binding proteins, dimerizes with CAAT/enhancer-binding proteins and directs their binding to cAMP response elements.* Proc Natl Acad Sci U S A, 1993. **90**(10): p. 4679-83.

112. Hsu, W., et al., *Fos and Jun repress transcription activation by NF-IL6 through association at the basic zipper region.* Mol Cell Biol, 1994. **14**(1): p. 268-76.

113. Ramji, D.P. and P. Foka, *CCAAT/enhancer-binding proteins: structure, function and regulation.* Biochem J, 2002. **365**(Pt 3): p. 561-75.

114. Wang, H., et al., *C/EBPbeta is a negative regulator of human papillomavirus type 11 in keratinocytes.* J Virol, 1996. **70**(7): p. 4839-44.

115. Oh, H.S. and R.C. Smart, *Expression of CCAAT/enhancer binding proteins (C/EBP) is associated with squamous differentiation in epidermis and isolated primary keratinocytes and is altered in skin neoplasms.* J Invest Dermatol, 1998. **110**(6): p. 939-45.

116. Martos-Rodriguez, A., et al., *Expression of CCAAT/enhancer-binding protein-beta (C/EBPbeta) and CHOP in the murine growth plate. Two possible key modulators of chondrocyte differentiation.* J Bone Joint Surg Br, 2003. **85**(8): p. 1190-5.

117. Darlington, G.J., S.E. Ross, and O.A. MacDougald, *The role of C/EBP genes in adipocyte differentiation.* J Biol Chem, 1998. **273**(46): p. 30057-60.

118. Tanaka, T., et al., *Defective adipocyte differentiation in mice lacking the C/EBPbeta and/or C/EBPdelta gene.* EMBO J, 1997. **16**(24): p. 7432-43.

119. Westmacott, A., et al., *C/EBPalpha and C/EBPbeta are markers of early liver development.* Int J Dev Biol, 2006. **50**(7): p. 653-7.

120. Lee, Y.H., et al., *Disruption of the c/ebp alpha gene in adult mouse liver.* Mol Cell Biol, 1997. **17**(10): p. 6014-22.

121. Swart, G.W., et al., *Transcription factor C/EBPalpha: novel sites of expression and cloning of the human gene.* Biol Chem, 1997. **378**(5): p. 373-9.

122. Maytin, E.V. and J.F. Habener, *Transcription factors C/EBP alpha, C/EBP beta, and CHOP (Gadd153) expressed during the differentiation program of keratinocytes in vitro and in vivo.* J Invest Dermatol, 1998. **110**(3): p. 238-46.

123. Bull, J.J., et al., *Contrasting expression patterns of CCAAT/enhancer-binding protein transcription factors in the hair follicle and at different stages of the hair growth cycle.* J Invest Dermatol, 2002. **118**(1): p. 17-24.

124. Chen, W., et al., *Expression of peroxisome proliferator-activated receptor and CCAAT/enhancer binding protein transcription factors in cultured human sebocytes.* J Invest Dermatol, 2003. **121**(3): p. 441-7.

125. House, J.S., et al., *C/EBPalpha and C/EBPbeta are required for Sebocyte differentiation and stratified squamous differentiation in adult mouse skin.* PLoS One, 2010. **5**(3): p. e9837.

126. Loomis, K.D., et al., *Genetic ablation of CCAAT/enhancer binding protein alpha in epidermis reveals its role in suppression of epithelial tumorigenesis.* Cancer Res, 2007. **67**(14): p. 6768-76.

127. Chen, S.S., et al., *C/EBPbeta, when expressed from the C/ebpalpha gene locus, can functionally replace C/EBPalpha in liver but not in adipose tissue.* Mol Cell Biol, 2000. **20**(19): p. 7292-9.

128. Johnson, P.F., *Molecular stop signs: regulation of cell-cycle arrest by C/EBP transcription factors.* J Cell Sci, 2005. **118**(Pt 12): p. 2545-2555.

129. Tsukada, J., et al., *The CCAAT/enhancer (C/EBP) family of basic-leucine zipper (bZIP) transcription factors is a multifaceted highly-regulated system for gene regulation.* Cytokine. **54**(1): p. 6-19.

130. Matsusaka, T., et al., *Transcription factors NF-IL6 and NF-kB synergistically activate transcription of the inflammatory cytokine interleukin 6 and interleukin 8.* PNAS, 1993. **90**: p. 10193-10197.

131. Akagi, T., et al., *Impaired response to GM-CSF and G-CSF, and enhanced apoptosis in C/EBPbeta-deficient hematopoietic cells.* Blood, 2008. **111**(6): p. 2999-3004.

132. Armstrong, D.A., L.N. Phelps, and M.P. Vincenti, *CCAAT enhancer binding protein-beta regulates matrix metalloproteinase-1 expression in interleukin-1beta-stimulated A549 lung carcinoma cells.* Mol Cancer Res, 2009. **7**(9): p. 1517-24.

133. Nakajima, T., et al., *Phosphorylaton at threonine-235 by a ras dependent mitogen-activated protein kinase cascade is essential for transcription factor NF-IL6.* Proc. Natl. Acad. Sci. USA, 1993. **90**: p. 2207-2211.

134. Zhu, S., et al., *CCAAT/enhancer binding protein-beta is a mediator of keratinocyte survival and skin tumorigenesis involving oncogenic Ras signaling.* Proc Natl Acad Sci U S A, 2002. **99**(1): p. 207-12.

135. Buck, M., et al., *Phosphorylation of rat serine 105 or mouse threonine 217 in C/EBPbeta is required for hepatocyte proliferation induced by TGFalpha.* Molecular Cell, 1999. **4**: p. 1087-1092.

136. Cho, I.J., N.R. Woo, and S.G. Kim, *The identification of C/EBPbeta as a transcription factor necessary for the induction of MAPK phosphatase-1 by toll-like receptor-4 ligand.* Arch Biochem Biophys, 2008. **479**(1): p. 88-96.

137. Lu, Y.C., et al., *Differential role for c-Rel and C/EBPbeta/delta in TLR-mediated induction of proinflammatory cytokines.* J Immunol, 2009. **182**(11): p. 7212-21.

138. Cloutier, A., et al., *Inflammatory cytokine production by human neutrophils involves C/EBP transcription factors.* J Immunol, 2009. **182**(1): p. 563-71.

139. Pope, R.M., A. Leutz, and S.A. Ness, *C/EBP beta regulation of the tumor necrosis factor alpha gene.* J Clin Invest, 1994. **94**(4): p. 1449-55.

140. Shirakawa, F., et al., *The human prointerleukin 1 beta gene requires DNA sequences both proximal and distal to the transcription start site for tissue-specific induction.* Mol Cell Biol, 1993. **13**(3): p. 1332-44.

141. Dunn, S.M., et al., *Requirement for nuclear factor (NF)-kappa B p65 and NF-interleukin-6 binding elements in the tumor necrosis factor response region of the granulocyte colony-stimulating factor promoter.* Blood, 1994. **83**(9): p. 2469-79.

142. Kunsch, C., et al., *Synergistic transcriptional activation of the IL-8 gene by NF-kappa B p65 (RelA) and NF-IL-6.* J Immunol, 1994. **153**(1): p. 153-64.

143. Xia, C., et al., *Cross-talk between transcription factors NF-kappa B and C/EBP in the transcriptional regulation of genes.* Int J Biochem Cell Biol, 1997. **29**(12): p. 1525-39.

144. Aguilar-Morante, D., et al., *Decreased CCAAT/enhancer binding protein beta expression inhibits the growth of glioblastoma cells.* Neuroscience. **176**: p. 110-9.

145. Anastasov, N., et al., *C/EBPbeta expression in ALK-positive anaplastic large cell lymphomas is required for cell proliferation and is induced by the STAT3 signaling pathway.* Haematologica. **95**(5): p. 760-7.

146. Bundy, L.M. and L. Sealy, *CCAAT/enhancer binding protein beta (C/EBPbeta)-2 transforms normal mammary epithelial cells and induces epithelial to mesenchymal transition in culture.* Oncogene, 2003. **22**(6): p. 869-83.

147. Duprez, E., *A new role for C/EBPbeta in acute promyelocytic leukemia.* Cell Cycle, 2004. **3**(4): p. 389-90.

148. Homma, J., et al., *Increased expression of CCAAT/enhancer binding protein beta correlates with prognosis in glioma patients.* Oncol Rep, 2006. **15**(3): p. 595-601.

149. Kim, M.H., A.Z. Minton, and V. Agrawal, *C/EBPbeta regulates metastatic gene expression and confers TNF-alpha resistance to prostate cancer cells.* Prostate, 2009. **69**(13): p. 1435-47.

150. Li, W., et al., *A gene expression signature for relapse of primary wilms tumors.* Cancer Res, 2005. **65**(7): p. 2592-601.

151. Pal, R., et al., *C/EBPbeta regulates transcription factors critical for proliferation and survival of multiple myeloma cells.* Blood, 2009. **114**(18): p. 3890-8.

152. Rask, K., et al., *Increased expression of the transcription factors CCAAT-rnhancer binding brotein-beta and C/EBP-zeta correlate with invasiveness of human colorectal cancer.* International Journal of Cancer, 2000. **86**: p. 337-343.

153. Sundfeldt, K., et al., *The expression of CCAAT/enhancer binding protein in human ovary in vivo: specific increase in C/EBPbeta dering epithelial tumour progression.* British Journal of Cancer, 1999. **79**: p. 1240-1248.

154. Buck, M., et al., *C/EBPbeta phosphorylation by RSK creates a functional XEXD caspase inhibitory box critical for cell survival.* Mol Cell, 2001. **8**(4): p. 807-16.

155. Ewing, S.J., et al., *C/EBPbeta represses p53 to promote cell survival downstream of DNA damage independent of oncogenic Ras and p19(Arf).* Cell Death Differ, 2008. **15**(11): p. 1734-44.

156. Piva, R., et al., *Functional validation of the anaplastic lymphoma kinase signature identifies CEBPB and BCL2A1 as critical target genes.* J Clin Invest, 2006. **116**(12): p. 3171-82.

157. Wessells, J., S. Yakar, and P.F. Johnson, *Critical prosurvival roles for C/EBP beta and insulin-like growth factor I in macrophage tumor cells.* Mol Cell Biol, 2004. **24**(8): p. 3238-50.

158. Balmain, A. and K. Brown, *Oncogene activation in chemical carcinogenesis.* Adv Cancer Res, 1988. **51**: p. 147-82.

159. Quintanilla, M., et al., *Carcinogen-specific mutation and amplification of Ha-ras during mouse skin carcinogenesis.* Nature, 1986. **322**(6074): p. 78-80.

160. Rehman, I., et al., *Frequent codon 12 Ki-ras mutations in mouse skin tumors initiated by N-methyl-N'-nitro-N-nitrosoguanidine and promoted by mezerein.* Mol Carcinog, 2000. **27**(4): p. 298-307.

161. Leder, A., et al., *v-Ha-ras transgene abrogates the initiation step in mouse skin tumorigenesis: effects of phorbol esters and retinoic acid.* Proc Natl Acad Sci U S A, 1990. **87**(23): p. 9178-82.

162. Shuman, J.D., et al., *Cell cycle-dependent phosphorylation of C/EBPbeta mediates oncogenic cooperativity between C/EBPbeta and H-RasV12.* Mol Cell Biol, 2004. **24**(17): p. 7380-91.

163. Sterneck, E., et al., *Conditional ablation of C/EBP beta demonstrates its keratinocyte-specific requirement for cell survival and mouse skin tumorigenesis.* Oncogene, 2006. **25**(8): p. 1272-1276.

164. Yoon, K., et al., *Decreased survival of C/EBP beta-deficient keratinocytes is due to aberrant regulation of p53 levels and function.* Oncogene, 2007. **26**(3): p. 360-7.

165. Mihara, M., et al., *p53 has a direct apoptogenic role at the mitochondria.* Mol Cell, 2003. **11**(3): p. 577-90.

166. Mihara, M. and U.M. Moll, *Detection of mitochondrial localization of p53.* Methods Mol Biol, 2003. **234**: p. 203-9.

167. Leu, J.I., et al., *Mitochondrial p53 activates Bak and causes disruption of a Bak-Mcl1 complex.* Nat Cell Biol, 2004. **6**(5): p. 443-50.

168. Linzer, D.I., W. Maltzman, and A.J. Levine, *The SV40 A gene product is required for the production of a 54,000 MW cellular tumor antigen.* Virology, 1979. **98**(2): p. 308-18.

169. Eliyahu, D., et al., *Meth A fibrosarcoma cells express two transforming mutant p53 species.* Oncogene, 1988. **3**(3): p. 313-21.

170. Finlay, C.A., et al., *Activating mutations for transformation by p53 produce a gene product that forms an hsc70-p53 complex with an altered half-life.* Mol Cell Biol, 1988. **8**(2): p. 531-9.

171. Baker, S.J., et al., *Chromosome 17 deletions and p53 gene mutations in colorectal carcinomas.* Science, 1989. **244**(4901): p. 217-21.

172. Honda, R., H. Tanaka, and H. Yasuda, *Oncoprotein MDM2 is a ubiquitin ligase E3 for tumor suppressor p53.* FEBS Lett, 1997. **420**(1): p. 25-7.

173. Oren, M., *Decision making by p53: life, death and cancer.* Cell Death Differ, 2003. **10**(4): p. 431-42.

174. Bode, A.M. and Z. Dong, *Post-translational modification of p53 in tumorigenesis.* Nat Rev Cancer, 2004. **4**(10): p. 793-805.

175. Meek, D.W. and C.W. Anderson, *Posttranslational modification of p53: cooperative integrators of function.* Cold Spring Harb Perspect Biol, 2009. **1**(6): p. a000950.

176. el-Deiry, W.S., et al., *Definition of a consensus binding site for p53.* Nat Genet, 1992. **1**(1): p. 45-9.

177. Funk, W.D., et al., *A transcriptionally active DNA-binding site for human p53 protein complexes.* Mol Cell Biol, 1992. **12**(6): p. 2866-71.

178. Li, M., et al., *Distinct regulatory mechanisms and functions for p53-activated and p53-repressed DNA damage response genes in embryonic stem cells.* Mol Cell, 2012. **46**(1): p. 30-42.

179. McMahon, M. and D. Woods, *Regulation of the p53 pathway by Ras, the plot thickens.* Biochim Biophys Acta, 2001. **1471**(2): p. M63-71.

180. Cazzalini, O., et al., *Multiple roles of the cell cycle inhibitor p21(CDKN1A) in the DNA damage response.* Mutat Res, 2010. **704**(1-3): p. 12-20.

181. Taylor, W.R. and G.R. Stark, *Regulation of the G2/M transition by p53.* Oncogene, 2001. **20**(15): p. 1803-15.

182. Itahana, K., G. Dimri, and J. Campisi, *Regulation of cellular senescence by p53.* Eur J Biochem, 2001. **268**(10): p. 2784-91.

183. Serrano, M., et al., *Oncogenic ras provokes premature cell senescence associated with accumulation of p53 and p16INK4a.* Cell, 1997. **88**(5): p. 593-602.

184. Lin, A.W., et al., *Premature senescence involving p53 and p16 is activated in response to constitutive MEK/MAPK mitogenic signaling.* Genes Dev, 1998. **12**(19): p. 3008-19.

185. Dimri, G.P., et al., *Regulation of a senescence checkpoint response by the E2F1 transcription factor and p14(ARF) tumor suppressor.* Mol Cell Biol, 2000. **20**(1): p. 273-85.

186. Favaloro, B., et al., *Role of apoptosis in disease.* Aging (Albany NY), 2012. **4**(5): p. 330-49.

187. Kerr, J.F., A.H. Wyllie, and A.R. Currie, *Apoptosis: a basic biological phenomenon with wide-ranging implications in tissue kinetics.* Br J Cancer, 1972. **26**(4): p. 239-57.

188. Savill, J. and V. Fadok, *Corpse clearance defines the meaning of cell death.* Nature, 2000. **407**(6805): p. 784-8.

189. Zou, B., et al., *XIAP-associated factor 1 (XAF1), a novel target of p53, enhances p53-mediated apoptosis via post-translational modification.* Mol Carcinog, 2012. **51**(5): p. 422-32.

190. Liston, P., et al., *Identification of XAF1 as an antagonist of XIAP anti-Caspase activity*. Nat Cell Biol, 2001. **3**(2): p. 128-33.

191. Miyashita, T., et al., *Tumor suppressor p53 is a regulator of bcl-2 and bax gene expression in vitro and in vivo.* Oncogene, 1994. **9**(6): p. 1799-805.

192. Nakano, K. and K.H. Vousden, *PUMA, a novel proapoptotic gene, is induced by p53.* Mol Cell, 2001. **7**(3): p. 683-94.

193. Oda, E., et al., *Noxa, a BH3-only member of the Bcl-2 family and candidate mediator of p53-induced apoptosis.* Science, 2000. **288**(5468): p. 1053-8.

194. Sax, J.K., et al., *BID regulation by p53 contributes to chemosensitivity.* Nat Cell Biol, 2002. **4**(11): p. 842-9.

195. Nicholson, D.W., *Caspase structure, proteolytic substrates, and function during apoptotic cell death.* Cell Death Differ, 1999. **6**(11): p. 1028-42.

196. Slee, E.A., C. Adrain, and S.J. Martin, *Serial killers: ordering caspase activation events in apoptosis.* Cell Death Differ, 1999. **6**(11): p. 1067-74.

197. Locksley, R.M., N. Killeen, and M.J. Lenardo, *The TNF and TNF receptor superfamilies: integrating mammalian biology.* Cell, 2001. **104**(4): p. 487-501.

198. Daniels, R.A., et al., *Expression of TRAIL and TRAIL receptors in normal and malignant tissues.* Cell Res, 2005. **15**(6): p. 430-8.

199. Waring, P. and A. Mullbacher, *Cell death induced by the Fas/Fas ligand pathway and its role in pathology.* Immunol Cell Biol, 1999. **77**(4): p. 312-7.

200. Peter, M.E. and P.H. Krammer, *The CD95(APO-1/Fas) DISC and beyond.* Cell Death Differ, 2003. **10**(1): p. 26-35.

201. Bagnoli, M., S. Canevari, and D. Mezzanzanica, *Cellular FLICE-inhibitory protein (c-FLIP) signalling: a key regulator of receptor-mediated apoptosis in physiologic context and in cancer.* Int J Biochem Cell Biol, 2010. **42**(2): p. 210-3.

202. Muller, M., et al., *Drug-induced apoptosis in hepatoma cells is mediated by the CD95 (APO-1/Fas) receptor/ligand system and involves activation of wild-type p53.* J Clin Invest, 1997. **99**(3): p. 403-13.

203. Tamura, T., et al., *Induction of Fas-mediated apoptosis in p53-transfected human colon carcinoma cells.* Oncogene, 1995. **11**(10): p. 1939-46.

204. Maecker, H.L., C. Koumenis, and A.J. Giaccia, *p53 promotes selection for Fas-mediated apoptotic resistance.* Cancer Res, 2000. **60**(16): p. 4638-44.

205. Wu, G.S., et al., *KILLER/DR5 is a DNA damage-inducible p53-regulated death receptor gene.* Nat Genet, 1997. **17**(2): p. 141-3.

206. Munoz-Fontela, C., et al., *Emerging roles of p53 and other tumour-suppressor genes in immune regulation.* Nat Rev Immunol, 2016. **16**(12): p. 741-750.

207. Zhang, F. and S. Sriram, *Identification and characterization of the interferon-beta-mediated p53 signal pathway in human peripheral blood mononuclear cells.* Immunology, 2009. **128**(1 Suppl): p. e905-18.

208. Miciak, J. and F. Bunz, *Long story short: p53 mediates innate immunity.* Biochim Biophys Acta, 2016. **1865**(2): p. 220-7.

209. Munoz-Fontela, C., et al., *Transcriptional role of p53 in interferon-mediated antiviral immunity.* J Exp Med, 2008. **205**(8): p. 1929-38.

210. Yu, Q., et al., *DNA-damage-induced type I interferon promotes senescence and inhibits stem cell function.* Cell Rep, 2015. **11**(5): p. 785-797.

211. Leaman, D.W., et al., *Identification of X-linked inhibitor of apoptosis-associated factor-1 as an interferon-stimulated gene that augments TRAIL Apo2L-induced apoptosis.* J Biol Chem, 2002. **277**(32): p. 28504-11.

212. Chawla-Sarkar, M., D.W. Leaman, and E.C. Borden, *Preferential induction of apoptosis by interferon (IFN)-beta compared with IFN-alpha2: correlation with TRAIL/Apo2L induction in melanoma cell lines.* Clin Cancer Res, 2001. **7**(6): p. 1821-31.

213. Howlander, N., et al. *SEER Cancer Statistics Review, 1975-2014*. 2017 April 2017 [cited 2017.

214. Goldenberg, M.M., *Trastuzumab, a recombinant DNA-derived humanized monoclonal antibody, a novel agent for the treatment of metastatic breast cancer.* Clin Ther, 1999. **21**(2): p. 309-18.

215. Luo, J., N.L. Solimini, and S.J. Elledge, *Principles of cancer therapy: oncogene and non-oncogene addiction.* Cell, 2009. **136**(5): p. 823-37.

216. Tischler, J., B. Lehner, and A.G. Fraser, *Evolutionary plasticity of genetic interaction networks.* Nat Genet, 2008. **40**(4): p. 390-1.

217. Fridman, J.S. and S.W. Lowe, *Control of apoptosis by p53.* Oncogene, 2003. **22**(56): p. 9030-40.

218. Tomasello, E., et al., *Harnessing Mechanistic Knowledge on Beneficial Versus Deleterious IFN-I Effects to Design Innovative Immunotherapies Targeting Cytokine Activity to Specific Cell Types.* Front Immunol, 2014. **5**: p. 526.

219. Cai, X., Y.H. Chiu, and Z.J. Chen, *The cGAS-cGAMP-STING pathway of cytosolic DNA sensing and signaling.* Mol Cell, 2014. **54**(2): p. 289-96.

220. Takaoka, A., et al., *Integration of interferon-alpha/beta signalling to p53 responses in tumour suppression and antiviral defence.* Nature, 2003. **424**(6948): p. 516-23.

221. Rivas, C., S.A. Aaronson, and C. Munoz-Fontela, *Dual Role of p53 in Innate Antiviral Immunity.* Viruses, 2010. **2**(1): p. 298-313.

222. Wiley, S.R., et al., *Identification and characterization of a new member of the TNF family that induces apoptosis.* Immunity, 1995. **3**(6): p. 673-82.

223. Micali, O.C., et al., *Silencing of the XAF1 gene by promoter hypermethylation in cancer cells and reactivation to TRAIL-sensitization by IFN-beta.* BMC Cancer, 2007. **7**: p. 52.

224. Zhao, J., Y. Lu, and H.M. Shen, *Targeting p53 as a therapeutic strategy in sensitizing TRAIL-induced apoptosis in cancer cells.* Cancer Lett, 2012. **314**(1): p. 8-23.

APPENDIX

Oncogenic Ras signaling in the absence of C/EBPβ does not induce apoptosis

To determine if the apoptotic phenotype in regressing tumors was dependent on oncogenic Ras signaling, we developed a mouse where we could turn on oncogenic Ras in the basal layer of the epidermis in the presence or absence of C/EBPβ. The K14-ER:Ras^{tam} (ER:Ras) mouse allows for the spatial and temporal control of oncogenic Ras as a keratin 14 promoter directs expression of an inducible H-Ras^{G12V} to the basal layer of the epidermis. This mouse was crossed with a conditional epidermal C/EBPβ knockout K5-Cre;*C/ebpβ*$^{flox/flox}$ (CKOβ) mouse to produce the K14-ER:Ras^{tam};K5-Cre;*C/ebpβ*$^{flox/flox}$ (ER:Ras;CKOβ) mouse as well as the K14-ER:Ras^{tam};K5-Cre (ER:Ras;Cre) control mouse. In this way expression of oncogenic Ras and deletion of C/EBPβ both occur in the basal layer of the epidermis. Following a single dose of tamoxifen, total amounts of C/EBPβ remained unchanged (Fig 1A) however there was a >2-fold increase in cells exhibiting positive IHC staining for phosphorylated C/EBPβ on threonine 188 (Fig 1B, C) indicating that C/EBPβ is phosphorylated downstream of oncogenic Ras in this model system. Dosing wildtype and ER:Ras mice topically with tamoxifen had no statistically significant effect on levels of apoptosis in the epidermis (Fig 2A). Activated oncogenic Ras signaling and induced proliferation in the epidermis (Fig 2B) which lead to an increase in epidermal thickness (Fig 2C). With a working model system, ER:Ras;CKOβ and ER:Ras;Cre mice were topically dosed with tamoxifen. Activation of oncogenic Ras signaling induced proliferation equally in mice with and without C/EBPβ (Fig 2D). Levels of the DNA damage as measured by IHC staining for γH2AX were also increased in the epidermis following activation of oncogenic

Ras signaling to an equal extent in mice with and without C/EBPβ (Fig 2E) however levels of p53 (Fig 2F) and apoptosis (Fig 2G) were unchanged.

APPENDIX FIGURE LEGENDS

Appendix Figure 1: Activation of oncogenic Ras in basal keratinocytes of the epidermis increases PO_4-T188 C/EBPβ but not total C/EBPβ protein. Wildtype and K14ER:Ras mice were topically dosed with a single application of 1mg Tamoxifen in acetone. (A) Western blot analysis for C/EBPβ in epidermal lysates from tamoxifen treated wildtype and K14ER:Ras mice. (B) IHC staining for C/EBPβ and PO_4-T188 C/EBPβ in K14ER:Ras mice 18hr post Tamoxifen. (C) Quantification of PO_4-T188 C/EBPβ in wildtype and K14ER:Ras mice 18hr post Tamoxifen (Wildtype n=3, K14ER:Ras n=3). *indicates significantly different from controls $p<0.05$ via the Student's t test.

Appendix Figure 2: Activation of oncogenic Ras in basal keratinocytes is non-lethal and induces proliferation, epidermal thickening, and phosphorylation of histone 2AX but not increases in p53 or apoptosis in the absence of C/EBPβ. Wildtype and K14ER:Ras mice were topically dosed with a single application of 1mg Tamoxifen in acetone. (A) Quantification of epidermal apoptosis in H&E stained skin cross-sections (n=3 for each group). (B) Quantification of epidermal IHC staining for BrdU incorporation in skin cross-sections (n=3 for each group). (C) Measurements of epidermal thickness measured in H&E stained skin cross-sections. (n=3 for each group with 30 fields measured for each mouse). (D) Quantification of epidermal IHC staining for BrdU incorporation in skin cross-sections (n=4 for each group). (E) Quantification of epidermal IHC staining for γH2AX in skin cross-sections (n=4 for each group). (F) Quantification of epidermal IHC staining for p53 in skin cross-sections (n=4 for each group). (G) Quantification of epidermal apoptosis in H&E

stained skin cross-sections (n=4 for each group). *indicates significantly different from controls $p<0.05$ via the Student's t test.

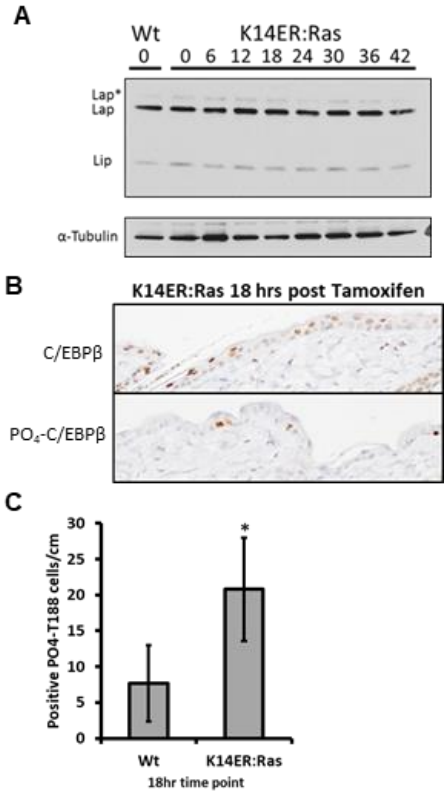

Appendix Figure 1: Activation of oncogenic Ras in basal keratinocytes of the epidermis increases PO_4-T188 C/EBPβ but not total C/EBPβ protein.

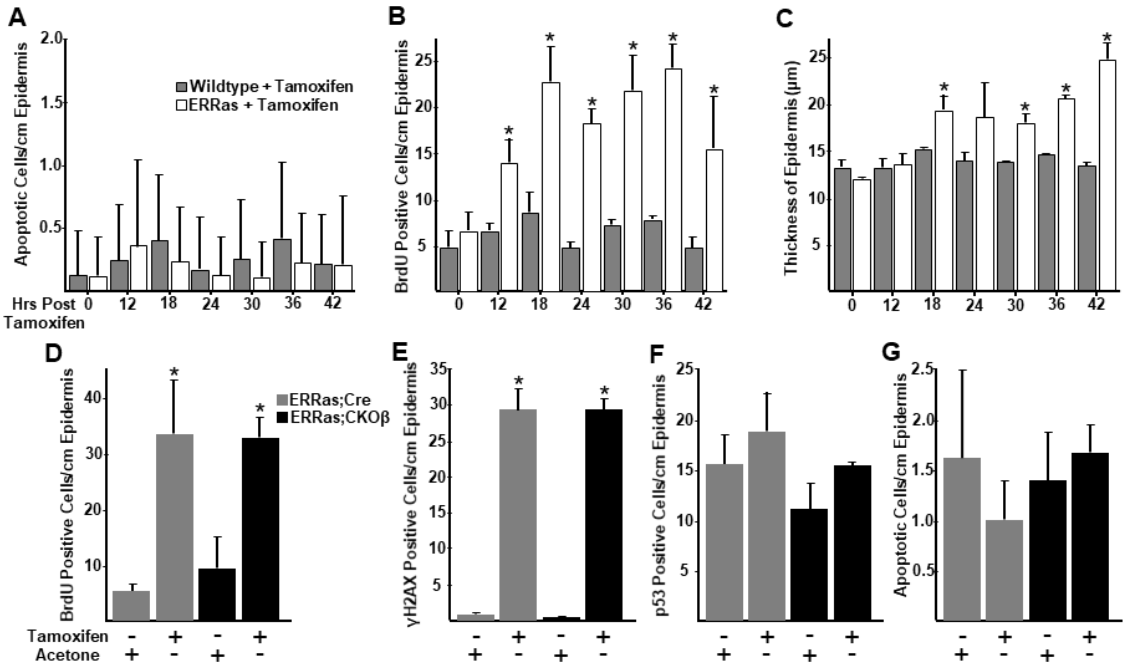

Appendix Figure 2: Activation of oncogenic Ras in basal keratinocytes is non-lethal and induces proliferation, epidermal thickening, and phosphorylation of histone 2AX but not increases in p53 or apoptosis in the absence of C/EBPβ